



**ENHANCED COST MINIMIZATION ALGORITHM FOR CONTROL
ARCHITECTURES**

THESIS

Laura L. Lucas

AFIT-ENV-MS-17-M-200

**DEPARTMENT OF THE AIR FORCE
AIR UNIVERSITY**

AIR FORCE INSTITUTE OF TECHNOLOGY

Wright-Patterson Air Force Base, Ohio

DISTRIBUTION STATEMENT A.
APPROVED FOR PUBLIC RELEASE; DISTRIBUTION UNLIMITED.

The views expressed in this thesis are those of the author and do not reflect the official policy or position of the United States Air Force, Department of Defense, or the United States Government. This material is declared a work of the U.S. Government and is not subject to copyright protection in the United States.

AFIT-ENV-MS-17-M-200

ENHANCED COST MINIMIZATION ALGORITHM FOR CONTROL
ARCHITECTURES

THESIS

Presented to the Faculty

Department of Systems Engineering and Management

Graduate School of Engineering and Management

Air Force Institute of Technology

Air University

Air Education and Training Command

In Partial Fulfillment of the Requirements for the
Degree of Master of Science in Systems Engineering

Laura L. Lucas, MS

March 2017

DISTRIBUTION STATEMENT A.
APPROVED FOR PUBLIC RELEASE; DISTRIBUTION UNLIMITED.

AFIT-ENV-MS-17-M-200

ENHANCED COST MINIMIZATION ALGORITHM FOR CONTROL
ARCHITECTURES

Laura L. Lucas, MS

Committee Membership:

Dr. D. R. Jacques
Chair

Dr. M. Pachter
Member

Lt. Col. A. M. Cox, Ph.D
Member

Abstract

This research emphasized control for missions with multiple unmanned vehicles (UVs). Extensions to an existing unified control architecture were developed. Line-of-sight (LOS) obstructions and total communication power limitations, such as battery capacity for communicating in multiple rover scenarios, were combined into one problem. The operational mission is summarized as follows: The operator initiates control transmissions between base and the UVs, while a small aerial vehicle provides a relay supporting flexible communications. During this mission, the system strives to maintain LOS communication with as many friendly UVs as possible. Automated enhanced placement software was designed to keep UVs visible to the relay. Manually determined relay placement might reduce performance and threaten safety; therefore, autonomous placement is under development. While there was documentation regarding midpoint placement for single rover scenarios, enhanced placement with battlespace obstructions and a flexible quantity of UVs was not completed previously. The algorithm provides two levels of decision support: first, it computes feasible destinations for the relay. Second, the algorithm reveals the minimum-cost destination from the finite set of candidates. Visibility computation ran in the background with three nodes and delivered relay coordinates to the operator. Flight test results are presented.

In loving memory:

CAP (1944 –2014), RCK (1931 –2016), & JPL (1929 –2016)

Table of Contents

	Page
Abstract	iv
In loving memory:.....	v
Table of Contents	vi
List of Figures	viii
List of Tables	ix
I. Introduction	1
Background.....	1
Motivation	4
Objective.....	5
Problem.....	5
Investigative Questions	6
Scope	7
Assumptions	8
Limitations.....	8
Thesis Organization.....	9
II. Literature Review	10
Key Concepts.....	10
III. Methodology	23
Overview	23
Data Sources	24
Ground Test Configurations	25
Flight Tests	26
Dynamic Simulation Tests	27

Dependent Variable	28
Notation	29
Simulation Process	32
Architecture	35
Hardware	42
Coordinate Frame Transformation and Scaling	43
Local Minima and Heuristics	43
Timeline.....	44
IV. Results of Algorithm for Simulation	45
Static Simulation	45
Dynamic Simulation.....	47
Conclusion.....	54
V. Results of Algorithm for Flight Test.....	55
Test Report	55
Obstacle-Free Centroid Test.....	55
Relay Positioning Test around Obstacle.....	58
Conclusion.....	63
VI. Conclusion and Recommendations.....	64
Investigative Questions Revisited	64
Potential Applications	67
Bibliography	69
Appendix.....	72
Appendix A: Working Article	72
Appendix B: Form 5028.....	92

List of Figures

	Page
Figure 1. Scene #2 in Table 2.	27
Figure 2. Operational View of Obstructed Communication Link.	30
Figure 3. Level 1 Flow Diagram.	32
Figure 4. Level 2 Flow Diagrams.	33
Figure 5. Level 3 Flow Diagrams, Part I.	34
Figure 6. Level 3 Flow Diagrams, Part II.	35
Figure 7. OV-1: Communication Relay for Single Vehicle [5].	36
Figure 8. SV-5a: System Function Traceability Matrix [5].	38
Figure 9. SV-1 Systems Interface Description Focused on Communication.	41
Figure 10. The quadrotor vehicle used for the implementation in this chapter.	42
Figure 11. Communication Power Cost Avoidance for Five Trials.	47
Figure 12. Simple Example of Dynamic Simulation Plot.	49
Figure 13. Overhead of Dynamically Simulated UV Paths.	50
Figure 14. Communication Cost Function over Time.	50
Figure 15. Comparative Cost Outcomes.	53
Figure 16. Comparative LOS Metrics.	53
Figure 17. Relay Centeredness ($dist_{\angle}$) and Rover Speed over Time. Part I.	57
Figure 18. Horizontal Position Variance Alert in Mission Planner.	57
Figure 19. Flight Test Set-up with Obstacle.	59
Figure 20. Relay Centeredness ($dist_{\angle}$) and Rover Speed over Time. Part II.	60
Figure 21. Overhead of Relay Following Algorithm Commands.	61

Figure 22. LOS between Nodes and Relay.....	62
---	----

List of Tables

	Page
Table 1. Decision Matrix to Choose the Level of Mission Autonomy and Information Exchange (recreated from [25])	15
Table 2. Test Cases with Computational Inputs	26
Table 3. Activity Descriptions by Vehicle Type (adapted from [5]).....	39
Table 4. Hardware details	42
Table 5. Execution Time Trials	46
Table 6. Sequence and Description of Events	51
Table 7. Table of Rules	52

ENHANCED COST MINIMIZATION ALGORITHM FOR CONTROL ARCHITECTURES

I. Introduction

Background

Unmanned vehicle (UV) technologies provide a crucial alternative to locally-piloted resources to accomplish the dull, dirty, dangerous tasks for which the UVs are specialized [1]. The multiple unmanned systems domain is based on interactive unmanned objects. Making a specialty of multiple unmanned vehicles requires UV coordination or, if the UVs are employed non-cooperatively, holding sway over non-cooperative UVs. The UVs considered in this paper are cooperative vehicles.

In over two decades of groundbreaking history, there has been a great deal of research on coupling multiple, coordinated vehicles to achieve cooperative control. *Autonomous Horizons* [2] shows the expected benefits of cooperative control. Tools that enhance situational awareness, decision-making, and speed-effectiveness will be conferred by autonomous software, seamlessly working and exchanging information with teams [2].

Cooperative control of multiple unmanned systems remains challenging for 2017 and beyond, because it represents a growth in autonomy that extends from the currently fielded fleet of unmanned vehicles. Different commercial and military platforms, and sometimes heterogeneous UV combinations, are flying with the current technology. Given budget constraints, some such combinations are subject to all the limitations (i.e., range and controllability) of current high frequency radio communications [3].

Intelligence collection and information flow are often the pursuits of UV control, a purpose which requires “transmission of states ... that is dependent on some communication data link [4].” If administering and supporting a communication data link requires an effort in the course of performing a mission, the user can incorporate a communication relay scenario. A communication relay scenario is defined as: “the act of passing information between a remote vehicle or sensor to a central ground control station (GCS) through an intermediate relay vehicle [5].” An intermediate relay vehicle is a class of multiple-UV coordination for operational missions, in order to allocate communication power and implement the communication data link.

An example operational mission is summarized as follows: the operator initiates control transmissions between a base station and the UVs, while a small aerial UV automatically flies into position and becomes a relay, supporting flexible communication. During the mission, the system communicates to as many friendly UVs as possible, in spite of line-of-sight (LOS) obstructions and communication power limits, which threaten mission performance. Allocating data link support to the relay vehicle is desired. The need is to operate the relay vehicle autonomously, thus helping the ground station operators narrow their focus and pay attention to the relayed information.

This mission applies to the defense and civilian sectors. Defense sector UV applications range from surveilling with a camera payload to harassing operational targets using a dangerous payload that the friendly UV carries. The breadth of civilian sector UV applications shows varying levels of autonomy, from agriculture to professional- and hobbyist-level videography. In those application areas, a

communication relay provides avoidance of blind sensor areas (missed spots) and relocation of itself, relative to multiple UVs, to improve link quality [6].

To complete the mission, the operator requires that UVs remain visible to the relay vehicle, without violating constraints (such as battery capacity) or affecting the operator's mental workload. Operator input includes activity other than waiting for actionable information. Operator workload comprises, depending on the scenario, a combination of effort to set the mode in which the aircraft is operating, create a waypoint path for one or more aircraft, and schedule settings to take effect for individual aircraft [6]–[9]. Automated positioning support must also follow lessons learned in the past, so to not increase workload for the operator [9].

Performance measures provide a quantitative means of reviewing data link effectiveness in simulations and flight tests. Timing transmission through the system communication sequence is an example of a performance measure for the communications capability [5]. Based on Wasserman et al.'s results [10], research improves measurement processes already performed. Established performance measures for the desired autonomous system likely need refinement, in parallel with the algorithmic implementation of the automated communication relay [11].

This research presents an algorithmic, single-relay implementation of optimal and heuristic control for a small aerial UV. The term “local minimum” is distinct from the term “heuristic.” “Local minimum” means the answer is the numerically determined local solution that minimizes an objective function to within a specific margin of error. “Heuristic” means the answer is an efficient design solution, based on knowledge of the

specific problem. In dynamic situations, part of heuristic knowledge comes from familiarity with the pattern of system evolution over time.

Upon use, the automated algorithm under design simplifies operational missions in which the operator invokes a communication relay. Other engineering approaches to automation for flight planning have included the game theoretical approach [3] and the genetic algorithm approach [6]. The consequences to those approaches have driven automation of different actors' capabilities—supposedly to enable a single operator to confidently perform operations [5]. Instead, the implementation of automation for flight planning has, so far, produced unexpectedly brittle systems [9], requiring the operator's input more frequently than intended.

Motivation

Robust single-operator control of multiple UVs near obstructions requires safe and effective flight planning. This research focuses on the automated communication relay's role in safe and effective positioning. Demonstrating the performance of a heuristic-based relay placement algorithm in a realistic flight environment is the rationale for this research effort.

The senior leader's perspective provides additional justification. Lt. Gen. Robert P. Otto told interviewers, "In the future, why wouldn't we have an integrated, cross-domain, high-capacity capability for targeting? ...The acquisition community [would] tell us how hard and expensive it would be [12]." Perspectives reflect the expectations leaders maintain for the future role of UV systems. Successful automated operation remains an important topic, especially for the acquisition community. Fact-finding,

design, and flight-testing are necessary to maximize the Air Force's systems in the context of their impact on the operational mission.

Increasing levels of autonomy should augment operator tasks to monitor and control remote vehicles, in terms of ease of operations and quality of intelligence aspects. Relaying communication has the potential to aid many tasks. These tasks include swarming, flying around obstacles, and operating across long distances.

Objective

The objective of this research is testing multiple rover scenarios to compare the efficacy of telemetry communications, while testing the experimental algorithm in control over automated relay positioning. The goal is to improve information provided by the multiple-UV system. Where previously signals were interrupted by physical obstructions, the information from signals will maintain continuity as a result of maintaining Line-of-Sight (LOS) in an environment with obstacles.

Problem

Operators desire the overall information-sensing range of small UVs to extend Beyond-Line-of-Sight (BLOS) and behind obstructions. "Range" in this case, means the regions across which a Command and Control (C2) source can propagate telemetry information and imagery to its neighbors. The system's communication solution potentially restricts the whole system's capability to utilize knowledge about the operating region.

Small, inexpensive UVs often have inexpensive communication components and may need a supportive relay vehicle to ensure that sensor data and vehicle information

reach their intended destination. However, manually determining relay placement is distracting to the operator. The workload required to select the most battery-efficient position and maintain LOS at all times during operation is excessive.

A solution that is portable, flexible, and provides greater LOS than traditional remote control benefits the Air Force. The Department of Defense (DOD) has recently been researching automation as a potential solution. With this research, automation may allow a small team to extend the overall information-sensing range of small UAVs to BLOS and behind objects.

Investigative Questions

- *What is an appropriate and effective means of autonomously positioning a communication relay in order to maintain the communication link between multiple vehicles and a ground control station?*

Gray's architecture [5], shown to be appropriate and effective for a single rover vehicle in previous thesis research, is also implemented in this research, and the desired details are added: additional vehicles and the positioning algorithm extended to accommodate obstacles, are added. These are testable in flight and in simulation.

- *Given an environment obstructed by obstacles, what is missing from established performance measures for quantitatively assessing aerial radio-frequency relays?*
Is there value in adding LOS metrics to supplement accuracy estimation?

The researcher tests the integrity of measures by comparison of simulations and flight test results. Gray's established measures [5] include: the average packets

(percentage) received due to a relayed network, and the timing of each component's transmission throughout the system communication sequence, are measures.

- *What is the effect on system performance, due to combining algorithmic local minima positioning with a heuristic approximation of the optimal positioning algorithm?*

In this research, the scenarios are controlled and the resulting performance is reviewed using local minimum and heuristic position candidates in the same decision algorithm. Scenarios involve different numbers of homogeneous remote UVs and up to two different obstacles, per scenario. The positioning algorithm accommodates extensive (but not unlimited) combinations.

“By controlling the experimental scenario the investigator is effectively creating a ‘closed’ environment and can therefore know ground truth. Thus, ‘ideal’ answers to subjective queries can be pre-defined [13].” However, an automated system can select between other options, which are not optimal but are heuristic answers and satisfy the constraints of the real environment [2]. These are testable in flight and in simulation.

Scope

The research scope includes three stages: (1) development of algorithms, (2) extension of the architecture and integration of communication relay scenarios, and (3) simulation, flight test, and evaluation. Critical thinking on performance measures, in direct response to the second investigative question, is a crosscutting step that aligns the systems engineering process to all stages of this research.

Assumptions

The researcher makes two simplifying assumptions. First, this research assumes conditions that allow Global Positioning System (GPS) satellite reception. Second, on-board processing is not used on the aerial relay (ultimately desired architecture); this research assumes that local minima and heuristic solutions are implementable in near-real time without constraining the location of processing to an off-board source location (current architecture).

Limitations

This research used pre-existing hardware and GCS options. This choice reduced the schedule risk involved with hardware and software integration. Additionally, it reduced the schedule duration of safety reviews, and avoided unnecessary customization. To further reduce cost, the set of UVs was limited to assets that had passed checkout at the Air Force Institute of Technology (AFIT). This possibly limited the configurations that could be implemented; the hardware was shared by different research projects over the same time period to accomplish integration and ground testing.

This research used virtual obstacles; for safety reasons, the direct pathways between the UVs and operators were not actually broken by tangible objects. The safety pilots must maintain LOS control of the UVs during AFIT tests. This constraint was imposed to assure ground personnel of safety. For that reason, it was necessary to employ traffic cones instead of more permanent structures (e.g., a building). The lack of a pre-surveyed obstacle introduced error, in that the obstacle footprint, as represented by traffic cones, was not accurately placed at its ground-truth coordinates.

The intended implementation of a positioning algorithm for keeping nodes (1) visible and (2) within communications range would have, ideally, focused on choosing the GCS as the node with greater priority. Losing the GCS was not considered for risk aversion in making relay placement decisions. The risk of losing the GCS was not realized during this research, however, GCS loss is a potential problem and limitation.

Thesis Organization

In Chapter 1, performance requirements for the communication relay system and motivations for achieving increased automation and autonomy are explored. The problem statement, assumptions, scope, investigative questions, and research objectives are established. In the next chapter, a thorough review of the literature is accomplished. In Chapter 3, a detailed description of the research method is outlined. Chapter 4 and Chapter 5 continue with the results of variable interactions extracted from the raw telemetry data, graphical solutions computed, and other system flight characteristics. Finally, in Chapter 6, the conclusions drawn, from the entirety of the research accomplished, and recommendations of future work to be done are described.

II. Literature Review

Key Concepts

Communication around obstacles and across a multi-UV system is the key focus of this research. Communication is a problem for applications that rely on LOS communication for controlling groups of small UVs performing: search, targeting, surveillance, status monitoring, firefighting, disaster management, ad-hoc networking and sensing, meteorology, surveying, and traffic management [14]. The communication that can occur between UVs, while they are directly tied to a ground infrastructure, is restricted to the limitations of that same infrastructure [14]. Under constrained conditions, successful mission execution requires knowledge of boundaries and location of system elements, which affect the total restriction.

Forces external to the system (obstacles, for example) reside in the path of the ground infrastructure. Any influence on line-of-sight potentially restricts the whole system's capability to utilize knowledge of the region. Statistical analysis in Garzón et al. [15] expressed the relationship between unknown environments and travelling robots in probabilistic terms. Simultaneous mapping of, and navigation around, terrain features was carried out. The simultaneous operational activities were accomplished by using reference imagery from an aerial sensor to assist a ground robot, which was equipped with an Inertial Measurement Unit (IMU) and a GPS. Garzón et al. performed simulated and outdoor environment tests. The problem of path planning BLOS of the ground control station affected the system as a whole [15].

Seah added Failure Modes and Effects Analysis to the scope of system architecture and analyzed the results of LOS loss to the GCS [16]. The system accomplished a GCS handoff to a remote teammate for economical operation across BLOS distances. Engineering solutions to these communication problems have been framed in architectures, thereby gaining advantages in testing and addressing system issues [16].

Short of omniscience, the best case for mission success occurs if system boundaries and agent responsibilities are well defined yet flexible enough to meet mission requirements [17]. Engineers researching this area have emphasized architecture, due to the complexity that would be associated with ad-hoc solutions. In this context, “ad-hoc” refers to temporary, loose teaming between a domain application and dynamic mission requirements [10]. For example, when pitted against obstacle adversities, one might look to ad-hoc networking solutions [14] and simulated aerial wireless communications [18], as one combined approach.

The database in Wasserman et al. [10] required a novel application of the Change 2.0 configuration management approach. Cross-domain network architectures have been challenged by changes in interfaces. Ad-hoc network maturation using distributed management showed potential benefits, especially when Commercial-off-the-Shelf (COTS) components were managed on the client end [10].

Bekmezci et al. published a scholarly bibliography of Flying Ad-Hoc Networks (FANETs) [14]. The bibliography used definitions and characteristics to explain differences between challenges and design features associated with infrastructure based, mobile ad-hoc (MANET), vehicle ad-hoc (VANET), and FANET communications.

Several portions of Bekmezci et al. [14] encouraged node distributed, ad-hoc computing and/or control mechanism research for Air Force applications. Communication through infrastructure was discouraged by Bekmezci et al. [14].

Some authors preferred to propose several new tools to develop traditional optimization approaches [19], [20]. Choi et al. applied optimization to balance energy loss due to communication and maneuver power requirements [19]. The function to maximize efficiency, however, had no closed form. Choi et al. formulated a closed-form approximation by employing the Taylor expansion [19].

The unique heuristics in Crawford et al. [20] were inspired by firefly lights and honeybee foraging. Application of metaheuristics to the set covering problem was proposed for teams composed of many adjacent robots. Although Crawford et al. used a lighthearted approach to develop new tools, the complexities of the algorithm were also problematic, as described in a separate article [21].

An optimization topic that engineers have explored is safety constraint handling due to “forbidden regions [22].” Defined by assignment, forbidden regions are regions to which visitation presents any type of unsafe operation or poses an unsafe constraint to the system [22]. The relationship between safety and Air Force interests is self-explanatory, but DOD continually has implemented policies indicative of safety and robustness concerns, according to Davendralingam [23].

The System of Systems (SOS) architecture framework in Davendralingam [23] explored the interdependencies, compatibilities, and time requirements that make individual systems more or less valuable in higher-level SOS architectures. For example, communication systems capable of connecting to up to four other systems, individual

systems that have commonly developed subsystems, and open systems all satisfy different constraints in Davendralingam's model. The governing rules are simplified from logical constraints, which were mined from manufacturing and development data [23].

In the area of communication, a successful experimental method has been that of a communication relay. Hansen, Pachter, Jacques, and Blue, in 2008 tested an important hypothesis: Hansen et al. proved mathematically that the midpoint between a stationary rover and the base was the optimum location for a communication relay [24]. The midpoint between the rover and the base is suboptimal during operations, because the midpoint is the ideal location which minimizes the radio frequency (RF) power required, only in the one-vehicle case and assuming that the rover is stationary [24].

Hansen et al. explained the utility of suboptimal methods with analytical solutions used as initial guesses [24]. "Using a geometric approach provides a suboptimal but easily implementable solution of the differential game [24]." Hansen et al. also recommended future work on the optimization topic, which instigated studies paving the way for the current body of knowledge.

Literature Search

In this review, the researcher searched for challenging problems that specifically addressed the use of communication relay systems to plan flights. The purpose was a desire to provide information to stakeholders, in particular, the U.S. Air Force. Authors who address the safe and effective operation of multiple-remote UV systems were well represented in the literature.

Like Bekmezci et al., Ali et al. published a scholarly bibliography [4], [14]. Ali et al. observed that there was a spectrum of robustness, which was determined by the general higher-level architecture [4]. Micro Unmanned Aerial Vehicle (UAV) applications for leader-follower, virtual structure, and behavioral approaches were discussed systematically. According to Ali et al., distributed, multiple-actor methods have grown popular for UV applications [4].

Lower-risk methods may need new tools that are emerging. Lower-risk methods were desired for fear that the ratio, or number of UVs a single human operator attempts to control, was approaching a saturation point. The ratio of the number of Small Unmanned Aerial Systems (SUASs) used in an architecture per human single-operator is rising [5]. This trend is not limited to developmental SUAS applications. A 2016 survey of civil applications found that infrastructure networks were employed for search and rescue operations using 1-8 UVs, and distributed ad hoc networks were employed using up to 50 UVs [25].

Hayat et al. provided an overview of key autonomy issues that promises challenges for multi-UV applications [25]. Autonomy was defined regarding UV networks as a multifaceted attribute of some systems [25].

“Device” (individual) and “Mission” (system) autonomy, both of which have a great impact on the communication demands of the aerial network...Device autonomy relates to the control of the UAVs and can be used to specify whether a UAV can fly autonomously or needs remote controlled (RC) navigation by a (human) pilot...Mission autonomy relates to the coordination between the entities in the network.

...For an aerial network, we define mission autonomy and corresponding traffic requirements depending on the [decision making entities (DMEs)] and the decision making process, as shown in Table 1, using a two dimensional decision matrix. We define the DMEs as either centralized or distributed, represented by

the rows of the matrix. The columns stand for the decision making process, which according to our definition can be either offline or online. The elements of the matrix describe the methods that can be adapted for the mission completion.

The level of autonomy in the network depends on a combination of entities and processes. An offline, centralized decision provides the least amount of mission autonomy, while an online decision, made in a distributed manner, ensures highest level of mission autonomy [25].

Table 1. Decision Matrix to Choose the Level of Mission Autonomy and Information Exchange (recreated from [25])

	Offline	Online	
		<i>Min Info</i>	<i>Max Info</i>
Distributed Individual	Telemetry	Telemetry	Telemetry Sensed
Distributed Consensus	Telemetry	Telemetry	Telemetry
Centralized		Coordination	Coordination Sensed

According to Clare, Cummings, and How, concerning the concept of operations for heterogeneous (air, sea, and land) UVs for all DOD systems:

A single operator will supervise multiple vehicles, providing high-level direction to achieve mission goals, and will need to comprehend a large amount of information while under time pressure to make effective decisions in a dynamic environment....The large amount of data generated by such a system could cause operator cognitive saturation, which has been shown to correlate with poor operator performance...at path planning [9].

While authors such as Hing [26] argued the potential for property damage and harm to civilians, Clare et al. instead made a performance-based argument [9]. The Clare et al. human factors studies focused their concerns on a mental workload saturation effect. Mental workload was defined as receiving no marginal benefit beyond a certain level, due to an inherent performance limitation [27].

The performance measurement model in Selva and Crawley [27] uniquely ranks architectures. The method is characterized by “handling large quantities of heuristic and subjective knowledge efficiently [27].” Although subjective measures are atypical for technical performance measures (TPMs), Selva and Crawley strove to apply a value-focused approach. Assessing value without TPMs indicated that Selva and Crawley sought to provide new development projects with a simplified alternative to traditional performance models [27].

At least two current studies indicated the desire for methods that are easy or convenient decision-support tools for a single operator to implement with multiple UAVs [15], [28]. Hitomi and Selva implemented agent based search experiments using combinations of computer and human agents [28]. Heuristic rules were included in the search algorithm, such as adding randomness and throwing out superfluous information. Tools were recommended that could “reduce the cognitive load on the user,” “potentially improve the performance of human users,” and “potentially allow them to participate in the search for longer periods of time [28].”

The human factors studies differed from the rest in their perspective and concerns, regarding treatment of safety for civilians and property. Hing argued the issue:

Future applications for UAVs will take them into low-flying areas populated with obstacles and civilians. Increased situational awareness for the pilots and operators controlling those UAVs will most certainly help decrease the potential for crashes and thereby decrease the chances of property damage or harm to civilians [26].

Based on that literature, there is a research gap in understanding whether a communication relay is beneficial when utilized to raise the potential for a single operator

to monitor and maintain control of multiple sensors. However, the demand for information about autonomous control in real-time is greater still.

The researcher found that communication relay was a theme of importance throughout the field. Eight different studies shared in investigating optimal UV position (but did so with a broad focus) [6], [9], [19], [20], [22], [29]–[31]. Five studies called for future research in areas utilizing RF transmission and one or more relays [6], [14], [19], [30], [32].

The optimal position was desired—but was not especially well supported with flight test results, which provided scarce tangible support for theoretical findings. According to Clare et al.’s research, with regard to further options for the objective function, “further investigation is necessary and underway to derive the full set of objective functions that could be used in various application scenarios [9].” Lin and Li found evidence that the optimal-power level control policy of multiple relays could be achieved for multiple sources and multiple destinations [30].

Another study by Rosal proposed Gauss pseudo spectral methods of optimal planning [8]. Choi, Pachter, and Jacques described a novel differential game theoretical approach, also for planning control trajectories [3]. Choi et al. found solutions to the maximization problem, described previously, that balances two efficiencies (aerodynamic maneuvers and communication relay), but the results were not physically implemented [19].

Jodeh [29] modeled the optimal trajectory problem that minimizes the time of a drone receiving information from all passive nodes in a widespread sensor network. In “a number of flight tests and demonstrations [33]” following Jodeh et al.’s initial work

[29], the drone returned real-time information about terrain features to the control station. Crawford et al. produced algorithms for the similar set-covering problem described previously [20].

Despite the breadth of control optimization algorithms, calculation of an advantageous relay waypoint location on realistic terrain, in the midst of small UVs, is a specific and complex problem. This problem was also featured in the literature. The convex form of an optimization problem to find the efficient number of robots needed to surveil an area, containing forbidden regions, was programmed in Arvelo, Kim, and Martins [22]. Although it was convex, the solution was non-trivial. Convex forms, in particular, are known for their suitability for precise and real-time path planning problems. Arvelo et al. formulated the restricted space problem using the element of time. Within parametric equations, states in the restricted space were held constant [22].

Tanil, Warty, and Obiedat detailed an optimized genetic algorithm for planning multiple, simultaneous trajectories around obstacles in two dimensions [6]. Tanil et al. adapted the UV cluster (up to six UAVs) for simulation to coordinate the area coverage problem in unknown environments. Stochastic paths, time synchronization, and spatial de-confliction were used to meet the requirements of collision-free area coverage and arrival at the simulation's end with the same total flight time. The results showed that intra-flight communication succeeded, even in obstacle-rich environments [6].

While optimal relay positioning was studied, emerging research was only partially successful at making flight test results available. Kim, Kwon, and Seo collected empirical data, providing tangible support for aerial unmanned support vehicles; they flight tested the prototype system performing path planning around obstacles for three-

dimensional (3D) motion capture [31]. Kim et al. used two aerial assistant UVs in a stereovision configuration. Since no relay was used, the pair of UVs had no capability beyond the base-to-UV's line of sight.

To summarize relevant peer-reviewed work, recent research was compartmented for each article within optimization or communication relay topics. The authors presented many unique topics related to cooperative control. There was a trend toward distributed, multiple-actor methods.

Potential methods of exploiting technology were not typically implemented in low- to moderate-risk flight tests. “Application to a problem with the vertical dimension,” Tanil, Warty, and Obiedat wrote, “would compose a useful future study [6].” Why four relevant optimization studies avoided implementing their results, physically, was never fully explained [4], [19], [21], [29].

In 2015, Hitomi and Selva developed a unique experimental method of formally investigating heuristics [28]. Heuristics methods follow paths used in the past to initiate the next new search at an open point of approach, for further improvement [34]. Hitomi and Selva investigated “hyper heuristic” methods to integrate humans with computer routines [28]. That experimental system included humans inside the system boundary, providing, gathering, and ranking possible architectures, using combinations of heuristics. In a broad sense, heuristics helped adapt computer assistance for operators dealing with information.

Within AFIT, one thesis included a view of moving toward eventual unification into a fail-safe control architecture for BLOS [16]. Shuck observed that, as of 2013,

open-source autopilot projects were still evolving and maturing [7]. These insights suggest a somewhat unstable hardware and software baseline in the COTS market sector.

Design and Implementation of Architecture

In 2015, Gray [5] architected and integrated a multi-UV system, which he envisioned for a collection of common DoD missions, including communication relay. Some improvements Gray recommended, based on his research, were: “further developing the system to utilize a closed loop controller, investigating other methods of determining the commanded position sent to the follower, and investigating the addition of more vehicles [5].” Extensions that Gray also recommended were: “close formation flight with other aircraft, relaying communication around obstacles and across long distances, and surveying or searching a long perimeter or a large area for a target of interest [5].” This research effort builds on his ideas by adding more vehicles and extending the architecture to include communication around obstacles.

System boundaries and multiple vehicle responsibilities were well-defined in Gray’s system architecture [5]. Only the COTS hardware and software needed, to force the path of communication from the GCS through the relay vehicles to remote vehicles, were included; most has been reused in this research. In Gray’s architecture, the relay vehicle stored an accurate and precise, relative physical location of the remote vehicles at each time step. The remote vehicles were responsible for transmitting and receiving all telemetry relayed to them from the GCS.

Gray included heterogeneous and homogeneous UV use cases [5]. The use case for communication relay is tersely defined as:

An operator desires to have a relay vehicle pass information between a remote vehicle and the GCS. The primary actor is the GCS operator. The operator determines the mission trajectory for the remote vehicle to complete. The GCS operator saves the mission to the remote vehicle's autopilot. The GCS operator launches the remote vehicle. The GCS operator commands the remote vehicle to initialize a loiter maneuver. The GCS operator launches the relay vehicle. The GCS operator commands the relay vehicle to initialize a loiter maneuver. The GCS operator initializes the relay C2 mode on the GCS. The GCS begins sending commands to the relay vehicle to continuously stay at the desired position relative to the remote vehicle. The GCS operator commands the remote vehicle to start the mission. This process ends when the mission is complete, when the GCS operator commands each vehicle to return home, or to be recovered [5].

Verification and data collection in Gray's predecessor thesis consisted of two tests. Two ground UVs (a relay vehicle and a remote vehicle) comprised Test 1. A multi-rotor aerial UV relay vehicle and a ground UV remote vehicle comprised Test 2. Outputs included the calculated destination, as a fixed point, to send the relay vehicle and the observed flight path. The results demonstrated that multi-UV systems implemented with COTS components, could exhibit effective control to accomplish multiple missions—especially when utilizing a unified architecture as the system foundation [5].

Positioning accuracy has already been measured. During Gray's communication relay test, when the vehicle arrived at a midpoint destination, the mean position error was 9.8m, and the root mean square (RMS) position error was 11.6m [5]. These values are conservative, because all communication nodes were manipulated in the test to force the GCS to lose and then reacquire the communication link [5].

A final topic was Gray's identification of particular difficulties affecting research methods similar to those used in this research effort. For one, Gray found that the autopilot unexpectedly drove the remote vehicle far out of range from the GCS during

flight. That problem drove errors in the positioning algorithm. The problem was never corrected, and as a result, there were spikes in position error in the communication relay test results [5].

Summary

Path planning BLOS has certainly been studied and may become a standard architectural component. When the obstacles are addressed, research that implements solution algorithms will fill a gap in the literature. The system may utilize knowledge received, relying on communication via relay; that is one solution to this research problem. To the best of this author's knowledge, this paper implements a unique method and unique flight test of an SUAS relay around obstacles and in a multi-UV system, based on an existing command and control architecture.

III. Methodology

Overview

This chapter describes the method used to simulate and implement a cost minimization algorithm for an existing architecture, Gray's [5] Unified C2 Architecture for teams of UVs. This research extended Gray's architecture, in that it generalized Gray's two-vehicle communication use case to alternative scenarios with additional vehicles and obstruction elements. Therefore, physical hardware implementation was accomplished with minimal change, relative to the predecessor study at AFIT. The significant change was the additional UV(s).

The formula for the minimization problem includes the explicit cost function and the calculated inequality constraints. Those constraints depend on the independent variables; up to nine feasible regions were observed during the research timeframe. Increasing the node distance downrange from a relay increases the immediate communication cost in a distance-squared relationship. The cost function is given as:

$$f = \sum_{i=1}^N (\overline{EO_i})^2 \quad (1) [35]$$

Where:

N = number of nodes produced by remote vehicles plus the home base station

E = relay position from which downrange distance to nodes is measured

O_i = node point location corresponding to a remote vehicle or the home base

The extension of functionality into more realistic terrain, in the midst of small, coordinated UVs, is a specific and complex problem. To answer the investigative

question, “What is an appropriate and effective means of autonomously positioning a communication relay in order to maintain the communication link between multiple vehicles and a ground control station?”, an adjustable simulation was conducted within MATLAB. Elements could easily be created, destroyed, or modified. The other investigative questions were answered by conducting short flights test using an SUAS communication relay.

Algorithm development followed a deterministic, local-optimum method, which required an intimate relationship between the automated positioning script, and numerical geometry. For a two-dimensional (2D) problem, sweeping or casting algorithms require more processing power and memory than determination of hidden and visible regions. A regional search method, to determine the visible regions in a scene analytically using geometry, is a process that has been around a long time and, being simpler, requires less sophisticated programming techniques than sweeping or casting in real time.

Obstacles were defined as forbidden regions in the battlespace. A circle was used to approximate each obstacle, representing the cross-section of a generic structure like a water tower or building. The implicit assumption was obstacles of infinite height and finite diameter. The researcher set up adjustable levels representing UV quantity and number and size of obstacles. The researcher then combined these into scenarios or “scenes” and used them to collect data.

Data Sources

The research method evolved in stages: (1) development of the algorithm in MATLAB and Python 2, (2) ground test—including static simulations and a brief

software-in-the-loop integration test, and (3) field data collection—including two flight tests and follow-on dynamic simulations were accomplished. Flight test scenarios were controlled to reduce risk while answering the investigative question, “What is the effect on system performance, due to combining algorithmic local minima positioning with a heuristic approximation of the optimal positioning algorithm?” The data were collected by propagating telemetry information through the relay vehicle, to and from the GCS and ground vehicles. Additionally, flight tests enabled a critical analysis of the data against the investigative question, “Given an environment obstructed by obstacles, what is missing from established performance measures for quantitatively assessing aerial radio-frequency relays?”

Ground Test Configurations

In Table 2, a matrix shows the developmental test case design. There were two controllable variables: number of obstacles and number of nodes (multiple nodes with two obstacles as opposed to multiple nodes with a single obstacle). It was hypothesized that the interactions between independent variables would have a significant effect at the design levels prepared for the last two columns.

The algorithm design allowed the software routine to accept an arbitrary number of N nodes. Due to time constraints, the design only allowed the software routine to accept one or two obstacles, although generalizability was desired. Extension to N obstacles would be extremely complex. Extension to two obstacles, however, makes little difference to the design variables’ definitions and mainly affects computation of the constraints of the problem.

Table 2. Test Cases with Computational Inputs

Scene #		1 or 2 Obstacles	Node Count
1		1	2
2		1	3
3		2	3
4		2	4
5		1	4

Flight Tests

The SUAS response and overall performance of the positioning script, the enhanced cost minimization algorithm, was determined by conduct of two brief flight tests. For the first test the single obstacle was placed at a predetermined coordinate out of the way from the system; the system demonstrated performance related to centroid following behavior. For the second test, the single obstacle was placed in the midst of the system nodes; the system demonstrated performance related to line of sight and no-fly-zone avoidance. The configuration for flight tests was Scene # 2 in Table 2, shown in Figure 1.



Figure 1. Scene #2 in Table 2.

Dynamic Simulation Tests

Dynamic simulation testing was used for characterizing best-case performance of the positioning script upon simplification of the test environment. This provided insight into how the algorithm performed in the absence of wind and other factors affecting GPS errors. Dynamic simulations to replicate flight tests and correct shortcomings in the algorithm were performed after flight test findings.

A notable difference in the control implementations for flight tests and dynamic simulation tests might have affected the results insofar as the obstacle could deny the algorithm perfect knowledge of where the system nodes are located. The relay positioning script for flight test allowed previous known locations for rover UVs to persist, if the true coordinates were unknown. The simulation, however, had perfect knowledge of node locations at every time step.

Dependent Variable

The response data needed for analysis in this research was the SUAS relay's response to the whole system, captured as telemetry from the quadrotor vehicle or MATLAB arrays from the simulation. The researcher also timed the algorithm's execution while the simulation platform was solving relay placement. This timing was performed to ensure adequate, near-real-time implementation capability.

After timing was recorded, a statistical summary of other performance metrics was developed for all tests. The statistical summary was related to the telemetry data as follows: the cost function (Equation 1) was evaluated at experimental relay position E, once per time step. The cost function was also evaluated at theoretical centroid position M, or average position of all available nodes, at the corresponding time steps. Then, the experimental results were expressed as a ratio at every time step over the theoretically optimal results. An additional summary data point was collected, which was the cumulative frequency of node visibility, in terms of outages that were detected through data post-processing. A centroid distance calculation for actual flight test data will be described subsequently.

Centroid Distance Calculation

During flight test, the theoretical centroid position was measured in Latitude Longitude Altitude (LLA) [degrees], rather than in the Cartesian frame. An alternate form of the statistical summary for flight test data was used. In post-processing, the researcher normalized observed flight paths to Euclidean distance (in radii). The local relay's link efficiency was evaluated by the distance to the system centroid. The normalized distance between the relay position and the system centroid is given as:

$$dist_{\angle} = \frac{\|\vec{EM}\|}{m_a} \quad (2)$$

Where:

M = system centroid coordinates

E = relay coordinates from which Euclidean dist. to system centroid measured

m_a = normalizing constant

Numerator calculation, once per time step, yielded a scalar value, which expressed GPS in normalized relay distance to the centroid, using the norm of Cartesian coordinates. The vector from E to M was calculated by subtracting components pairwise, e.g., translated latitude 1 – translated latitude 2, etc. A larger numerator represents a greater distance to the experimental relay position from the theoretically optimal position. The denominator, which was the normalizing constant, took an arbitrary scalar; for m_a, an estimate was used of the maximum distance between E and M. That maximum distance was the diagonal of the rectangular battlespace per the problem definition.

Node Visibility Calculation

After the test, the researcher decomposed observed flight paths to understand the ground UVs' telemetry. LOS to the relay was counted across the test timeframe. The cumulative relative amount of outage equals the sum of all seconds of outage divided by the length of the test.

Notation

Figure 2, below, represents an overhead view of the two-dimensional battlespace. Conceptually, a successful communication relay extends the reach of command

transmissions, from the house, exchanged with the friendly UVs downrange. The relay also helps telemetry, from the UVs, reach the house. Without loss of generality, the home base appears at node B. In fact, nodes usually are not specified in the software routine as UV locations or home base locations.

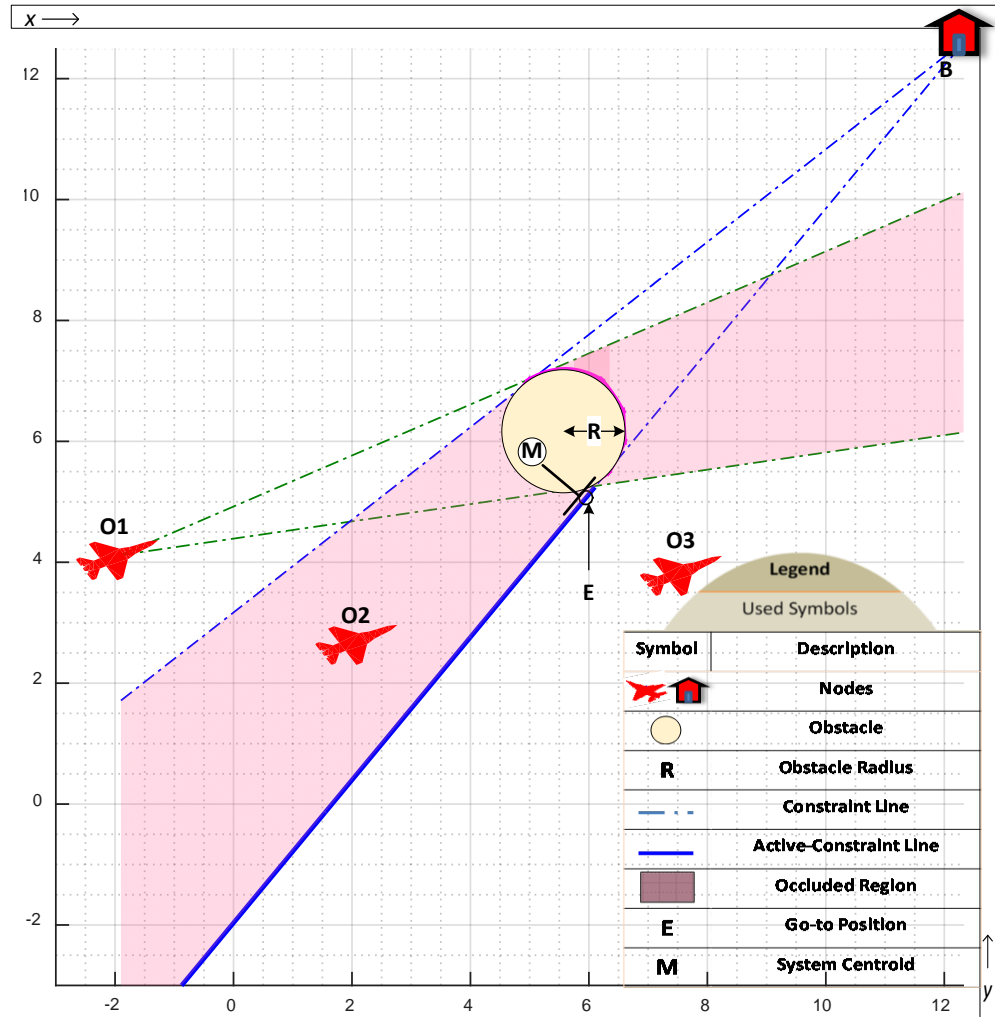


Figure 2. Operational View of Obstructed Communication Link.

Go-to positions like E were defined as finite, discrete placement options for the relay at a snapshot in time, which implies an assumption that the elements of the

battlespace are momentarily stationary. Go-to positions are also referred to as *feasible vertex* points and, in guided mode, *go-to-here command* points.

Nodes like O1 or B were defined as point sources that communicate messages straight to the relay and remain at similar elevations above ground level. Occluded regions were defined as part of the infeasible region within the battlespace. The lack of LOS from the relay to any node in that area would indicate a poor link, or no link, which means that a successful communication relay could not lie inside the shaded area. From an operator's perspective, it would be a poor decision to send the relay inside that area. There are two other boundary lines, not shown in Figure 2, which could extend each from O2 and O3; they were omitted to reduce the number of visual elements for a clean-looking operational view. O2 lies in the shaded area, because it is an obscured node from the point-of-view of B.

Point M is the centroid. M lies on a short vector, with tail at E, which is orthogonal to the active-constraint line as shown. That vector is associated with the Centroid Distance Calculation, Equation 2. For communication cost efficiency, a shorter vector is better.

Relay placement entailed executing the operational mission with an operator manually commanding the remote vehicles, the cost minimization algorithm running in a loop in the background, and Drone Kit delivering relay coordinates in Guided mode without operator intervention. The Python code used to command the SUAS relay will be made available electronically at AFIT. A paper describing the numerical, geometric basis of the algorithm can be found in Appendix A.

Simulation Process

During simulation tests, loop frequency was not an issue; the real-time aspect of flight test will be described with the flight test results in Chapter 5. Some parts of the simulation process were necessary modifications that were not implemented in flight test. These will be explained with the dynamic simulation results in Chapter 4.

The maneuver waypoints and sub-optimal or local minimum solutions, produced by the enhanced placement algorithm, contain the UV position, bearing, and velocity. The vehicle movements were ruled by this behavior. Waypoint information is produced from the following simulation process:

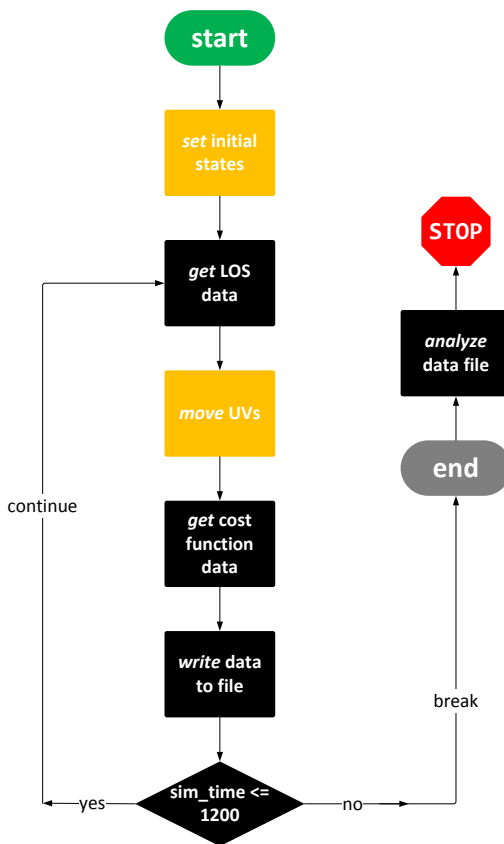


Figure 3. Level 1 Flow Diagram.

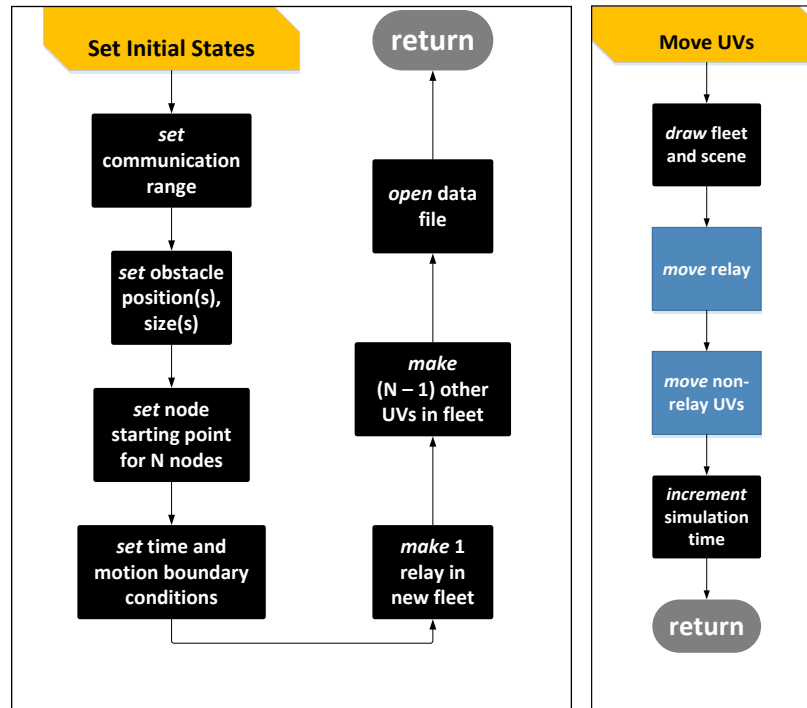


Figure 4. Level 2 Flow Diagrams.

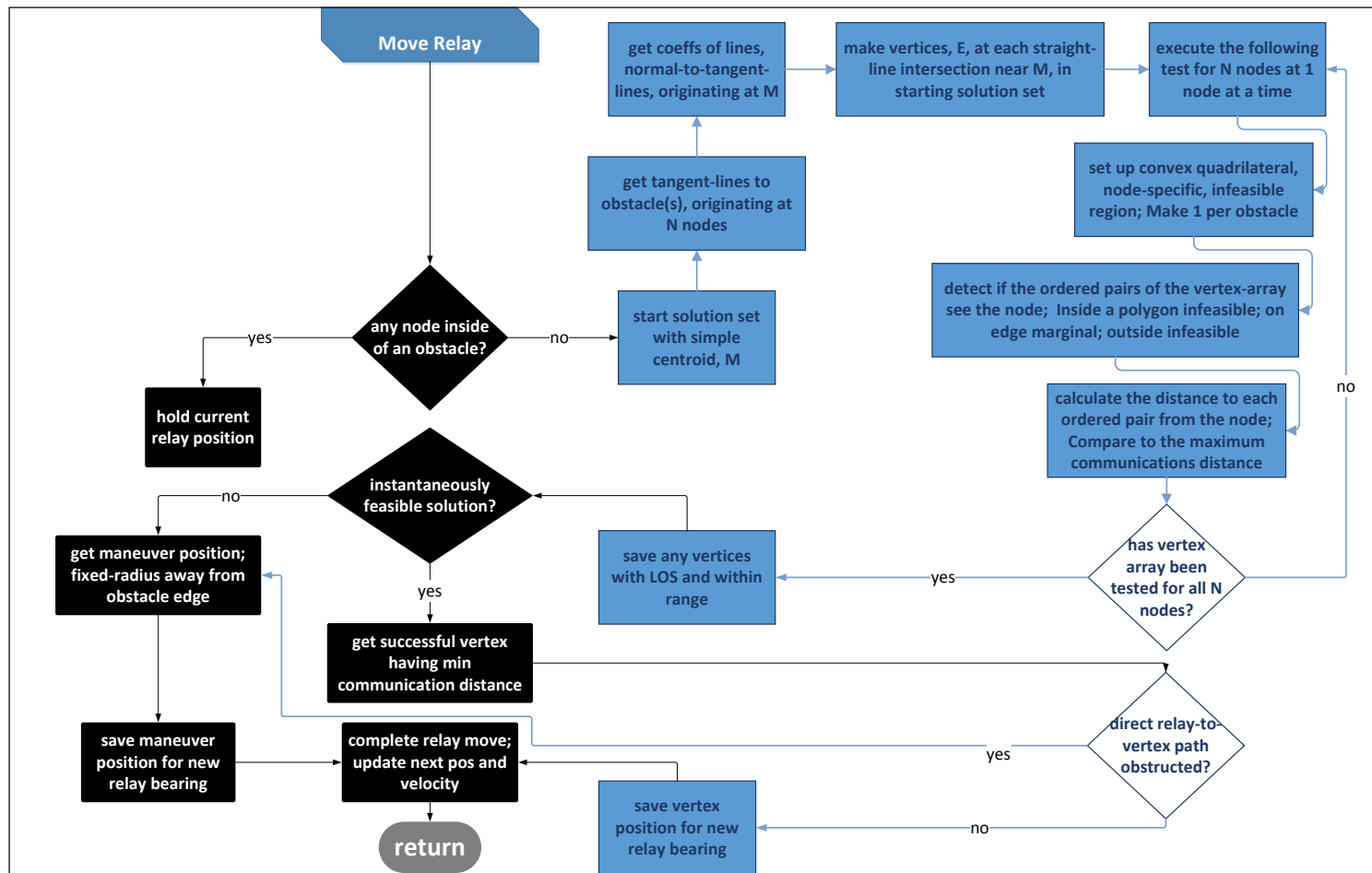


Figure 5. Level 3 Flow Diagrams, Part I.

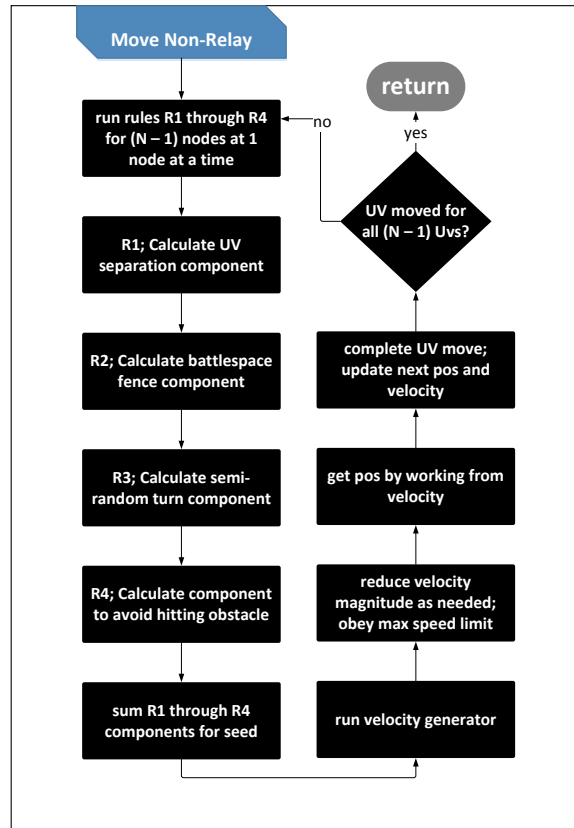


Figure 6. Level 3 Flow Diagrams, Part II.

Another option in the event of no instantaneous solution would be to hold the relay's current position. However, a position that is a fixed-radius away from the edge, of the obstacle that is nearer to the relay, prevents drift away from the vehicle driving area. If the relay was close to an obstacle, the maneuver also provides more separation.

Architecture

Gray [5] describes the architecture for the desired system. This section incorporates the reused and adapted architectural design at a high level; repeating low-level function descriptions and decomposition diagrams is avoided. All View (AV)-1 summarizes the vision and purpose of the architecture as:

The vision for...Unified C2 Architecture for teams...will allow the operator to control a team of autonomous vehicles to perform cooperative missions scenarios. These scenarios include performing formation flocking and performing communication relay. ...The purpose of this system is to provide a single operator the ability to control a team of multiple homogeneous and heterogeneous vehicles to accomplish missions requiring formation flocking or relaying communications through local vehicles [5].

Operational View (OV)-1, below, depicts the relay local vehicle position using one remote vehicle, whereas Figure 2 depicts generalization to account for multiple vehicles.

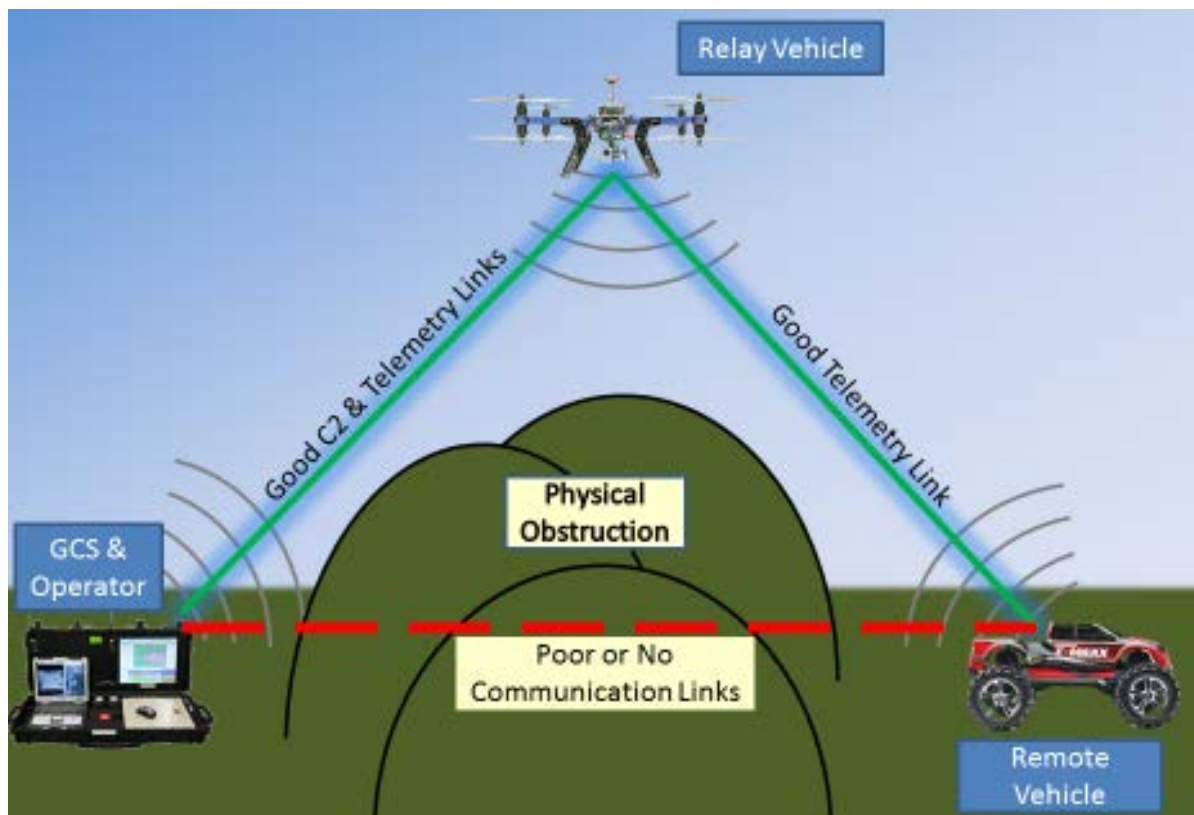


Figure 7. OV-1: Communication Relay for Single Vehicle [5].

Operational Activities

System operations are allocated to GCS & Operator, SUAS Relay Vehicle, and Unmanned Ground System (UGS) Remote Vehicle swim lanes. Communication operational activities (Send/Receive) affect all swim lanes. The GCS and operator are responsible for C2 operational activities, such as Command launch; Start positioning script; Calculate desired position of Relay Vehicle; Command go-to-here location; Write mission plan to autopilot; Command recovery, etc.

		System Function (SV-4)												
		Perform Command	Send Command	Receive Information	Send Information	Pass Information	Write Mission	Plan Mission	Perform Calculation	Display Information	Move Vehicle	Perform steady level movement	Provide Navigation Measurement	Receive User Input
Operational Activities (OV-5a)	Perform launch	X												
	Perform Recovery	X												
	Perform idle maneuver	X												
	Perform go to location	X												
	Perform stored mission	X												
	Command go to location		X											
	Command start mission		X											
	Command perform cooperative activity		X											
	Command idel maneuver		X											
	Send command		X											
	Receive telemetry			X										
	receive command			X										
	Send telemetry				X									
	Pass telemetry					X								
	Pass command					X								
	Write mission to autopilot						X							
	Plan Mission							X						
	Calculate desired vehicle 2 position								X					
	Provide visual information									X				
	Propel vehicle										X			
	Maneuver vehicle										X			
	Maintain steady level movement											X		
	Provide GPS solution												X	
	Receive user inputs													X

Figure 8. SV-5a: System Function Traceability Matrix [5].

Table 3, below, describes common activities performed by each type of vehicle.

Gray has already mapped the operational activities to lower-level functions, and he

produced a traceability matrix to ensure each system function is carried out by a system element [5].

Table 3. Activity Descriptions by Vehicle Type (adapted from [5])

Activity	Action by UGS	Action by SUAS
Perform Launch	Start driving.	Initialize propellers. Lift off the ground and hover at designated altitude and position.
Perform Idle Maneuver	Stop driving.	Stabilize and hover at the current location.
Perform Go-to-here Location	Drive by stick inputs to the location and perform an idle maneuver.	Fly by GPS guide to the location and perform an idle maneuver.
Perform Recovery	Start driving and drive by stick inputs to the landing location. Stop driving.	Start flying and fly by stick inputs to the landing location. Reduce altitude and speed. Touch down. Stop propellers.

System Elements and Interfaces

“The System View (SV)-1 is a graphical representation of the physical architecture. This representation displays the allocation of components to sub-systems and the information exchanged between components [5].” Figure 9 narrows the SV-1 scope to a view of the desired communication system. Additionally, without loss of generality, Figure 9 uses the name “UGS” instead of the agnostic term, “Vehicle 1.” Since this research is focused on the communication link, each element depicted is either directly responsible for a portion of the communications sent and received by the system, or is required to enable another element in the accomplishment of communication.

According to the SV-1, the operator provides inputs to the GCS and receives feedback from the GCS software via the display. The GCS and RC transmitter send commands. The GCS receives telemetry from each vehicle through the networked communication nodes. The infrastructure uses the GCS communication transceiver on a network with less powerful vehicle transceivers. The SUAS requires a split port allowing only commands addressed to the vehicle to reach its autopilot, while allowing the GCS software to use GPS position addressed to the GCS computer, so that the GCS computer may display the information to the operator.

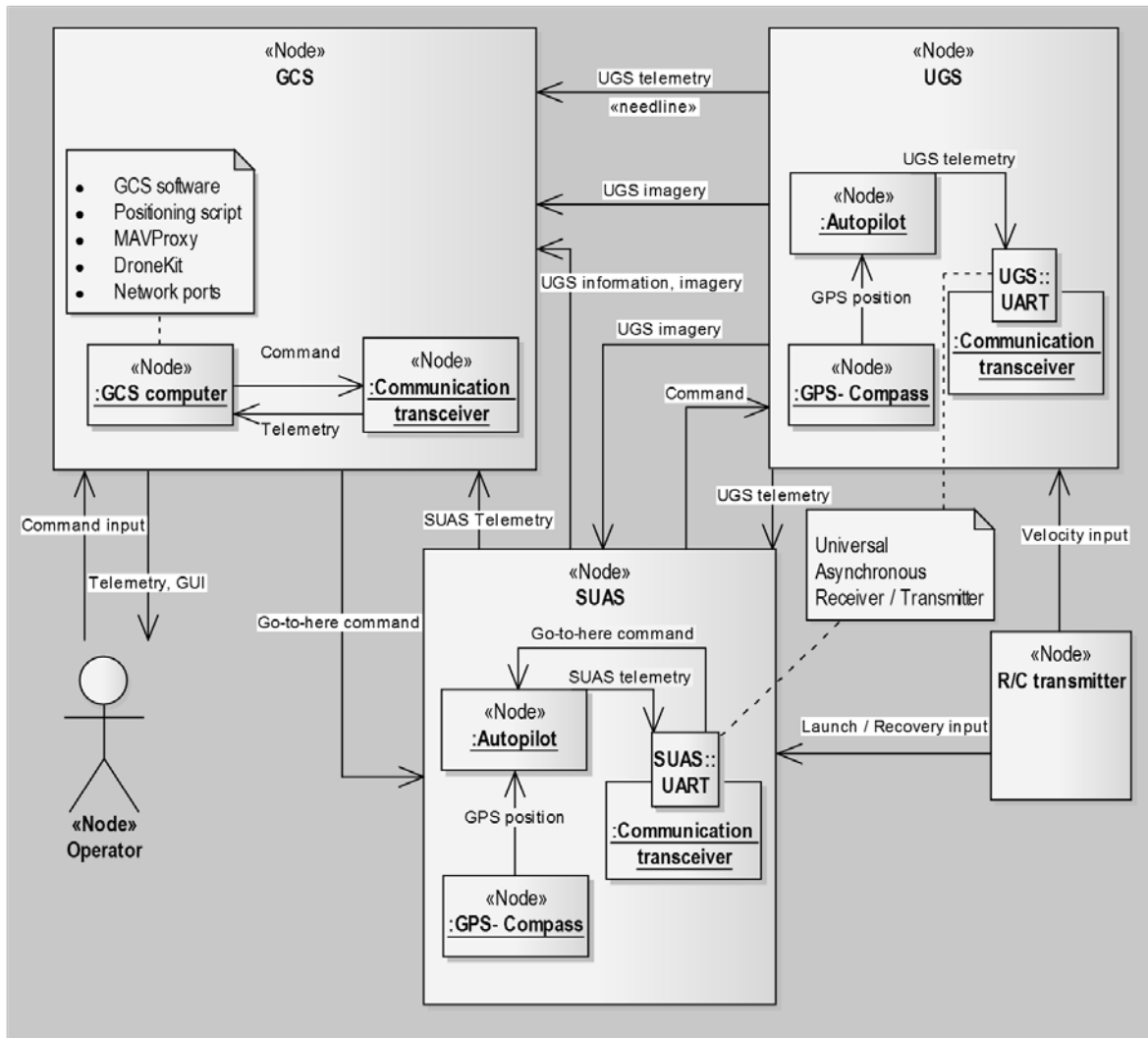


Figure 9. SV-1 Systems Interface Description Focused on Communication.

Hardware



Figure 10. The quadrotor vehicle used for the implementation in this chapter. Details on the specific hardware in Table 2.

Table 4. Hardware details

Component		Description
Multi-rotor vehicle		3D Robotics X8, COTS propulsion components
Avionics		Pixhawk and current firmware
Power source		4S 10,000 mAh LIPO battery
Mission equipment		Wave Relay MANET node, 3DR GPS/compass
Safety component		FrSky RC transmit/receiver

For the GCS, a 10/100Mbps Ethernet connection provided communication between the laptop computer and the Wave Relay ground antenna. The system used Transmission Control Protocol (TCP) above Internet Protocol (IP) and split the SUAS

address into two port numbers. One instance of the SUAS address was a DroneKit input, while the other was a Mission Planner input.

Coordinate Frame Transformation and Scaling

The scaling framework in the Cartesian frame normalized distances relative to the obstacle radius. This method allowed for the flexible use of optimization to calculate the SUAS' next position. For flight test, the researcher integrated a coordinate frame transformation utility into the Python script. This method allowed for the use of GPS coordinates in degrees, enabling compatibility between the algorithm and DroneKit. The value used for the radius of Earth was 6,371.0087714 km.

Local Minima and Heuristics

The formulation of the constraining obstacle as an infinite vertical cylinder allows for analytical treatment of the problem, so that the algorithm can exploit local minima and heuristic solutions.

A less conservative formulation would be to allow the SUAS to ascend to a safe altitude and fly above the problem. However, that approach would lead to complex balancing based on the power cost of climbing maneuvers.

Timeline

The proposed timeline was to build a dynamic simulation prior to flight test. Times proposed differed from the researcher's actual timeline, because flight test must conclude prior to the onset of winter weather. The dynamic simulation developed as a facsimile of flight tests that had already occurred. As the simulation progressed through development, the researcher used the simulated environment to test system performance following a use case exception. The simulation achieved the original goal and a capability to implement use cases without weather interruptions.

IV. Results of Algorithm for Simulation

This chapter describes the results of the algorithm in the MATLAB integrated development environment. The researcher tested the single-relay algorithm in 2D, including optimal and heuristic positioning. The extent of this testing, if it had been accomplished using flight test, would have been prohibitively difficult within academic time constraints and under safety requirements.

Static Simulation

Static simulation took place during software development. Trials demonstrated software functionality; ultimately, each trial automatically produced cost-efficient local relay locations with verifiable LOS and feasible outcomes. Precise point outcomes validated that this system would meet the sponsor's need to rationally guide relay vehicles using rules. Documentation of systematic example trials appears in Appendix A.

The algorithm was tested by processing the data from 150 simulation trials. Processing included execution time measurement in scenes with potentially voluminous feasible regions. Table 5 shows that, if it were necessary, the algorithm could afford implementing a loop frequency surpassing 10 Hz.

Table 5. Execution Time Trials

Rank	Scenario	Median Elapsed Time [msec]
<i>1st Place</i>	<i>Scene #1</i> , 1 Obst. 2 Nodes	3.2
<i>2nd Place</i>	<i>Scene #2</i> , 1 Obst. 3 Nodes	3.8
<i>3rd Place</i>	<i>Scene #5</i> , 1 Obst. 4 Nodes	4.4
<i>4th Place</i>	<i>Scene #3</i> , 2 Obst. 3 Nodes	5.4
<i>5th Place</i>	<i>Scene #4</i> , 2 Obst. 4 Nodes	5.8

For a reasonable expectation that successful flight tests would be accomplished later, the beginnings of heuristic rules were required in early algorithm trials. Even pertaining to simple Scene #1 (one obstacle and one rover), the simple centroid is insufficient for two reasons. First, the centroid does not predict or preclude the undesirable times when the centroid's position lacks LOS to the GCS or to the rover. Second, the centroid does not predict or preclude an undesirable vector to the centroid's position, which passes through the edge of the obstacle and into the forbidden region.

The cost function was evaluated at feasible vertex points for all trials. The global minimum position was the centroid of the system nodes. Even if the centroid was in an infeasible position, it was used as the reference point, a 1.0 value for cost avoidance (see Figure 11).

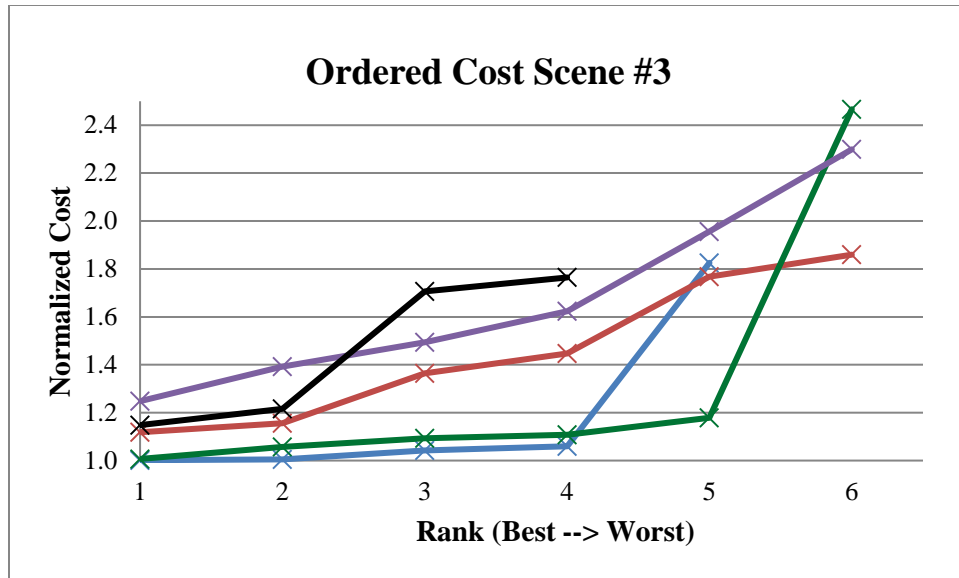


Figure 11. Communication Power Cost Avoidance for Five Trials.

A mapping of 10 trials onto the MATLAB solver utility, “fmincon,” confirmed that ranked point outcomes were the local minima for their respective feasible regions, based on Equation 1, the cost function. However, that mapping was not always necessary. In many cases, the centroid was a feasible location; the centroid was also the global minimum, and therefore the ideal case. Conversely, in few cases there were no feasible regions.

Dynamic Simulation

As described in Chapter 3, the research timeline put dynamic simulation trials after flight tests, based on the flight test opportunities offered by the weather. Ideally, the simulation-tested algorithm (written in MATLAB) would have been completed first. The first product would have been an input into the flight-tested algorithm (rewritten in Python 2). Then, the products would have been analogous to each other; however, new fail-safes were added under dynamic simulation. Chapter 5 will present the flight test

results, complete with the problems encountered, which the researcher actually resolved in simulation.

The researcher considered the integrated system, starting from the flight tests, as the baseline. From the baseline, the algorithm again was tested by processing the data after collecting for 20 minutes. MATLAB's "drawnow" function was selected to display vehicle movements during testing.

Cost Function Calculation

The researcher evaluated the cost function and calculated the relative visibility, or cumulative ratio of direct LOS uptime and downtime. The cost function was normalized according to the centroid's cost function values. The cost function results varied noticeably, depending on the semi-random initial states and driving of simulated rover vehicles.

In most cases, as shown in Figure 12, the single-relay algorithm in 2D performed satisfactorily. Viewing the vehicle paths from overhead, the relay path appears green, while the node paths appear red; the ground antenna node is always located at the origin. The rings around the node positions represent the nodes' positions when the simulation stopped. The relay path begins at the origin and follows the three nodes along the desired route to the system centroid.

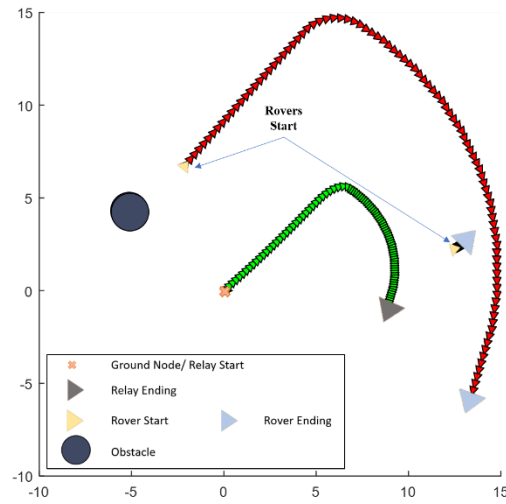


Figure 12. Simple Example of Dynamic Simulation Plot.

Figure 13 depicts the end of a sequence of events that led to an undesirable result. Three time markers were chosen to narrate each vehicle's movements during testing. In the case of Figure 14, the simulated relay performed well for the first 815 s, and then performance gradually declined. The average result was 1.5 times the function evaluated at the centroid.

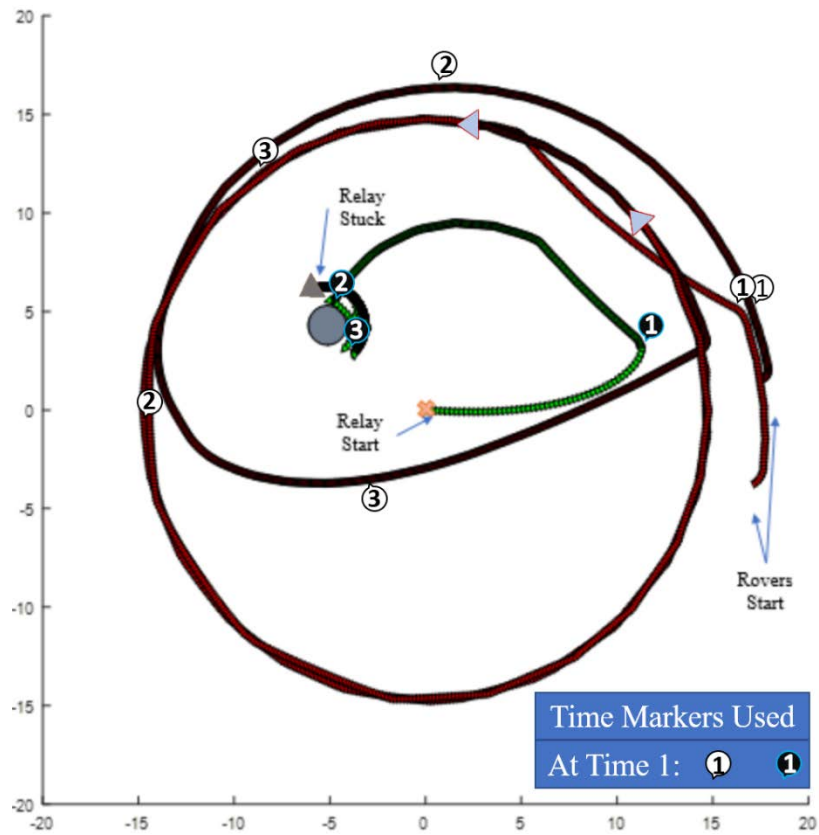


Figure 13. Overhead of Dynamically Simulated UV Paths.

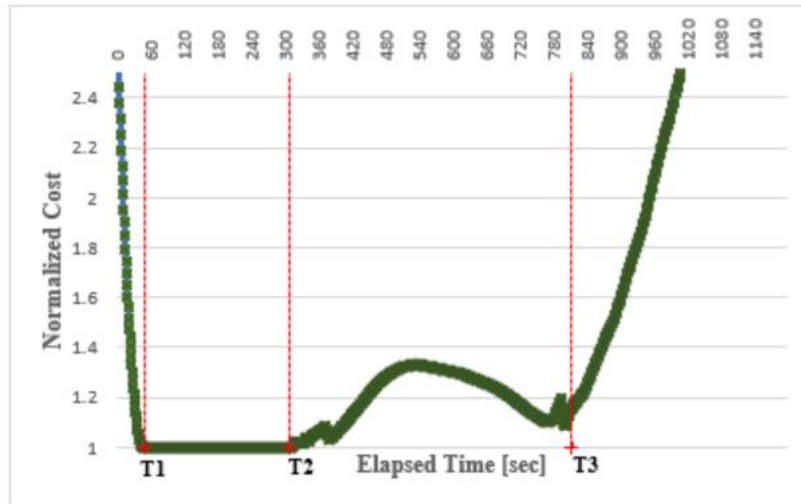


Figure 14. Communication Cost Function over Time.

Table 6. Sequence and Description of Events

Time Marker	Action of Vehicles before Time Marker
T1 50 s	The rovers drove toward the y-axis and away from the x-axis. The relay followed the desired path to the centroid of the three nodes.
T2 310 s	The rovers drove toward the opposite side of the obstacle from the ground node at (0, 0). The relay took the path that exactly followed the centroid.
T3 815 s	The rovers moved into the region occluded by the obstacle, from the relay's point-of-view. Since the centroid lacked LOS to at least one node, the relay took the path that circled around the obstacle with direct LOS to the ground node.
End	The rovers turned back toward the ground node, and the centroid regained LOS to all three nodes. The relay failed to turn back; instead, it became stuck. The relay did not recover by the end of the simulation.

Summary Table 6 shows the value a dynamic simulation's capability added by presenting many trials in succession. Using the results shown, the researcher caught mistaken logic. The relay shown above was programmed to avoid turning into the obstacle. However, the relay was not programmed to turn clockwise under the condition that a counterclockwise turn would provide a more direct approach to the centroid near (5, 8). Therefore, it spent time in one place, while performance gradually declined.

Node Visibility Calculation

Like the cost function results, varying depending on initial states and simulated driving, the node visibility calculation was variable. For the case shown in Figure 13, node visibility was 91.7% when taken by the average across all nodes. At 815 s, node visibility was 92.1%. This declining data set was the worst observed case: The simulated rovers' average visibility was 85.7% and 90.3%, respectively. The ground node's average cumulative visibility was more typical at 99.0%.

Table of Rules

As planned, the researcher developed solutions to problematic simulation results, using rules. The purpose of the following heuristics was enabling the algorithm to search for a better path than that which chance would generate from random UV progress.

Table 7 lists movement rules that underwent development after flight test ended.

Table 7. Table of Rules

<u>Idle maneuver</u> : If a node was inside the obstacle, the relay was commanded to hold its current position.
<u>Range</u> : A default range was assumed, but the user should use actual range if it differs from the default.
<u>Add randomness</u> : A semi-random turn direction was used to avoid a stuck relay.

Figure 15 and Figure 16 depict improved cost outcomes (which coincide with improved LOS metrics) due to the final increment of movement rules. The updated simulation handled the problem constraints better than the original. The comparison of

performance levels against flight test was imperfect, but it was included to emphasize that the flight test results, which will be described subsequently, had room for improvement.

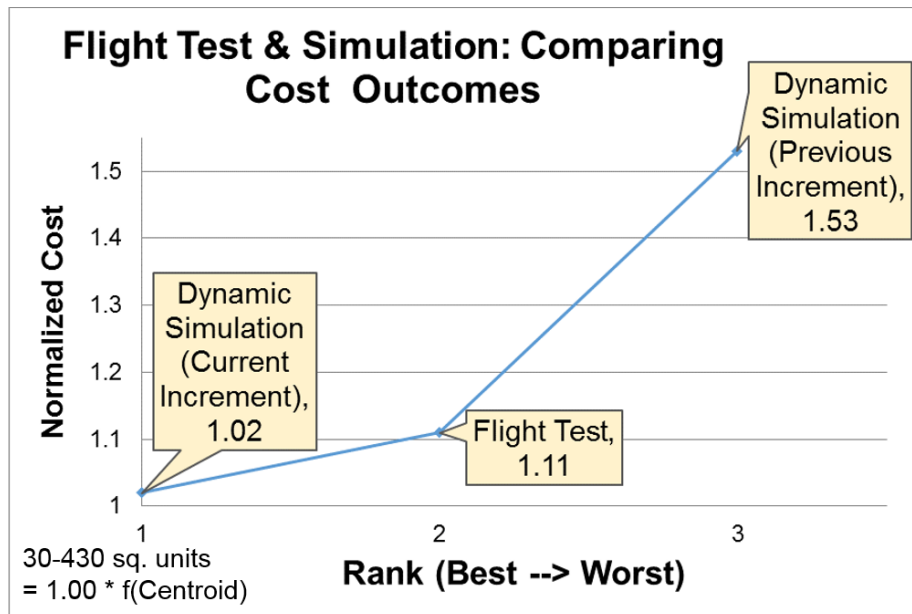


Figure 15. Comparative Cost Outcomes.

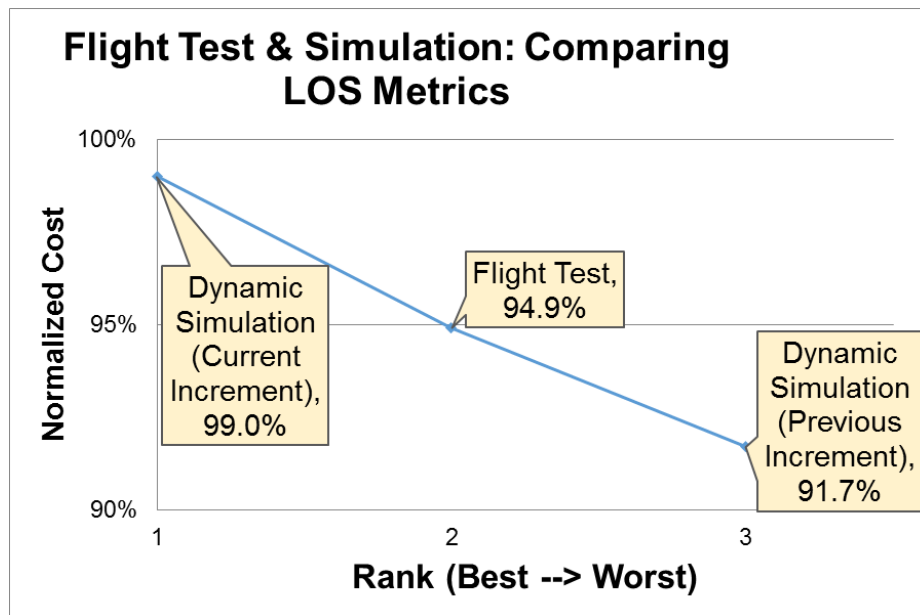


Figure 16. Comparative LOS Metrics.

Conclusion

The use case was implemented during a medium-sized sample of trial runs and 20 minutes of dynamic simulation. How much of *an appropriate and effective means* the cost-minimizing algorithm became, for autonomously positioning a communication relay to maintain the communication link, was clarified. Chapter 5 will continue with the results of algorithm implementation during flight test. The impact of this means of minimizing cost on the investigative questions will be described in Chapter 6.

V. Results of Algorithm for Flight Test

This chapter describes the results of flight test implementation. The use case relates to the flight test as follows: one extension includes multiple rovers, while another extension allows multiple rovers and includes one or two obstacles present. Thus, flight test consisted of two different set-ups including/excluding the obstacle as a factor.

Test Report

All major flight test changes for this research are described in Appendix B. Prior to flight test, the researcher made significant modifications to the test requirements described in Gray's [5] Test Project Technical and Safety Review documentation. This set of changes was necessary for unique flight-testing of an SUAS relay around one obstacle and in a two-UV system.

Obstacle-Free Centroid Test

In the first flight test, the no-fly zone was located well away from the system. Two drivers controlled the two rovers, which were moving at times and, at other times, briefly stationary. The rovers' speed while moving was below 5 m/s. The algorithm's purpose was to send the SUAS to the centroid of the system. The system contained three nodes: one home base and two rover UVs.

The loop frequency input affecting telemetry rates was approximately 6 Hz. The looped algorithm led the SUAS relay through a real environment using GPS for 3.4 minutes, including launch and recovery, leaving 74% of battery remaining. The researcher investigated GPS positions for the system, in relation to the cost function.

Additionally, using normalized GPS positions, the researcher mathematically verified unobstructed line-of-sight. The limiting factor to the calculations' accuracy was the coordinate frame transformation discussed in Chapter 3.

Average Distance from Nodes

As shown in Figure 15, the algorithm continually commanded the relay into the desired position at the centroid of the three nodes. The rovers' movement caused the centroid position to diverge from the relay's current position. After allowing the rovers to transmit GPS positions, the relay followed the centroid, as expected. While the rovers' increasing speed resulted in increasing relay distance to the centroid, the relay's path to its cost-minimizing, centroid position appeared to lag slightly, also as expected.

Figure 15 reveals apparent oscillation in the SUAS' heading, following the 60-second mark on the time axis. The wind had increased to barely within operating range (about 15 kts). Suddenly, the GCS computer displayed an "error position (horizontal) variance" alert, a red status message, and the Pixhawk's Extended Kalman Filter (EKF) label (see Figure 16). This incident demonstrated an unexpected offset between the magnetic compass and GPS signals. The rovers moved slowly for several seconds, and soon the relay had reconciled its commanded position and its actual position. This incident was resolved, and the test continued.

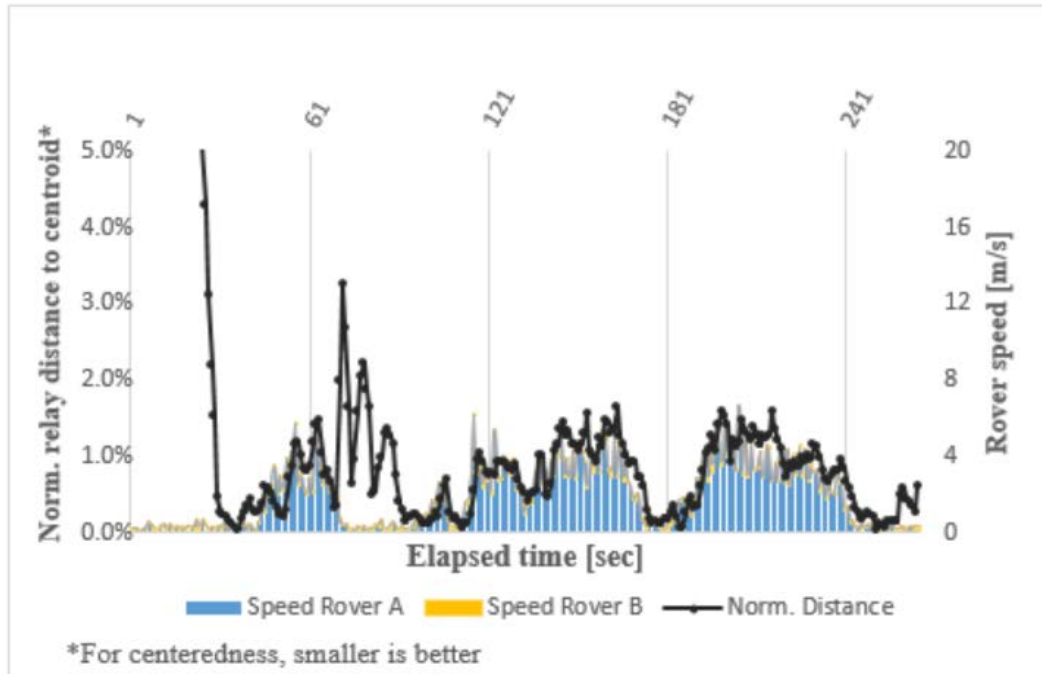


Figure 17. Relay Centeredness ($dist_{\Delta}$) and Rover Speed over Time. Part I.

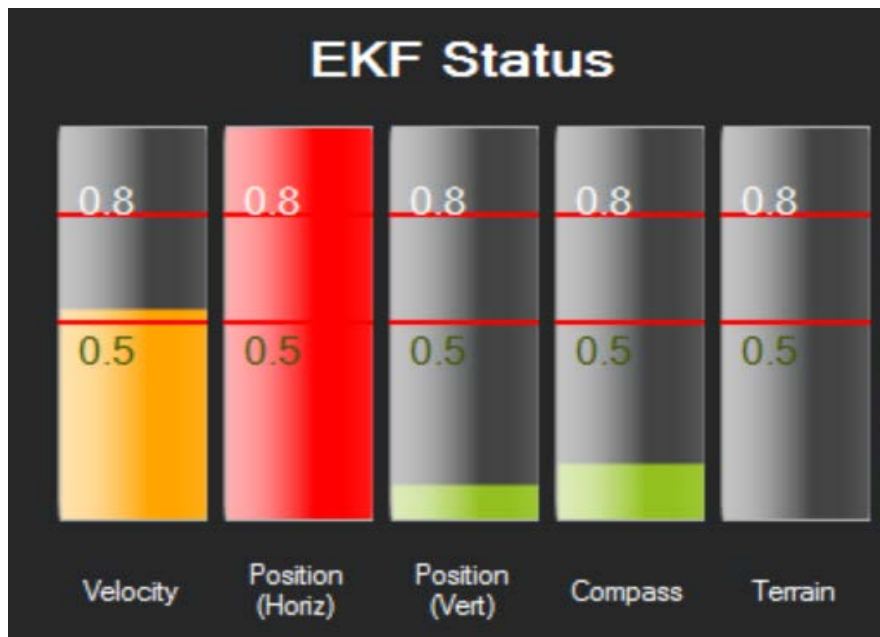


Figure 18. Horizontal Position Variance Alert in Mission Planner.

Node Visibility Calculation

Node visibility was 100%, meaning that the communication link retained all three nodes in direct LOS from the SUAS' point-of-view throughout the centroid test timeframe. 100% node visibility was expected without obstacles present, of course. However, the relay was observed unexpectedly changing direction when the relay flew straight above a rover vehicle; the response was minor and possibly due to an excessive loop frequency input. The researcher corrected the frequency between the two tests, by changing the loop frequency input from 6 Hz to 1 Hz.

Relay Positioning Test around Obstacle

In the second flight test, the no-fly zone was in the same operational area as the relay, the two rovers, and the ground node. The loop frequency input affecting telemetry rates was decreased to 1 Hz, to improve stability during the more difficult test. The algorithm was the same as before; only the problem configuration changed to reflect a more challenging scenario.

The size differential between the SUAS and the virtual obstacle was more than 300%. The field obstacle covered a circle 7.5 m in radius. A satellite image, Figure 17 below, shows how these dimensions translated on the flight test range.

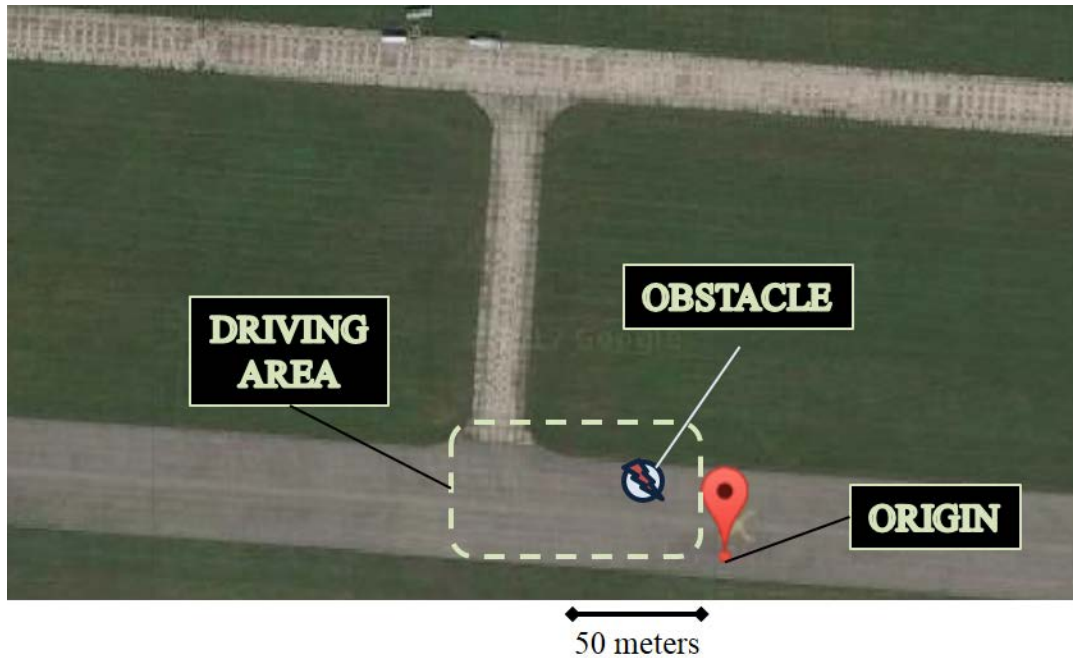


Figure 19. Flight Test Set-up with Obstacle.

The algorithm corrected nodes that were occluded by the virtual obstacle from the SUAS point-of-view. It also identified advantageous cost function contours at feasible positions. The algorithm issued commanded waypoints as a corrective action, or else the SUAS stayed on its current cost function contour while no corrective action was needed, as presented in Figure 18. The bad LOS calculation, defined later in this chapter, accounts for the discontinuity in the graph below, at around 104 s. A normalized relay distance to the centroid of 0.5% equals about 1 m error.

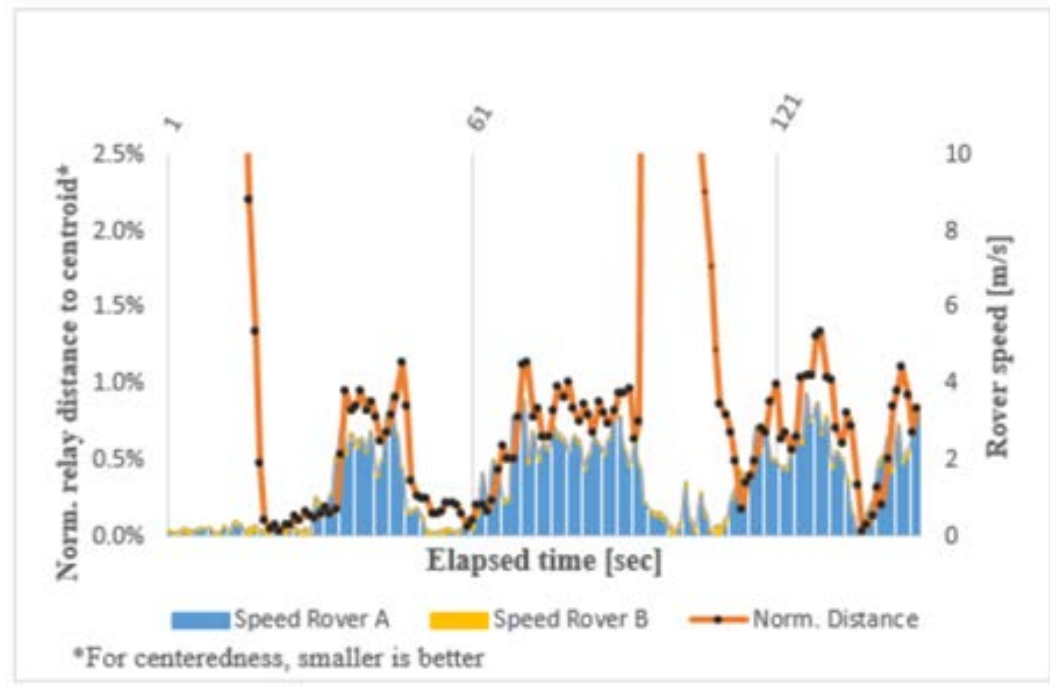


Figure 20. Relay Centeredness ($dist_{\angle}$) and Rover Speed over Time. Part II.

One driver controlled both rovers, independently; Rover B remained stationary and continually communicated its current position (a node). A top view of the 3D path of the SUAS flight is in Figure 19 below. The SUAS relay (autonomously) and Rover A (under manual control) travelled in the direction of the arrow; Rover B and the Ground Node were stationary.

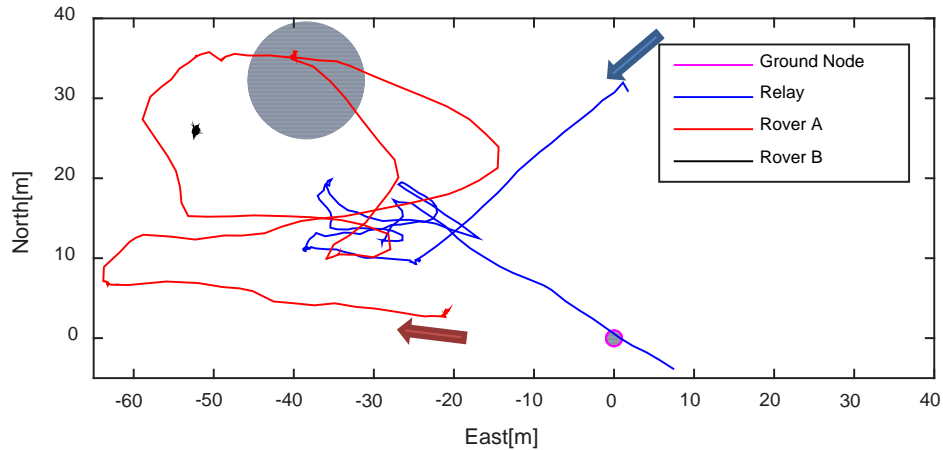


Figure 21. Overhead of Relay Following Algorithm Commands.

Rover A started driving from $(-21.0, 3.4)$. The relay flew smoothly to $(-24.7, 9.3)$ to start following the centroid towards the West. When Rover A's GPS position solution found that the rover had driven through the obstacle and out the other side at $(-44.7, 35.3)$, the relay was at $(-19.4, 14.4)$, farther to the Southeast than expected. However, the algorithm commanded the relay back to the Northwest until the relay reestablished direct LOS with Rover A.

Notice that even though the obstacle radius was 7.5 m, the SUAS stopped approaching the obstacle upon arriving at a buffer zone at $(-35.3, 19.9)$. Without position errors, the zone would have its edge at exactly 3 m from the obstacle edge. That buffer was deliberately programmed at $0.4 * \text{radius}$. After the relay reestablished LOS with Rover A, the system performed as expected for 55 s.

The looped algorithm led the relay through the real environment using GPS for 7.5 minutes, leaving 66% of battery remaining. Node visibility was 94.9% when taken by average of the averages, which will be described subsequently. After the relay left the

driving area and accelerated towards the Southeast, passing over the ground node, the safety pilot took back control of the aircraft.

The reason behind the relay departure will be described following the Loss of LOS Evaluation. In Figure 19, two Southeastern departure legs, a short leg and a long leg, are visible on the relay path. The short leg represents when Rover A was perceived driving through the obstacle and out the other side. The long leg represents when Rover A was perceived driving inside the obstacle and remaining inside.

Loss of LOS Evaluation

Two LOS “outages” occurred (one at a time) during the obstacles test. First, the SUAS relay spent 10 seconds to acquire direct LOS with one of the rovers. 84 seconds passed before the other rover drove out of LOS. Then, the relay spent 13 seconds to reacquire LOS. This results in a mean time to reacquire LOS equal to 11.5 s.

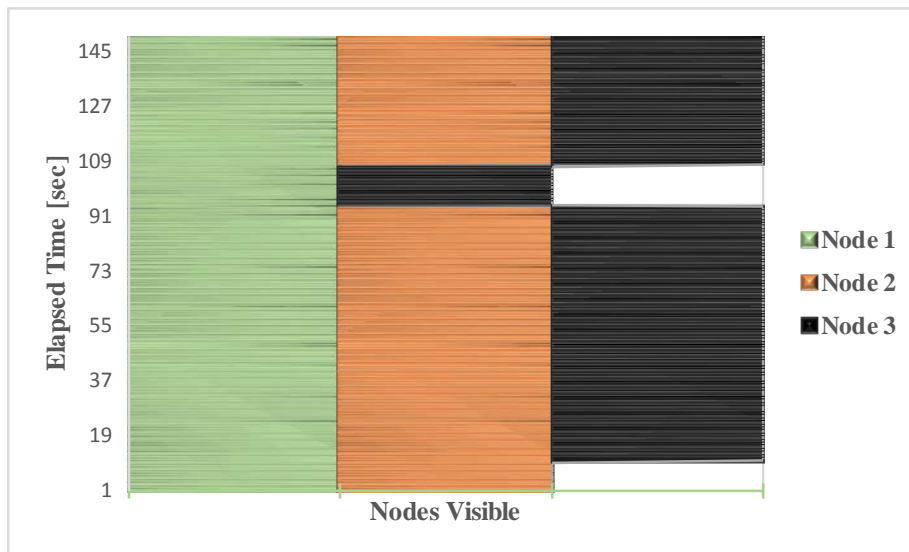


Figure 22. LOS between Nodes and Relay.

Bad Line-of-Sight Calculation and Potential Flyaway

The researcher excluded a time interval from the Loss of LOS Evaluation, due to a bad LOS calculation and potential flyaway in that interval. The GPS position estimate for one of the rovers found, erroneously, that a node drove inside the edge of the obstacle and stayed there. That position estimate was captured in Figure 19.

The data showed that the LOS calculation passed *Nan* to Mission Planner instead of guided go-to-here coordinates. Typically, Mission Planner takes values appropriate for translation into integers, of data type “format short.” Mission Planner attempted an unsigned integer translation and displayed gigantic numbers—values up to 65,500 meters.

The algorithm continued its execution loop throughout the events corresponding to the potential flyaway time interval. However, the safety pilot stopped the flyaway by taking back control of the SUAS. The researcher integrated software modifications to fix the infinite value calculation and tested the modifications using dynamic simulation.

Conclusion

The use case was implemented during 11 minutes of flight tests. The *effect on system performance*, due to combining a local minimum search with a heuristic approximation of the optimized position, was quantified. The impact of system performance on the investigative questions will be described in Chapter 6.

VI. Conclusion and Recommendations

This chapter presents the responses to the investigative questions preceding the investigative experiment and recommends areas for future investigation.

Investigative Questions Revisited

The objective leading into the investigative questions was to design an experiment, develop route-planning software, and demonstrate its autonomous relay placement capability for multiple rover scenarios with an obstacle. Chapter 1 explained the objective, and then posed three investigative questions. The subsequent explanation will address the series of investigative questions, based on the experimental results.

What is an appropriate and effective means of autonomously positioning a communication relay in order to maintain the communication link between multiple vehicle nodes and a ground node?

This question led to a realistic investigation of appropriateness in terms of algorithm execution time, prior to real-time applications. Although a midpoint placement method had been documented and tested for single rover scenarios [5], the enhanced placement software had not existed prior to this research. This research specifically extended the algorithm to support for multiple rovers and up to two obstacles.

The results of field data collection revealed that the script executed faster than the loop frequency input flight-tested, implying that the simulation also executed fast enough to be called appropriate for real time implementation. The slowest time trial and the loop

frequency used were 5.8 msec and 1 Hz, respectively. These values show that a system based on computational geometry continues to offer a viable solution.

This question also led to investigation of system effectiveness as a means of maintaining the communication link. The performance of how long and how often the system lost direct node line-of-sight from the relay's perspective addresses the question. Information regarding LOS metrics was not previously documented.

Results showed that the experimental system was 91.7%-94.9% effective at maintaining LOS with an obstacle present. These values apply to cooperative systems only, but 95% may be optimistic. The researcher observed that a rover that moved toward the obstacle and slowed or stopped as an outage occurred could gradually erode effectiveness. However, the outage was corrected in an average of 11.5 s. This question is answered if the decision-maker accepts an occasional outage. Otherwise, this is an area for improvement.

Is there value in adding LOS metrics to supplement accuracy estimation?

This question is answered by the value placed on having the simulation data. A simple centroid calculation, even with only one obstacle, is insufficient for performance measurement. For instance, the global minimum cost position does not predict or preclude the undesirable times when the local relay vehicle flies into the no-fly zone. The difference between results using heuristics and those using the global minimum is measurable—accounting for the LOS metrics that this research specifically added.

Gray found [5] that GPS position error was 11.6m using this architecture. The results of the data collection were consistent with Gray's estimate. That is, accuracy

estimation on its own provided the same information for technically different solutions to the problem stated in Chapter 1.

A practical set of measures that included LOS was capable of differentiating between two experimental scenarios. The data showed that the flight test with one moving and one stationary rover outperformed simulated test with two moving rovers, even though simulation simplified the test environment. It would not have been possible to measure packet loss directly in that simplified environment. LOS metrics were easy to implement, as well.

What is the effect on system performance, due to combining algorithmic local minima positioning with a heuristic approximation of the optimal positioning algorithm?

This question relates to getting the heuristic into a clean form and implementation. The flight tests showed that the algorithm worked well with some heuristic rules. However, there are still considerations to address.

The total communication cost (equation 1) was lower using optimal solutions in the static simulation, compared to the dynamic simulation, which was implemented with the heuristic table of rules (heuristic in Chapter 4). Additional analysis of simulation data revealed mistaken logic; the mistaken logic caused the relay to become stuck, which was corrected. Thereafter, the dynamic simulation performed well with the heuristics update. However, optimal positioning was easier to test than heuristic positioning.

The simulated, dynamic relay positioning test around one or two obstacles showed the realism of replicated flight test scenarios. With the operator commanding UVs, the node visibility computation ran in the background and delivered relay coordinates.

Dynamic simulation was difficult to implement, but it was a practical method of showing the relative success of heuristics implementation.

Potential Applications

A suggested objective for future research is mathematical: prove that the intersection of a tangent line with the perpendicular reference line originating at the centroid is optimal (see Appendix A). Accomplishing a mathematical proof would provide the increased theoretical foundation to justify fully researching the topic.

Heuristics offer a growth path for the 2D problem. Program a delay in the decision loop and a mildly predictive calculation of where the centroid will be in the future, relative to the no-fly zone. Recreating scenarios when the current algorithm does not find an instantaneous solution would make an interesting future test of the predictive capability.

A robust capability around real obstacles, as opposed to virtual obstacles, is needed; the user requires a robust capability to maintain communications from the relay to the GCS. To support this capability, modifications to the algorithm are recommended. Those modifications would ensure identification of which node is the GCS, as well as choosing the GCS as the node with greater priority.

One area that the researcher did not address is the three-dimensional optimization problem. That optimal solution would be applied in the multiple-UV domain to iterate further upon the current architecture. The researcher attempted to develop a written product containing a hypothetical approach in this area. However, there are many possibilities for solving the problem that did not fit within the scope of this research activity.

Bibliography

- [1] U. S. Navy, “The Navy Unmanned Surface Vehicle (USV) Master Plan,” 2007.
- [2] M. R. Endsley, “Autonomous Horizons: System Autonomy in the Air Force—A Path to the Future,” Washington, D.C., 2015.
- [3] Y. Choi, M. Pachter, and D. Jacques, “Optimal Relay UAV Guidance—A New Differential Game,” in *Conf. Decision Contr.*, 2011, pp. 1024–1029.
- [4] Q. Ali, N. Gageik, and S. Montenegro, “A Review on Distributed Control of Cooperating Mini UAVs,” *Int. J. Artif. Intell. Appl.*, vol. 5, no. 4, pp. 1–13, 2014.
- [5] J. Gray, “Design and Implementation of a Unified Command and Control Architecture for Multiple Cooperative Unmanned Vehicles Utilizing Commercial Off the Shelf Components,” Air Force Inst. of Technology, 2015.
- [6] C. Tanil, C. Warty, and E. Obiedat, “Collaborative Mission Planning for UAV Cluster to Optimize Relay Distance,” in *Aerosp. Conf. Proc.*, 2013, pp. 1–11.
- [7] T. J. Shuck, “Development of Autonomous Optimal Cooperative Control in Relay Rover Configured Small Unmanned Aerial Systems,” Air Force Inst. of Technology, 2013.
- [8] J. D. Rosal, “Centralized Cooperative Control for Route Surveillance with Constant Communication,” Air Force Inst. of Technology, 2009.
- [9] A. S. Clare, M. L. Cummings, and J. P. How, “Operator Objective Function Guidance for a Real-Time Unmanned Vehicle Scheduling Algorithm,” *J. Aerosp. Comput. Information, Commun.*, vol. 9, no. 4, pp. 161–173, 2012.
- [10] B. Wasserman, H. Ludwig, J. Laredo, K. Bhattacharya, and L. Pasquale, “Distributed Cross-Domain Change Management,” in *Int. Conf. Web Services*, 2009, pp. 59–66.
- [11] D. K. Ahner and C. R. Parson, “Workshop Report: Test and Evaluation of Autonomous Systems,” Wright-Patterson AFB, OH, 2016.
- [12] B. Iannotta, “Sharp Intelligence, Tight Budget,” *Aerosp. Am.*, vol. 53, no. 2, pp. 24–27, Feb. 2015.
- [13] G. Lai and T. Lamoureux, “Development of Measures of Effectiveness and Performance from Cognitive Work Analysis Products,” Ottawa, ON, 2012.
- [14] I. Bekmezci, O. Sahingoz, and Ş. Temel, “Flying Ad-Hoc Networks (FANETs): A Survey,” *Ad Hoc Networks*, vol. 12, no. 4, pp. 1–17, 2013.
- [15] M. Garzón, J. Valente, D. Zapata, and A. Barrientos, “An Aerial-Ground Robotic System for Navigation and Obstacle Mapping in Large Outdoor Areas,” *Sensors (Switzerland)*, vol. 13, no. 1, pp. 1247–1267, 2013.

- [16] K. S. Seah, "System Architecture of Small Unmanned Aerial System for Flight Beyond Visual Line-of-Sight," Air Force Inst. of Technology, 2015.
- [17] T. Diamond, A. Rutherford, and J. Taylor, "Cooperative Unmanned Aerial Surveillance Control System Architecture," Air Force Inst. of Technology, 2009.
- [18] M. J. Vincie, "Airborne Wireless Communication Modeling and Analysis with MATLAB," Air Force Inst. of Technology, 2014.
- [19] D. H. Choi, S. H. Kim, and D. K. Sung, "Energy-efficient Maneuvering and Communication of a Single UAV-based Relay," *IEEE Trans. Aerosp. Electron. Syst.*, vol. 50, no. 3, pp. 2320–2327, 2014.
- [20] B. Crawford, R. Soto, R. Cuesta, M. Olivares-su, F. Johnson, and E. Olgu, "Two Swarm Intelligence Algorithms for the Set Covering Problem," in *9th Int. Conf. Software Eng. Applicat.*, 2014, pp. 60–69.
- [21] R. Soto, B. Crawford, and R. Olivares, "The Complexity of Designing and Implementing Metaheuristics," *HCI Int.*, 2015.
- [22] E. Arvelo, E. Kim, and N. C. Martins, "Maximal Persistent Surveillance under Safety Constraints," in *Proc. IEEE Int. Conf. Robot. Autom.*, 2013, pp. 4048–4053.
- [23] D. Davendralingam, "A Robust Portfolio Optimization Approach to System of System Architectures," *Syst. Eng.*, vol. 18, no. 3, pp. 269–283, 2015.
- [24] J. Hansen, M. Pachter, D. Jacques, and P. Blue, "Optimal Guidance of a Relay MAV for ISR Support beyond Line-of-Sight," in *Guid. Navig. Contr. Conf. and Exhibit*, 2008, pp. 1–27.
- [25] S. Hayat, E. Yanmaz, and R. Muzaffar, "Survey on Unmanned Aerial Vehicle Networks for Civil Applications: A Communications Viewpoint," *IEEE Commun. Surv. Tutorials*, vol. 18, no. 4, pp. 2624–2661, 2016.
- [26] J. T. Hing, K. W. Sevcik, and P. Y. Oh, "Improving Unmanned Aerial Vehicle Pilot Training and Operation for Flying in Cluttered Environments," in *Int. Conf. Intell. Robots Syst.*, 2009, pp. 5641–5646.
- [27] D. Selva and E. Crawley, "VASSAR: Value Assessment of System Architectures Using Rules," in *Aerosp. Conf. Proc.*, 2013.
- [28] N. Hitomi and D. Selva, "Experiments with Human Integration in Asynchronous and Sequential Multi-agent Frameworks for Architecture Optimization," *Procedia Comput. Sci.*, no. 44, pp. 393–402, 2015.
- [29] N. M. Jodeh, "Optimal UAS Assignments and Trajectories for Persistent Surveillance and Data Collection from a Wireless Sensor Network," Air Force Inst. of Technology, 2015.
- [30] R. Lin and Y. Li, "A Novel Distributed Automatic Resource Allocation Scheme in Cooperative Relay Network," in *3rd Int. Conf. Consumer Electron. Commun. Networks*, 2013, pp. 23–25.

- [31] J. H. Kim, J.-W. Kwon, and J. Seo, "Multi-UAV-Based Stereo Vision System without GPS for Ground Obstacle Mapping to Assist Path Planning of UGV," *Electron. Lett.*, vol. 50, no. 20, pp. 1431–1432, 2014.
- [32] N. M. Jodeh, R. G. Cobb, and R. A. Livermore, "Optimal Airborne Trajectories for Data Collection from Wireless Sensor Networks by Direct Collocation Methods," in *AIAA Guid. Nav. Contr. Conf.*, 2015, pp. 1–14.
- [33] H. Jordan, "AFRL COUNTER team wins Air Force Outstanding Scientist Team Award," *Wright-Patterson Air Force Base News*, 13-Aug-2008.
- [34] G. P. Potdar, R. C. Thool, and S. G. Singhji, "Comparison of Various Heuristic Search Techniques for Finding Shortest Path," *Int. J. Artif. Intell. Appl.*, vol. 5, no. 4, pp. 63–74, 2014.
- [35] M. Pachter, J. Hansen, D. Jacques, and P. Blue, "Optimal Guidance of a Relay Aircraft to Extend Small Unmanned Aircraft Range," *Int. J. Micro Air Veh.*, vol. 2, no. 3, pp. 157–180, Sep. 2010.
- [36] J. T. Hing and P. Y. Oh, "Mixed Reality for Unmanned Aerial Vehicle Operations in Near Earth Environments," in *Int. Conf. Intell. Robots Syst.—Proceedings*, 2010, pp. 2509–2510.
- [37] J. I. Abeygoonewardene, "Scaling Flight Tests of Unmanned Air Vehicles," Air Force Inst. of Technology, 2006.
- [38] I. Quilez, "Sphere Ambient Occlusion," *Fractals, Computer Graphics, Mathematics, Demoscene and More*, 2006. [Online]. Available: <http://www.iquilezles.org/www/articles/sphereao/sphereao.htm>. [Accessed: 01-Jan-2016].

Appendix

Appendix A: Working Article

(For Information Only. Draft Paper is under Revision.)

ENHANCED COST MINIMIZATION ALGORITHM FOR CONTROL ARCHITECTURE—
21SEP2016 DRAFT BY LAURA LUCAS

Keywords

Optimization, Numerical Geometry, Visibility, BLOS, Communication, Telemetry

Abstract

This research emphasizes command and control for specialized operational missions, in which an operator controls multiple unmanned vehicles (UVs). The operational mission is summarized as follows: the operator initiates control transmissions between a base station and the UVs, while a small aerial vehicle provides a relay supporting flexible communications. During this mission, the system can communicate to as many friendly UVs as possible. Relay routing software ensures UVs remain visible to the relay vehicle. Line-of-sight obstructions and limits on total communication power, such as battery capacity, impact relay placement. However, manually determining relay placement can reduce performance and threaten safety. Therefore autonomous placement is under development. Unlike the midpoint method, an enhanced placement algorithm accounts for battlespace obstructions and a flexible quantity of UVs. The algorithm provides two levels of decision support: first, it computes a finite number of feasible destinations for the relay. Second, the algorithm reveals the minimum-cost destination from the finite set of candidates. When the operator is online and commanding UVs, the node visibility computation runs in the background, which delivers relay coordinates but is unobtrusive to the operator.

Introduction

The unmanned vehicle is known for its dull, dirty, and dangerous tasks; its capability to accomplish such specialized tasks is an asset [1]. With the growth occurring in unmanned vehicle (UV) fleet sizes, the desire for cooperative control in the commander's battlespace follows the fleet's upward trend. The Department of Defense (DoD) needs methods that will enable an airman to guide groups of UVs through mixed environments—urban, forested, and mountainous [24]. Moreover, the DoD desires multiple-UV sensor systems that provide better

information and speed than current systems [12]. This research studies the command and control element participating in specialized operational missions, in which a single operator controls multiple unmanned vehicles (UVs).

This specific system is the research focus: a communication link provided by a dedicated relay and non-proprietary relay routing software messages. The developmental system's operational mission is summarized as follows: first, the operator initiates command transmissions between a base station and one or more UVs. Then, the system retains communication capabilities to as many UVs as needed to enable sensor activities (for instance, wide area search). A small unmanned aerial vehicle system (SUAS) provides the relay supporting the communications. Relay routing software ensures that all system nodes remain visible to the SUAS, supporting an integrated communication link. The operator relinquishes relay placement decisions during the time between launch and recovery.

A well-known midpoint heuristic has proven useful in the past, under the previous architecture where no obstructions were present [5]. The researcher extends that architecture by analyzing additional, cooperative remote UVs, while another extension incorporates obstructions within the battlespace. However, in adding the logical elements to either component of the architecture, the past midpoint heuristic is no longer sufficient to maintain communications. Therefore, the researcher develops an original software solution, comprising a new rule for finite, discrete relay locations in several scenarios.

Using rules for link integrity, the algorithm provides a command for the relay vehicle—e.g., a small unmanned aerial vehicle system (SUAS)—to go to a fixed position in each scene and enable transmission to and telemetry from the UVs. This is accomplished, due to applied geometry and optimization of the solution, without losing command and control from the GCS. In short, the proposed solution is automated placement of the communication relay. The researcher's rule is used for demonstration. The algorithm drives recommended go-to positions in each scenario based on minimizing total power cost of communication under visibility constraints.

Literature Review

The purpose of architecting efforts is to unify “portable” engineering ideas from different domains, thereby gaining an advantage in addressing system issues, such as the aforementioned communication problem [16]. Benefits of architecting, such as accessibility and risk reduction, provide motivation for further systems engineering research. In the context of SUAS, architecture is a present resource that is potentially available for expansion.

Previously, in a study with a rover and a home base, the operator utilized the rule, “head straight toward the midpoint between the rover and the base,” to command the relay downrange

[24]. That optimal placement rule was useful to extend small UV survey range. Gray [5] demonstrated an unmanned cooperative control system utilizing an original architecture which Gray developed for a collection of common Department of Defense (DoD) missions, including communication relay missions. Hansen, Pachter, Jacques, and Blue also verified that the midpoint was the best automated solution for the communication relay scenario with a rover and a home base, when no obstructions were present [24].

The communication relay scenario by definition is: “the act of passing information between a remote vehicle or sensor to a central GCS through an intermediate relay vehicle [5].” In academia, the communication relay theme touched on new sub-topics, viewpoints, and experiments in recent years. For example, Choi, Kim, and Sung solved the efficiency maximization problem that balances two power costs under circular maneuvering conditions: aerodynamic maneuver cost and communication cost [19]. When the mission allows, multiple relays can work together; Lin and Li [30] found evidence that the optimal power-level control policy of the multiple-relay system could be achieved for communication networks involving multiple sources and multiple destinations. As another example, Tanil, Warty, and Obiedat [6] detailed an optimized genetic algorithm for planning multiple, simultaneous trajectories around obstacles in two dimensions.

Both Lin and Li’s article and Tanil et al.’s article described forwarding algorithms, in which the role of the communication link was spread across multiple actors [6], [30]. A likely benefit of that trend toward distributed, multiple-actor methods is its emphasis on adoption of a state-of-the-art technology to achieve accuracy. A drawback to that trend is cost growth; for example, the additional actors introduced a cost driver when Kim, Kwon, and Seo’s [31] method required the camera payloads attached to several UVs to produce overlapping information. This research assumes that teams of UVs are virtually connected to ground infrastructure comprising a central base of control; the researcher also assumes that the communication link relies upon a single relay. Considering the knowledge that exists, the system architecture may allow for further research with substitution of distributed methods for comparative information.

Arvelo, Kim, and Martins programmed the convex form of a minimization problem in which they planned for deploying a limited number of robots, who were tasked to surveil an area containing forbidden regions [22]. Safety, for civilians and property on the ground below the vehicle, is a primary concern specifically affecting SUAS missions and is of utmost importance. Some authors have been concerned about safety, arguing that the combination of many urban environments and many line-of-sight-limiting factors is part of today’s “mixed reality [36].”

Defined by assignment, “forbidden regions” are areas to which visitation presents any type of unsafe operation or poses an unsafe constraint to the system [22]. To relate safety constraints to U.S. Air Force interests, consider the term “no-fly zone.” Hing, Sevcik, and Oh

explained [17] that path planning around forbidden regions is related to both safety and risk. However, Clare, Cummings, and How [9] argued that brittle optimization rules only threaten system performance. Hing and Oh [36] expressed additional concern that disuse of fragile pre-decisional information systems can introduce broken methodologies into hands-on-aircraft training and evaluation systems, leading to vulnerable civilians and endangered property. Continued research is required, comprising robust methods of flight planning for safe and effective single-operator control of multiple UVs.

Automation is crucial as part of the solution, however, automation has been described as “brittle,” indicating that the operator’s input may be required more frequently than is sometimes advertised [9]. The literature left a research gap in understanding whether autonomous communication relays help a human single-operator, in the multi-UV system context, to mitigate the threat of workload saturation [27]. At least two recent studies indicated methods are wanted that are easy or convenient decision-support tools for a single operator to implement multiple UVs [15], [28]. The researcher, therefore, steps aside from assertions or rebuttals about the effects of communication relays on the operator’s workload saturation; instead, the researcher focuses on delivering decision support, similar to the midpoint rule used in the past.

Computational Method

The researcher populates a simulation of scenes with up to two obstructions and multiple stationary nodes, representing UVs and a ground control station (GCS) located at home base. During each scene, the algorithm under design calculates the average position, known as the system centroid, of all the UVs. A problem arises, because the geometry of a scene with obstructions can cause an immediate line-of-sight (LOS) communication outage due to occlusion; the obstructions interrupt the visibility lines passing through the centroid and to/from the nodes. That problem drives the algorithm’s role to extend and include geometric calculations.

In Table 8, a matrix shows the developmental test case design; there are two controllable variables (number of obstacles and number of nodes) and an interaction between the input variables (multiple nodes with multiple obstacles). The researcher hypothesizes that the interaction between variables has significant effect at the design levels prepared for the last two columns (number of obstacles and number of nodes). Therefore, the dependent variables, execution time and solution space complexity, are related to the two controllable variables.

Table 8. Test Cases for Computational Analyses

Scene #		1 or 2 Obstacles	Node Count
1		1	2
2		1	3
3		2	3
4		2	4
5		1	4

This section specifies the elements used to design and demonstrate the algorithm when a single obstacle is present. This research enables specific scenarios in stages, evolving toward the algorithm that will undergo operational test and evaluation. The objective is to have robust algorithms for scenes with up to two obstacles. Extension to two obstacles, however, makes little difference to the design variables' definitions and mainly affects computation of the constraints of the problem. That extension is discussed after the basic flow of the algorithm is broken out.

Effective placement of the communication link is the key decision throughout the scenarios in this research. What distinguishes the proposed SUAS placement algorithm from other existing solutions is that analytical, rather than probabilistic or random, fixed-point methods are used. Due to MATLAB utilization, this occurs in no more than two seconds.

Figure 21, below, represents an overhead view of the two-dimensional battlespace. Conceptually, a successful communication relay extends the reach of command transmissions, from the house, exchanged with the friendly UVs downrange. The relay also helps telemetry, from the UVs, reach the house. Without loss of generality, the home base appears at node B. In fact, for most of this paper, nodes are not specified as UV locations or home base locations.

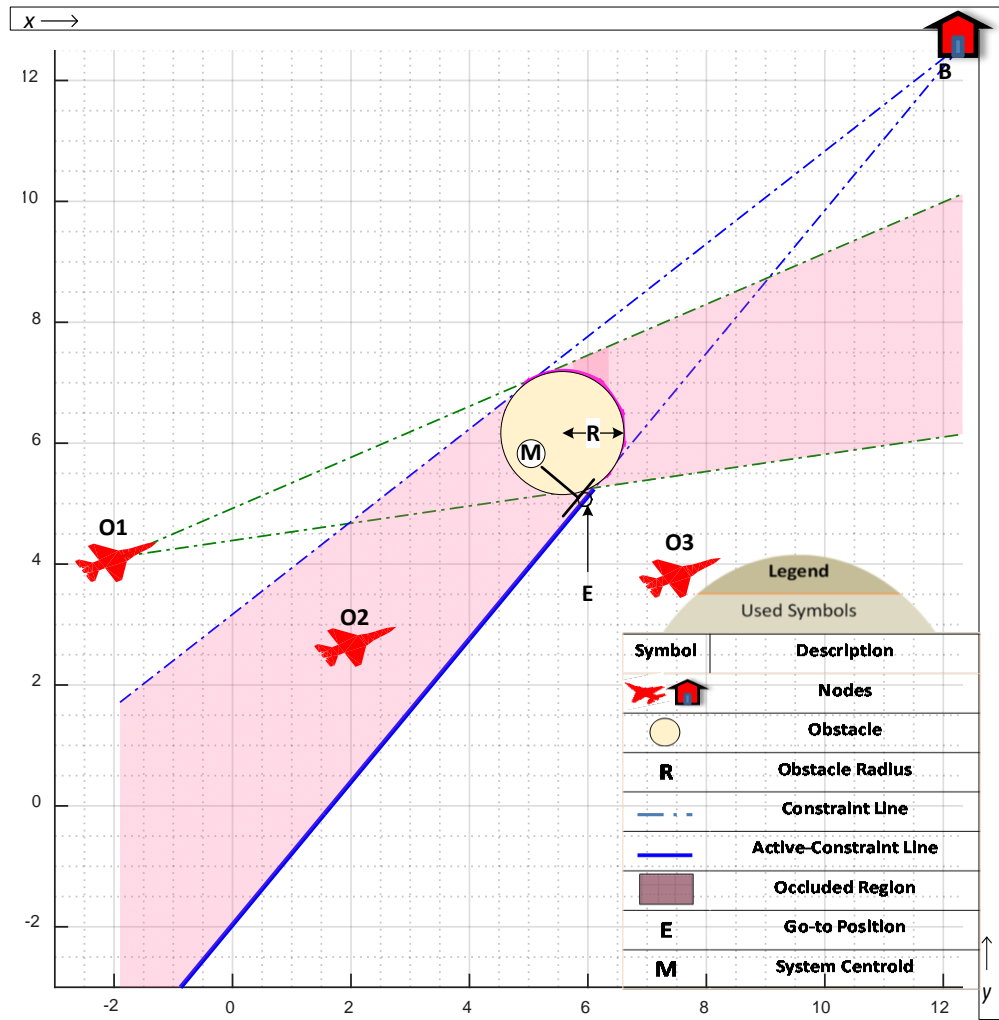


Figure 23. Operational View of Obstructed Communication Link.

Nodes are defined as point sources which communicate messages straight to the relay. B and O1 – O3 in Figure 1 represent nodes. BLOS point locations are allowed. Nodes at matching elevations above ground level, including the relay, are the baseline case. A flat Earth assumption is made in this baseline case.

The shaded area represents part of the occluded region, in which the lack of LOS from O1 or B to any relay in that area would indicate a poor link, or no link, from one or both nodes. The shaded area is part of the infeasible region of the battlespace, which means that a successful communication relay cannot lie strictly inside the shaded area. From an operator's perspective, it would be a poor decision to send the SUAS relay inside that area. There are two other boundary lines, not shown, which could extend each from O2 and O3. O2 lies in the shaded area, because it is an obscured node from the point-of-view of B.

Obstacles are defined as forbidden regions in the battlespace. The filled obstacle circle approximates the cross-section of a generic structure like a water tower. Two-dimensional obstacles of infinite height and finite diameter are the baseline case. Active-constraint lines are defined as tangent lines to the obstacle surface from nodes which are unable to view all other nodes.

Go-to positions are defined as finite, discrete placement options for the SUAS relay at a snapshot in time, meaning an assumption is made that the elements of the battlespace are momentarily stationary. Point E in Figure 21 represents a go-to position. Point E is also known as a feasible vertex point.

The average of node positions is defined as the system centroid. Point M is the centroid. M lies on a short vector, with tail at E, which is orthogonal to the active-constraint line as shown. The normalized length of this vector has a positive relationship to the communication cost of a relay located at E.

Scaling the SUAS Algorithm

In Abeygoonewardene's MATLAB simulation, all equations and vehicles were described in non-dimensional terms. This allowed for scaling, which in turn allowed for successful comparisons between dissimilar scenes, with different-sized craft moving under different acceleration profiles [37]. This research takes a simple, non-dimensionalized length, version of that approach by scaling the x and y axes relative to the obstacle radius.

Scaling is useful to simplify the problem and ensure the algorithm is robust for different users. For example, visibility from a point around an obstruction is a function of a unitless ratio, which is

$$\text{visibility ratio} = \frac{i^{th} \text{ node distance away from the } j^{th} \text{ obstruction}}{\text{diameter of the } j^{th} \text{ obstruction}} \quad (1a)$$

$$v_{ij} = D_{ij}/(2R_j) \quad (1b)$$

R is the obstacle radius in units of length [38]. A distance of one unit in any direction is one radius in length. Even more convenient is the fact that communication power is proportional to the square of communication distance. Thus, the use of scaling predictably affects the entire optimization problem, including the constraints, the coordinate plane, and the cost function.

Algorithm Method

The researcher-designed software applies a four-step computational method. The proposed routine is a method for testing a moderate number of vertex points, and the main steps of this method are given as:

Step 1—define $2N$ tangent lines to the circle through external points at the nodes, where N is the number of nodes.

Step 2—find the few vertices that meet two go-to location requirements, which are discussed below.

Step 3—rank the few vertices that meet both requirements, from least cost to greatest cost.

Step 4—the recommendation is, “head toward the top-ranking vertex.”

Of these four total steps, Step 2 requires a more detailed explanation. There are two go-to location requirements. The first go-to location requirement is that the go-to location either is point M or is a vertex at the intersection of any tangent line from Step 1 with the short vector that runs perpendicular from the tangent line to point M . If the system centroid is strictly inside of any occluded region from the point-of-view of one of the nodes, then the algorithm continues to try to find point E . The algorithm accomplishes this by finding, listing, and testing a moderate number of candidate points for a moderate number of nodes. Specifically, the candidate points in the list number thusly:

$$\text{length}(\text{list of vertices}) = 2N \quad (2)$$

One point is found per each tangent line drawn to the obstacle. These points are found using the intersection of every tangent line from Step 1 with the corresponding short vector that runs perpendicular from that tangent line to point M . Step 2 states that the vertices also meet a second requirement, which makes them feasible go-to locations. At this stage, range becomes important.

Because of scaling the SUAS algorithm, a battlespace is defined as X radii long by X radii wide, based on the radius of the largest obstacle in the space. Suppose $X = 20$, in other words, it takes ten diameters of the large obstacle to span the length of the space. Then, the maximum straight path within the battlespace is the diagonal that segments the battlespace into two isosceles right triangles. The default maximum communication range is set at the length of that segment:

$$\text{maximum comm range} = 20\sqrt{2} \times R \quad (3)$$

Regions of the battlespace stem from the constraints bearing on the recommended go-to location. The vertices require testing, to ensure the go-to location is not strictly inside of the occluded region from each node’s point-of-view. Actually, the algorithm nudges the vertices away from the obstacle by a tiny distance before it tests them, because they otherwise might fail the second requirement due to a machine accuracy issue.

The researcher's method of approximation reduces the occluded region from each node's point-of-view to a convex quadrilateral polygon, which is defined by its corners. Since every tangent line intersects the obstacle at one and only one point, two of four corners are the two points of tangency based on the node location and obstacle parameters. The other two corners are found by following the two tangent lines farther away from the node by the fixed distance from (3). Setting the fixed length of the test region differently from the default is optional. This method results in the shaded regions shown in Figure 21 and concludes derivation of the feasibility requirements.

Step 2, Detailed

The algorithm tests every vertex with respect to every infeasible region/ convex quadrilateral polygon. The algorithm accomplishes this by executing the researcher-written “can I see it” function. The approximation has reduced the occluded region from each node’s point-of-view to a convex quadrilateral polygon defined by four corner points. The “can I see it” function is completed by using MATLAB’s “inpolygon” command in a loop.

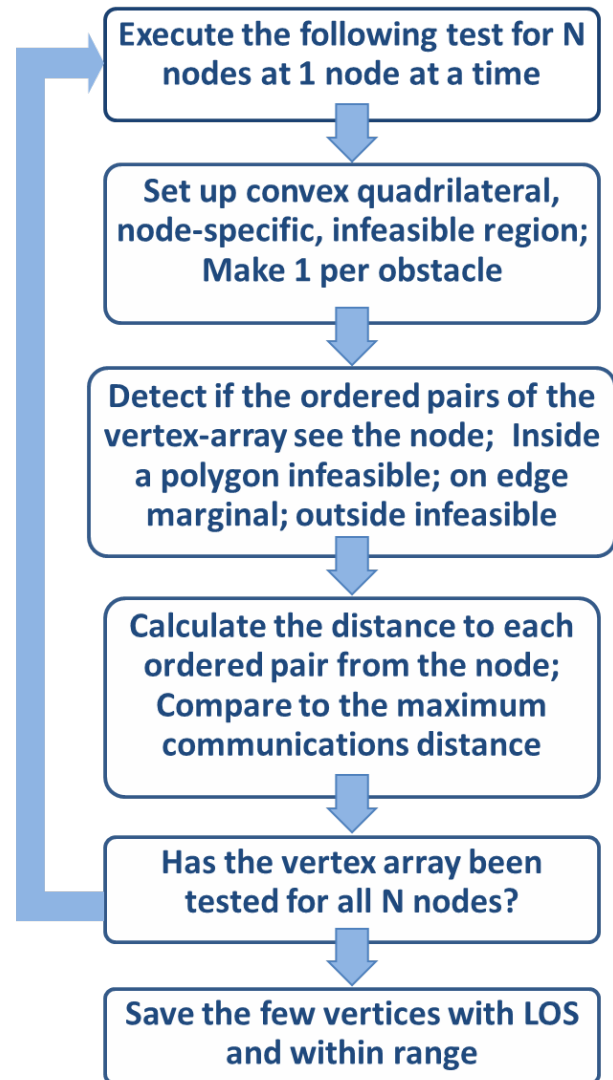


Figure 24. Flow Diagram for the “can I see it” Function.

After the “can I see it” function eliminates vertices having no LOS to one or more nodes, the few vertices (if any) that remain are retained for cost function evaluations. This method results in all the possible guesses that meet both the first and second go-to location requirements,

which means that the algorithm prefers a location with LOS as well as located on a constraint line and close to the system centroid.

Increasing the node distance downrange from a relay increases the immediate communication cost in a distance-squared relationship. The cost function is given as:

$$f = \sum_{i=1}^N (\overline{EO_i})^2 \quad (4)$$

This relationship is based on the radio frequency power requirements [35].

As the following two examples will show, the cost minimization point is relatively intuitive and practical. That is because the solutions are found where at least one constraint line is active. This is fortunate, because the results will show that the communication power budget can significantly improve.

The algorithm, including the step described by Figure 2, follows much the same method in the two-obstacle case. In general, an array of length $2N$ extends into an array of length $4N$. The first go-to location requirement is the same, and one centroid point, M , is again added to the array. Conversely, the second go-to location requirement is more difficult to meet, as the algorithm tests the two occluded regions for both obstacles at once. The vertices require testing, to ensure the go-to location is not strictly inside of either occluded region from each node's point-of-view. The algorithm nudges the vertices away from the average of both obstacles' centers by a tiny distance before it tests them.

Analytical Examples

Analytical Example 1

In this example, the obstacle is a circle of radius R . There are two nodes $O1$ and $O2$ located at $(11.7, 1.82)$ and $(-1.12, 12.2)$, respectively, in units of R . The obstacle is centered at $(5.6, 6.2)$. Obviously, $O1$ is closer to the obstacle than $O2$. Intuitively, the active-constraint line should be a line that passes through $O1$. The algorithm calculates the feasible solutions based on rules. Figure 23 shows points $E1$ and $E2$ as the best relay positions. $E1$ and $E2$ are on the two tangent lines that pass through $O1$. The better-value decision between $E1$ and $E2$ is delayed, until cost results are created.

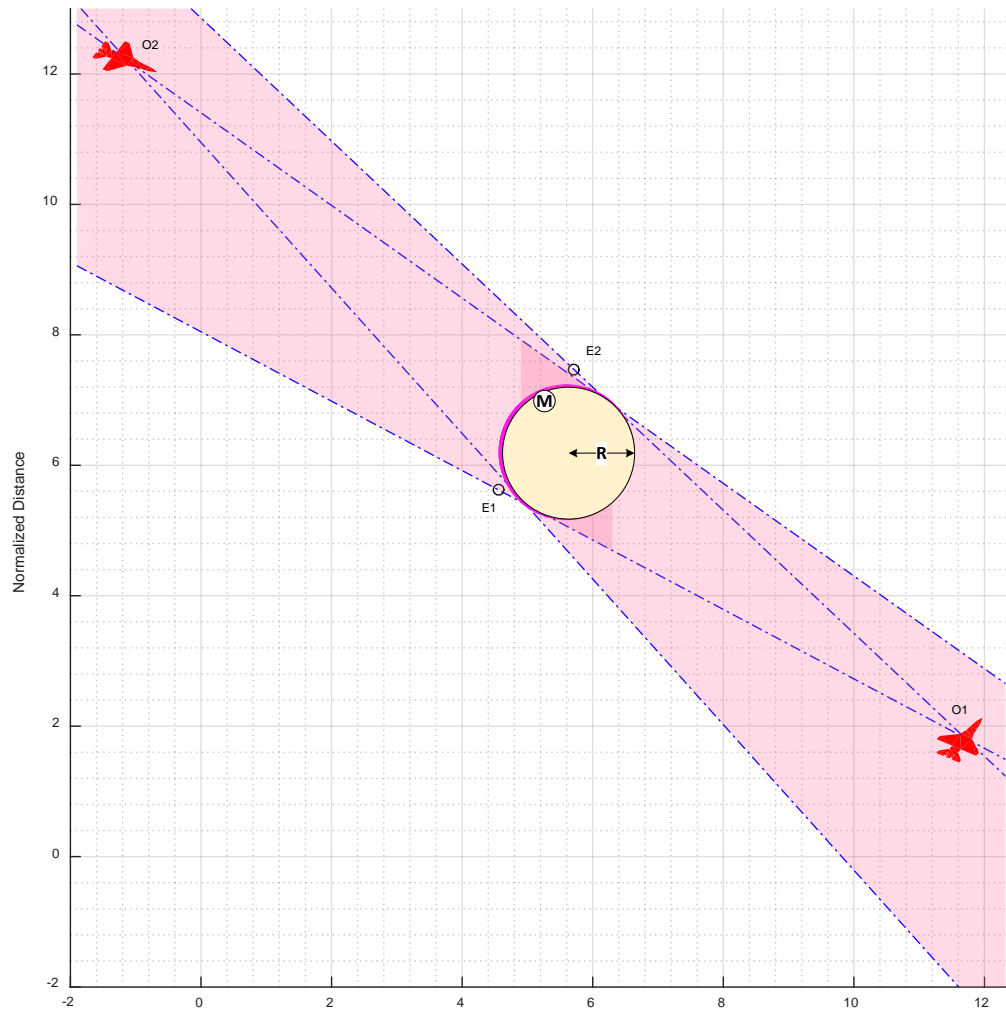


Figure 25. Scene #1 Example with Two Feasible Regions.

The main steps of the algorithm follow:

Step 1—there are four tangent lines to the circle through two nodes. Their equations are calculated as:

$$O1 \text{ Line 1: } -3.50x - 6.57y + 52.88 = 0 \quad (5a)$$

$$O1 \text{ Line 2: } -5.11x - 5.41y + 69.61 = 0 \quad (5b)$$

$$O2 \text{ Line 3: } 5.18x + 7.30y - 83.24 = 0 \quad (5c)$$

$$O2 \text{ Line 4: } 6.67x + 5.98y - 65.43 = 0 \quad (5d)$$

In this case Line 1 and Line 2, connected to O1, bound the feasible (unshaded) region on the “northwestern” side of the obstacle. Locations strictly inside the circle are always considered infeasible.

$$M = \text{mean}([O1; O2]) = (5.29, 7.01) \quad (6)$$

Step 2—there are two vertices that meet both requirements: [E1; E2].

$$E1 = (4.55, 5.62) \mid \overrightarrow{E1M} \perp \text{Line 1} \quad (7a)$$

$$E2 = (5.72, 7.46) \mid \overrightarrow{E2M} \perp \text{Line 2} \quad (7b)$$

Step 3—the algorithm performs two cost function evaluations, utilizing Equation 4, to provide decision support.

$$f(E1) = 140.97 > f(E2) = 136.83 \quad (8)$$

The communication cost reflects R-squared units.

Step 4—the algorithm recommends, “Head toward the cost-minimizing vertex E2 at (5.72, 7.46).”

In this example, there are two feasible regions and two Feasible Vertices (FVs). A mapping of this example into the MATLAB solver function, “fmincon,” confirms that E1 and E2 are the local minima for their respective feasible regions, based on the cost function. Therefore, the recommendation E2 is the global minimum-cost point in this scenario, for this snapshot in time.

Analytical Example 2

In this example, the two obstacles are circles of radius R and 3R/7. There are four nodes O_i located at (0.90, 2.43), (3.75, -0.43), (8.12, -0.85), and (10.23, 16.99), respectively, in units of R. The obstacles are centered at (7, 12) and (5, 1). Figure 24 shows three points E_n as the best relay positions. Cost results will show that the boxed go-to point at (5.07, 4.67) is the best feasible vertex.

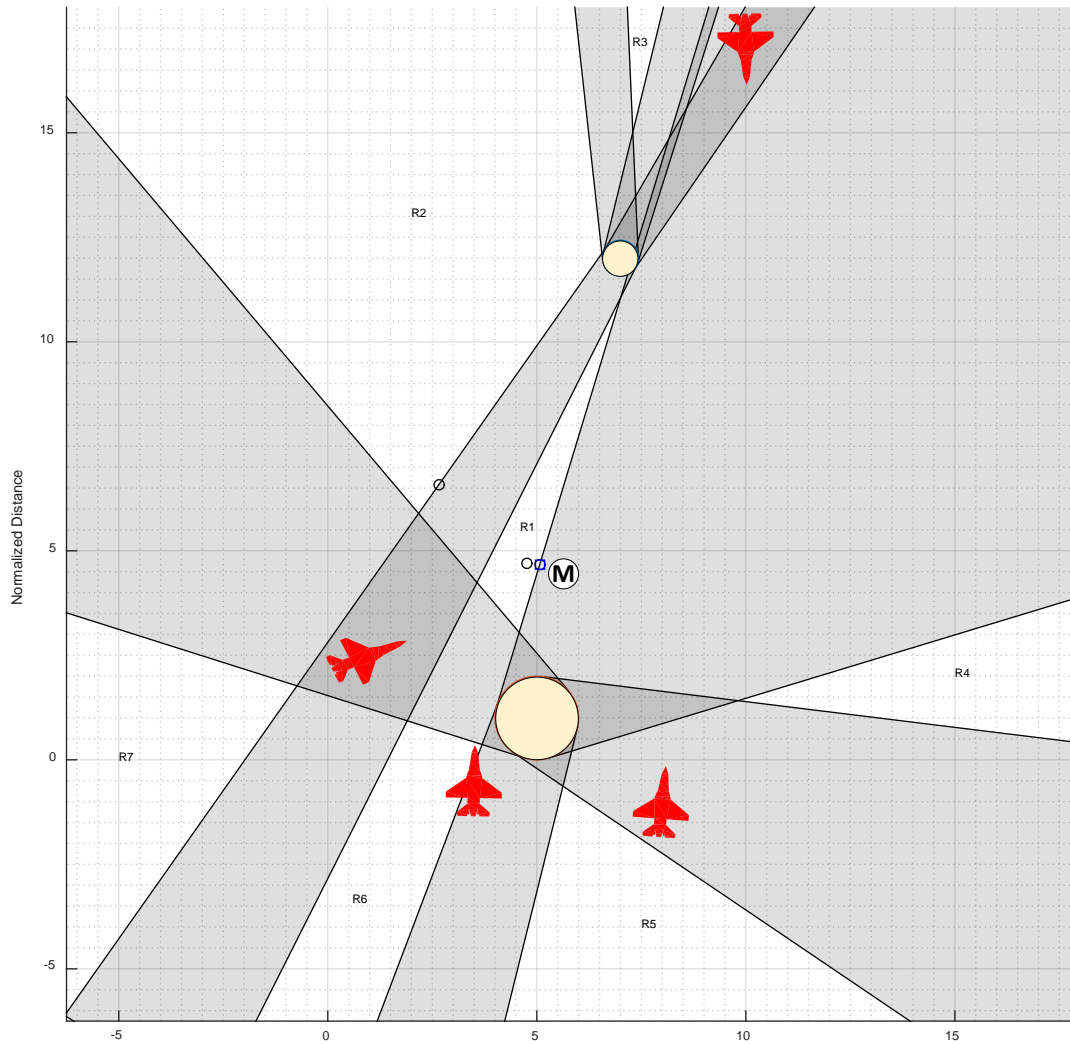


Figure 26. Scene #4 Example with Seven Feasible Regions.

Step 1—there are 16 tangent lines to the circles through four nodes.

Step 2—there are three vertices that meet both requirements.

Step 3—the algorithm performs three cost function evaluations, utilizing Equation 4.

$$f(E1) = f(2.66, 6.59) = 318.77 > \quad (9a)$$

$$f(E2) = f(4.77, 4.71) = 269.25 > \quad (9b)$$

$$f(E3) = f(5.07, 4.67) = 267.54 \quad (9c)$$

Step 4—the algorithm recommends, “Head toward the cost-minimizing vertex E3.”

In fact, mapping Example 2 into the MATLAB solver function, “fmincon,” confirms the local minimum for the feasible region at R1, based on the cost function. R2 – R7 are clearly

farther away from M than R1. Therefore, the recommendation E3 is the global minimum-cost point in this scenario, for this snapshot in time.

Results

Qualitatively, as long as the algorithm finds a feasible solution, the results of the numerically calculated recommendation include an efficient design solution, tailored to the specific problem. Quantitatively, the researcher times the algorithm's execution, from start through solving the relay placement point, in milliseconds. The cost avoidance of the low-cost relay placement point in comparison to the other feasible placement points, which are computed but not displayed, also produces numerical results. The results are assessed according to these ground rules: shorter execution time is better, and a larger discriminator delta between the recommendation and the non-recommendation points is better. Also, the researcher tracks whether the algorithm finds a solution.

A benefit of utilizing the algorithm is that it runs fast. In a medium-sized (75 trial) sample, the worst case is 26.2 msec when one obstacle is present. If much worse results occur, that may be because the memory is not being pre-allocated for maximum performance. The algorithm finds a solution in 75 out of the 75 trials when one obstacle is present, though it has been observed, manipulating the nodes and circles, that the algorithm does not always find a solution. The overall median elapsed time is 3.7 msec, and the mode is 3.0 msec.

In a medium-sized (75 trial) sample, the worst case is 41.5 msec when up to two obstacles are present. This version of the algorithm uses "if" statements, as needed, to handle different methodologies for one vs. two obstacles. The algorithm finds a solution in 75 out of the 75 trials when up to two obstacles are present, though it has been observed, manipulating the nodes and circles, that this algorithm also does not always find a solution. The overall median elapsed time is 5.5 msec, and the mode is also 5.5 msec.

A second benefit of utilizing the algorithm is that it works well in spite of having multiple, non-contiguous feasible regions. The algorithm only has to loop through a moderate number of polygons to determine which points are infeasible; everything else is feasible. As shown in Table 9, the feasible solution set becomes complex as the number of nodes increases, with up to eight distinct regions on a plot of the solution space for two obstacles and four nodes. The researcher uses a few different simulated obstacles for observation of the feasible solutions and feasible regions. The user should keep in mind that, in exceptional cases, no feasible solutions may be found. The user should also be aware that there are infinitely many possible solutions in a feasible region, even though several are calculated via the algorithm.

Table 9. Simulation Results

Scene		Median [msec]	Observed Feasible Solutions and Regions
#1, 1 Obst. 2 Nodes		3.2	2 Feasible Regions: 1-2 Feasible Vertices (FV)
#2, 1 Obst. 3 Nodes		3.8	2 or 3 Feasible Regions
			2 Regions: 2-4 FV
			3 Regions: 1-4 FV
#3, 2 Obst. 3 Nodes		5.4	2 to 5 Feasible Regions
			2 Regions: 4 FV
			3 Regions: 5 FV
			4 Regions: 3-6 FV
			5 Regions: 1-6 FV
#4, 2 Obst. 4 Nodes		5.8	3 to 8 Feasible Regions
			3 Regions: 4 FV
			4 Regions: 4 FV
			5 Regions: 2-6 FV
			6 Regions: 2-13 FV
			7 Regions: 4-7 FV
			8 Regions: 7 FV
#5, 1 Obst. 4 Nodes		4.4	3 or 4 Feasible Regions
			3 Regions: 2-7 FV
			4 Regions: 1-6 FV

A disadvantage is that the algorithm requires an input based on a guess, potentially. That is, the maximum communication range of the relay vehicle is a scalable unknown variable. By default, the fixed length of the test region is set at:

$$\text{maximum comm range} = 20\sqrt{2} \times \pi \quad (10)$$

Results based on a guess might include questionable go-to point solutions, because vertices sometimes lie far apart from one another. However, the cost function evaluation step prioritizes better go-to point solutions in terms of cost, which tend to be near the system centroid. Even so, it is best for the user to calibrate the algorithm by entering a reasonable maximum range—if the default is not reasonable.

A commonplace finding is that algorithm-generated scenes often require no relay at all, having all nodes on the same side of the obstruction and within the battlespace. In these cases, as noted in Section 0, the algorithm returns Point M. In general, the algorithm finds solutions which are at best no more efficient than the midpoint, or its multiple-node analogue—the centroid. The researcher proposes that it is realistic to sometimes find all nodes on the same side of the obstruction in static, point-in-time snapshots of aerial relay missions.

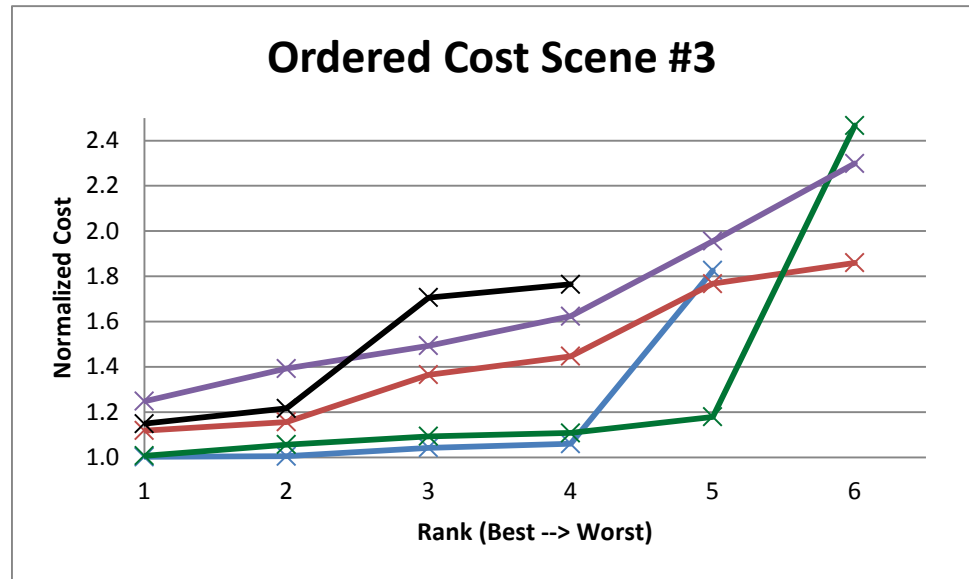


Figure 27. Cost Avoidance Charts.

Conclusion

The researcher has addressed extensions to pre-existing architecture by writing an enhanced algorithm and has found the algorithm to be original among optimization methods in the literature. A human operator can run the algorithm in the background to implement multiple-vehicle and multiple-obstruction scenarios for a relay that effectively meets the operator's requirements. Furthermore, the solution is accessible and can be replicated. In order to enhance the execution speed and consolidate information about multiple feasible regions, this paper has described the results of waypoint planning of a system of cooperative UVs which are motionless.

In the real-time operational mission, the relay adjusts its trajectory autonomously to maintain communications, based on the UVs' dynamic positions relative to terrain features. A conservative time step for the simulation is twice per second, based on preliminary results. MATLAB will handle the dynamic simulation, and the solution should also be prototyped for operational test after hardware integration. The researcher's new rule is used for demonstration; demonstration in flight test is the objective of future research. Activity is planned and ongoing for application of the algorithm in real-time.

References

- [1] U. S. Navy, “The Navy Unmanned Surface Vehicle (USV) Master Plan,” 2007.
- [2] M. R. Endsley, “Autonomous Horizons: System Autonomy in the Air Force—A Path to the Future,” Washington, D.C., 2015.
- [3] Y. Choi, M. Pachter, and D. Jacques, “Optimal Relay UAV Guidance—A New Differential Game,” in *Conf. Decision Contr.*, 2011, pp. 1024–1029.
- [4] Q. Ali, N. Gageik, and S. Montenegro, “A Review on Distributed Control of Cooperating Mini UAVs,” *Int. J. Artif. Intell. Appl.*, vol. 5, no. 4, pp. 1–13, 2014.
- [5] J. Gray, “Design and Implementation of a Unified Command and Control Architecture for Multiple Cooperative Unmanned Vehicles Utilizing Commercial Off the Shelf Components,” Air Force Inst. of Technology, 2015.
- [6] C. Tanil, C. Warty, and E. Obiedat, “Collaborative Mission Planning for UAV Cluster to Optimize Relay Distance,” in *Aerosp. Conf. Proc.*, 2013, pp. 1–11.
- [7] T. J. Shuck, “Development of Autonomous Optimal Cooperative Control in Relay Rover Configured Small Unmanned Aerial Systems,” Air Force Inst. of Technology, 2013.
- [8] J. D. Rosal, “Centralized Cooperative Control for Route Surveillance with Constant Communication,” Air Force Inst. of Technology, 2009.
- [9] A. S. Clare, M. L. Cummings, and J. P. How, “Operator Objective Function Guidance for a Real-Time Unmanned Vehicle Scheduling Algorithm,” *J. Aerosp. Comput. Information, Commun.*, vol. 9, no. 4, pp. 161–173, 2012.
- [10] B. Wasserman, H. Ludwig, J. Laredo, K. Bhattacharya, and L. Pasquale, “Distributed Cross-Domain Change Management,” in *Int. Conf. Web Services*, 2009, pp. 59–66.
- [11] D. K. Ahner and C. R. Parson, “Workshop Report: Test and Evaluation of Autonomous Systems,” Wright-Patterson AFB, OH, 2016.
- [12] B. Iannotta, “Sharp Intelligence, Tight Budget,” *Aerosp. Am.*, vol. 53, no. 2, pp. 24–27, Feb. 2015.
- [13] G. Lai and T. Lamoureux, “Development of Measures of Effectiveness and Performance from Cognitive Work Analysis Products,” Ottawa, ON, 2012.
- [14] I. Bekmezci, O. Sahingoz, and Ş. Temel, “Flying Ad-Hoc Networks (FANETs): A Survey,” *Ad Hoc Networks*, vol. 12, no. 4, pp. 1–17, 2013.
- [15] M. Garzón, J. Valente, D. Zapata, and A. Barrientos, “An Aerial-Ground Robotic System for Navigation and Obstacle Mapping in Large Outdoor Areas,” *Sensors (Switzerland)*, vol. 13, no. 1, pp. 1247–1267, 2013.

- [16] K. S. Seah, "System Architecture of Small Unmanned Aerial System for Flight Beyond Visual Line-of-Sight," Air Force Inst. of Technology, 2015.
- [17] T. Diamond, A. Rutherford, and J. Taylor, "Cooperative Unmanned Aerial Surveillance Control System Architecture," Air Force Inst. of Technology, 2009.
- [18] M. J. Vincie, "Airborne Wireless Communication Modeling and Analysis with MATLAB," Air Force Inst. of Technology, 2014.
- [19] D. H. Choi, S. H. Kim, and D. K. Sung, "Energy-efficient Maneuvering and Communication of a Single UAV-based Relay," *IEEE Trans. Aerosp. Electron. Syst.*, vol. 50, no. 3, pp. 2320–2327, 2014.
- [20] B. Crawford, R. Soto, R. Cuesta, M. Olivares-su, F. Johnson, and E. Olgu, "Two Swarm Intelligence Algorithms for the Set Covering Problem," in *9th Int. Conf. Software Eng. Applicat.*, 2014, pp. 60–69.
- [21] R. Soto, B. Crawford, and R. Olivares, "The Complexity of Designing and Implementing Metaheuristics," *HCI Int.*, 2015.
- [22] E. Arvelo, E. Kim, and N. C. Martins, "Maximal Persistent Surveillance under Safety Constraints," in *Proc. IEEE Int. Conf. Robot. Autom.*, 2013, pp. 4048–4053.
- [23] D. Davendralingam, "A Robust Portfolio Optimization Approach to System of System Architectures," *Syst. Eng.*, vol. 18, no. 3, pp. 269–283, 2015.
- [24] J. Hansen, M. Pachter, D. Jacques, and P. Blue, "Optimal Guidance of a Relay MAV for ISR Support beyond Line-of-Sight," in *Guid. Navig. Contr. Conf. and Exhibit*, 2008, pp. 1–27.
- [25] S. Hayat, E. Yanmaz, and R. Muzaffar, "Survey on Unmanned Aerial Vehicle Networks for Civil Applications: A Communications Viewpoint," *IEEE Commun. Surv. Tutorials*, vol. 18, no. 4, pp. 2624–2661, 2016.
- [26] J. T. Hing, K. W. Sevcik, and P. Y. Oh, "Improving Unmanned Aerial Vehicle Pilot Training and Operation for Flying in Cluttered Environments," in *Int. Conf. Intell. Robots Syst.*, 2009, pp. 5641–5646.
- [27] D. Selva and E. Crawley, "VASSAR: Value Assessment of System Architectures Using Rules," in *Aerosp. Conf. Proc.*, 2013.
- [28] N. Hitomi and D. Selva, "Experiments with Human Integration in Asynchronous and Sequential Multi-agent Frameworks for Architecture Optimization," *Procedia Comput. Sci.*, no. 44, pp. 393–402, 2015.
- [29] N. M. Jodeh, "Optimal UAS Assignments and Trajectories for Persistent Surveillance and Data Collection from a Wireless Sensor Network," Air Force Inst. of Technology, 2015.

- [30] R. Lin and Y. Li, "A Novel Distributed Automatic Resource Allocation Scheme in Cooperative Relay Network," in *3rd Int. Conf. Consumer Electron. Commun. Networks*, 2013, pp. 23–25.
- [31] J. H. Kim, J.-W. Kwon, and J. Seo, "Multi-UAV-Based Stereo Vision System without GPS for Ground Obstacle Mapping to Assist Path Planning of UGV," *Electron. Lett.*, vol. 50, no. 20, pp. 1431–1432, 2014.
- [32] N. M. Jodeh, R. G. Cobb, and R. A. Livermore, "Optimal Airborne Trajectories for Data Collection from Wireless Sensor Networks by Direct Collocation Methods," in *AIAA Guid. Nav. Contr. Conf.*, 2015, pp. 1–14.
- [33] H. Jordan, "AFRL COUNTER team wins Air Force Outstanding Scientist Team Award," *Wright-Patterson Air Force Base News*, 13-Aug-2008.
- [34] G. P. Potdar, R. C. Thool, and S. G. Singhji, "Comparison of Various Heuristic Search Techniques for Finding Shortest Path," *Int. J. Artif. Intell. Appl.*, vol. 5, no. 4, pp. 63–74, 2014.
- [35] M. Pachter, J. Hansen, D. Jacques, and P. Blue, "Optimal Guidance of a Relay Aircraft to Extend Small Unmanned Aircraft Range," *Int. J. Micro Air Veh.*, vol. 2, no. 3, pp. 157–180, Sep. 2010.
- [36] J. T. Hing and P. Y. Oh, "Mixed Reality for Unmanned Aerial Vehicle Operations in Near Earth Environments," in *Int. Conf. Intell. Robots Syst.—Proceedings*, 2010, pp. 2509–2510.
- [37] J. I. Abeygoonewardene, "Scaling Flight Tests of Unmanned Air Vehicles," Air Force Inst. of Technology, 2006.
- [38] I. Quilez, "Sphere Ambient Occlusion," *Fractals, Computer Graphics, Mathematics, Demoscene and More*, 2006. [Online]. Available: <http://www.iquilezles.org/www/articles/sphereao/sphereao.htm>. [Accessed: 01-Jan-2016].

Appendix B: Form 5028

TEST PROJECT TECHNICAL AND SAFETY REVIEW					
SECTION I		PROJECT INFORMATION			
Test Project Title		Overall Risk Level	Control #	Test Dept.	
Positioning Algorithm for Cooperative C2 Architecture		LOW	1612	ENV	
Typed Name and Grade	Signature	Email Address	Phone Number	Date	
Principal Investigator					
Dr. David Jacques		david.jacques@afit.edu	X3329		
Alt Principal Investigator					
Dr. John Colombi		john.colombi@afit.edu	X3347		
Ms. Laura Lucas		laura.lucas@afit.edu			
Safety Pilot					
Mr. Rick Patton		rick.patton@afit.edu	X4911		
SECTION II		TECHNICAL/SAFETY REVIEW			
Typed Name and Rank	Position	Signature	Date	Coord. Comments?	
AFIT Flight Test Safety Officer				Yes	No
Chad S. Hale, Lt Col	AFIT FTSO				
Rob M. Eninger, Lt Col	AFIT/ENV				
Scott J. Pierce, Maj	AFIT/ENG				
SECTION III		COORDINATING COMMENTS			
(Reviewer should initial next to any comments)					

PROJECT DESCRIPTION

1. SUMMARY OF CHANGES

- a. The architecture behind this repeat test shares almost complete commonality with Jeremy Gray's Cooperative Control Architecture (AFIT 5028 #1504, 20 Oct 2015), which has been flight tested on two previous occasions —with the same ground control station (GCS) software, the same autopilot, the same wireless network system for command and control (C2) communications, and the same type of aircraft and ground vehicles. This flight test has a *significantly modified* set of test objectives from Jeremy Gray's thesis. It will focus entirely on the autonomous communication relay concept, and it constitutes a follow-on thesis activity to Gray's work. The GCS uses a unique algorithm (Python script), which is new for this test. As it was for Gray's flight test, the single air vehicle will be placed in Guided mode, with the waypoint determined by the Python script running on the ground station.
- b. This test has one less identified hazard than Gray's 2015 test. Since only one air vehicle will be used, the hazard associated with impacting another vehicle was removed.
- c. The *significant modifications* are a second ground vehicle and a virtual obstacle.

2. BACKGROUND

- a. Description:

These tests are developed to measure performance of and network support for heterogeneous cooperative unmanned vehicles in teams of three during a specific mission. The mission is to relay a C2 communication link from a GCS through an intermediate relay vehicle to two remote vehicles, which may be out of range of the GCS and/or have an obstruction blocking the link.

These tests will utilize a single (1) 3D Robotics X8 multi-rotor aircraft "relay," and two (2) Traxxas Remote Controlled (RC) trucks, all equipped with geolocation (GPS) to collect data about the communication relay mission. The aircraft falls under the small Unmanned Aerial System (UAS) Group 1 category, and the trucks will be indicated as Unmanned Ground Vehicles (UGVs). The team of three vehicles is monitored and controlled from a central GCS, which is comprised of an operator, a laptop with Mission Planner ground control software for the X-8 multi-rotor, DroneKit for receiving ground vehicle telemetry, and a Python Script for calculating guided waypoints for the X-8. This system has been tested and proven on the ground with two UGVs before flight testing.

The objective of these tests is to collect the required telemetry from the three vehicles to characterize the relative duration of uninterrupted C2 time for the UGVs during the communication relay mission. The required flight/ground data, including geo-location, attitude, and time, will be transmitted to the GCS from each vehicle's C2 transceiver. This data will be saved by the GCS software. The UGVs' data will be saved on the first laptop, and the UAS relay data will be saved on the second laptop. The data will be post-

processed to determine the communication status of the relay vehicle relative to the rover vehicles and the GCS.

The X8 multi-rotor air vehicle will be conducting maneuvers controlled by the onboard Pixhawk autopilot connected to the ground using a 2.3~2.5 GHz Wave Relay mobile ad-hoc network (MANET) communications modem. For communications redundancy and safety, a separate 2.4 GHz RC radio link is also integrated into the aircraft system. The GCS contains the flight plan processing, to determine the waypoint commands sent to the relay vehicle to perform the communication relay mission. The RC trucks will be RC controlled in manual mode.

b. Purpose:

The purpose of these tests is to collect data for a master's research thesis in pursuit of a degree in Systems Engineering at Air Force Institute of Technology (AFIT/ENV). These tests are designed to verify the intended capabilities of a relay positioning algorithm.

c. List of AFIT and non-AFIT assets at risk:

- i. One (1) 3D Robotics X8 multi-rotor UAS with Pixhawk autopilot and Wave Relay communication node
- ii. Two (2) Traxxas RC Truck UGVs with Pixhawk autopilots and Wave Relay communication nodes
- iii. Wave Relay ground node
- iv. AFIT Personnel (a mix of military and civilian staff and students)
- v. A vehicle and trailer owned and operated by CESI (civilian contractor)
- vi. Adjacent facilities around airfield

d. Location of test:

Primary: Wright-Patterson Air Force Base, OH

Backup: Himsel Airfield, Camp Atterbury Joint Maneuver Training Center, IN

e. Planned dates of the test:

31 OCT 2016-4 NOV 2016

f. Number of projected flights during the test period:

Approximately 3-5 flights during the test period.

3. MISHAP RESPONSIBILITIES

- a. Should an incident occur in which the UAS is damaged or destroyed, the AFIT Flight Test Safety Officer (FTSO) will be notified via the After Action Report.
- b. WPAFB. If an incident occurs in which property or personnel on WPAFB is damaged/injured, the installation emergency 911 service will be notified immediately. In addition, the AFIT Safety Office will be notified within 5 working days per AFIT's Mishap Notification Procedures. Serious mishaps must be reported immediately.
AFIT Safety Office (Tim Thomas, 255-3636 x3627, Cell Phone 937-479-9715)

- c. If an incident occurs in which property owned by the Army (backup/alternate location only), or civilians is damaged and/or any personnel are injured, the Camp Atterbury Range Control will be notified immediately. That office will make a determination on whether or not to initiate an investigation.

Camp Atterbury Range Control (812) 526-1351

- d. If an injury or illness results in lost duty time or hospitalization, then the AFIT Safety Office will be notified immediately. The Principal Investigator will be responsible for submitting any of the required mishap reports as defined in AFIT's Mishap Notification Procedures. For further information, refer to the Mishap Notification Procedures posted in the Safety folder under the 'Mishap Reporting' tab on the AFIT Intranet site.

4. TEST OBJECTIVES

- a. Objective 1 – Verify Vehicles' Manual and Guided Mode Response to Gain Settings
- b. Objective 2 – Demonstrate Multi-Rotor UAS Automatic Positioning

5. TEST ITEM DESCRIPTION

- a. Vehicle description
 - i. X8 Multi-rotor
 - 1. Vendor:
 - a. 3D Robotics, Berkeley, CA
 - 2. Model:
 - a. X8
 - 3. Characteristics:
 - a. Dimensions – 13.7" x 20.1" x 11.8"
 - b. Propeller Size – 11x4.7 SF (4), 11x4.7 SFP (4)
 - c. Weight – 10 lbs.
 - 4. Payload description:
 - a. none
 - 5. Avionics description (autopilot):
 - a. Pixhawk and loaded firmware
 - 6. Power plant:
 - a. 800KV brushless out runner motor
 - b. 3D Robotics 2A Speed Controller
 - c. 3D Robotics Power Distribution Board
 - d. 4S 14.8V 10,000 mAh 10C LIPO battery
 - 7. Datalink:
 - a. Wave Relay MANET Transceiver Node (2.3 – 2.5 GHz),
 - b. FrSky Taranis (RC) transmitter with FrSky D8R-II plus receiver (2.4 GHz)
 - 8. Range:
 - a. Visual Line-of-Sight (LOS) distances only.
 - 9. Airframe Modifications
 - a. None
 - ii. Traxxas E-Maxx Truck

1. Vendor
 - a. Traxxas
2. Model
 - a. E-Maxx Truck
3. Characteristics:
 - a. Dimensions – 16” x 16” x 10”
4. Payload description:
 - a. none
5. Flight computer (autopilot):
 - a. Pixhawk and loaded firmware
6. Power plant system:
 - a. 2200KV brushless out runner motor
 - b. Castle waterproof speed controller
 - c. 7S 9.4V 5000 mAh NiMH battery (speed control, flight computer)
 - d. 3S 11.1V 2200 mAh LiPo battery (wave relay)
7. Datalink:
 - a. Wave Relay MANET Transceiver Node (2.3 – 2.5 GHz)
 - b. FrSky Taranis (RC) transmitter with FrSky D8R-II plus receiver (2.4 GHz)
8. Range: Visual Line-of-Sight (LOS) distances only
9. Airframe Modifications
 - a. Plastic housing replaced with wooden platform for flight computer, data link modules, Wave Relay battery, and other sensors.

b. Flight Conditions

- i. Launch Method

Vehicles will be manually controlled by the safety pilot during launch. Multi-rotor aircraft will perform a vertical takeoff in manual mode from a level stationary position away from personnel and equipment. Both the pilot and safety observer will maintain positive communication and ensure the aircraft is free from obstructions.
- ii. Method of Piloting

Manual pilot control will be used for takeoff and landing. This will be switched over to autopilot control when UAS achieves normal operating altitude range, which is monitored on the GCS. Flight plans are uploaded to the GCS prior to flight. Autopilot commands are provided by ground station or flight computer. Safety pilot can take manual control at any time during operations. If communications between GCS and UAS are lost, the aircraft autopilot is pre-programmed to return to the rally point and maintain altitude at that point.
- iii. Recovery Method

Aircraft will be manually controlled by the safety pilot during recovery. All landings will be completed on a level surface away from equipment and personnel for multi-rotor aircraft.

iv. Flight Altitude(s)

The maximum allowable altitude at WPAFB is 130 meters above ground level (AGL), or lower if restricted by airspace limitations. The minimum operating altitude is set at 3 meters AGL for multi-rotor aircraft. Planned altitudes for this test are 7-10 m. At all altitudes, the safety pilot shall maintain visual LOS. Altitudes are monitored on the GCS.

v. Flight Range

Visual LOS distances only. Maximum tested range of Radio Control (RC) radio link is one mile. Maximum specified range of Autopilot Command link is two miles.

vi. Flight Duration

Maximum duration of flight with charged batteries has been tested to 20 minutes.

vii. Flight Speed

Maximum speed setting for this test will be 5 m/sec (18 kph).

viii. Weather Conditions

Operation is not allowed under rain or when lighting warning is issued. Electronics are not shielded and water will result to short circuits in the system. Operation is limited to a maximum wind speed (including gusts) of 28 kph, with a cross wind of less than 28 kph.

c. Failure Modes

A complete list of failure modes is found in the Small Multi-rotor Air Worthiness Attachment Memo, 2016 Update.

d. Describe the test facilities to be used:

- i. WPAFB Area B: The (primary) SUAS airfield is maintained by AFRL and located adjacent to the AF museum. This airfield is in good condition and is often used by AFRL and the RAMS model aircraft club. See *figure 1*.
- ii. Camp Atterbury: The (alternate) SUAS airfield is fully functional airfield located on Army property and under restricted airspace. Himsel Army Airfield has a single north/south runway with an adjacent parking apron. An alternate SUAS airstrip, approximately one mile east of Himsel airfield, has been recently paved providing an excellent surface for takeoff and landing. The SUAS field is located in an isolated area of the base adjacent to the weapons range. SUAS operations at both Himsel airfield and the SUAS field are controlled by the Himsel tower controller.

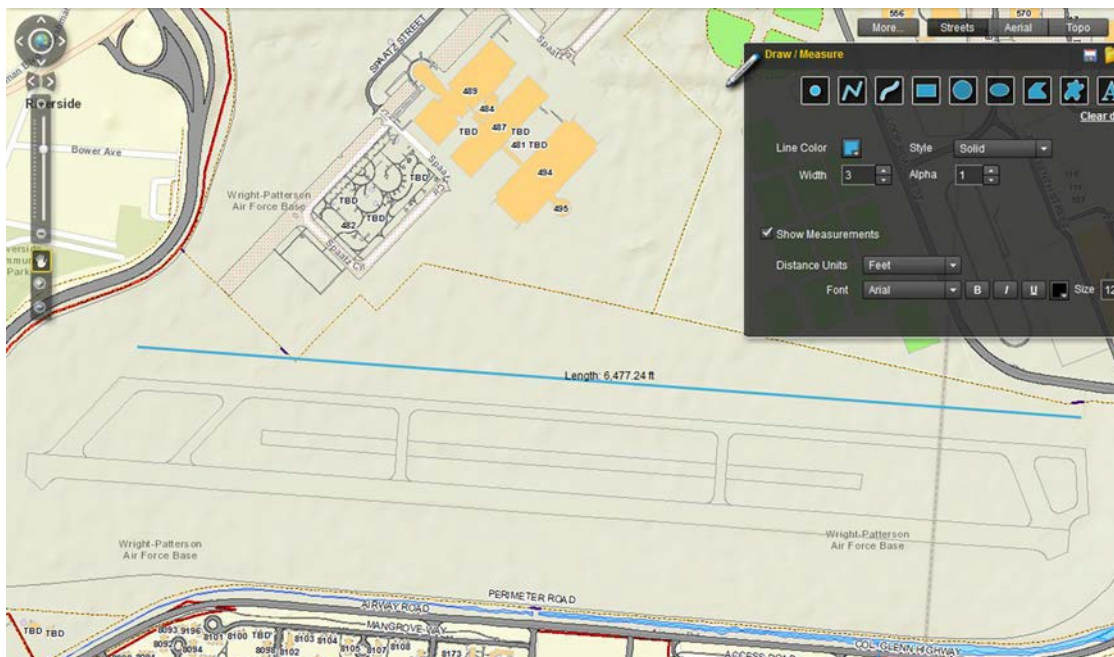


Figure 1: WPAFB UAS Flight area



Figure 2: Camp Atterbury Himsel Field Test Area

6. SYSTEM MATURITY

a. Describe testing that supports readiness:

The integrated architecture has been tested, and verified in two previous flight tests, including the same Wave Relay communication system and GCS software. The new algorithm has been tested on the ground. Additionally, AFRL utilizes the Wave Relay communication system as a C2 link for performing similar autonomous aircraft research, which increases the validity of using this system for a C2 link. This C2 link's available frequency band does overlap with that of the safety pilot's RC link. As a primary safety measure, the script on the GCS laptop includes a safety switch, which has been verified to ensure the control of the aircraft defers to the RC link when the safety pilot switches the mode to manual. As worst case scenario, the overlap in frequency spectrums has been verified in flight not to impede the ability of the RC radio to maintain or regain control of the vehicle. This is attributed to the safety pilot radio's use of frequency hopping to maintain a strong signal and the reduction of the C2 links to the lower end of the band.

b. Previous lessons learned:

In similar research, the C2 script run on the GCS did not allow the safety pilot to place the vehicle in manual mode. This was caused by a mode change command sent at a high frequency from a command script over the C2 link to the vehicle. This high frequency command did not allow the autopilot enough time to register the change in the RC mode channel for the safety pilot radio. This issue has been solved through the addition of a logic loop in the command script, which does not allow the script to send a new guided command if the RC mode channel is receiving a manual mode command. This solution has been tested on the ground using two UGV performing formation flocking.

Additionally, the safety pilot has gained experience how to quickly regain control if the command script inadvertently commands the vehicle into guided mode.

c. Authorized flight:

This flight requires authorization under the AFIT MFR which has been reviewed and approved by the Airworthiness office at AFLCMC.

Small Multi-rotor: Ref#: AFIT-R0013 Signed: 17 Oct 2016, Expires: 16 Oct 2018

ORM Checklist Form

Date: _____

Control #: _____

	GREEN	YELLOW	RED
Crew Rest	Good	Marginal	Poor
Crew/Personal Concerns	None	Minor	Major
Primary Crew Qualified	All Qualified	1 Unqualified	2+ Unqualified
7+ Days TDY/Leave	2 nd duty day back or later	1 st duty day back	
Perceived Scheduling Pressure	None	Some	Significant Pressure to Complete Mission
Duty Day	<8 hours	>8 hrs.	>12 hours
Showtime	0600-1600	0300-0600/1600-2200	2200-0300
Planning Changes (Last 24 hrs.)	Minimal/No impact	Minor	Major
Mission Complexity	Low/Normal	Demanding	Extremely Demanding
Test Mission/Safety Risk	Low	Medium	High
Cross Winds/Wind Speed	<10 kts	10-13 kts	13-15 kts
Time of Day	Day	Night	0200-0500 TO/Landing
Airframe Modification	Minor	Significant	Severe
Maturity-Hardware/Software	Nothing New	1 st Flight of Hardware/Software Mod	1 st Flight of NEW Hardware/Software
Additional Risk Not Addressed	Low	Medium	High

This checklist is to be briefed at the beginning of each test day.

Each green box is 0 points. Each yellow box is 1 point. Each red box is 2 points.

A score of 0-3: Attempt to mitigate any red boxes to reduce the risk. Test director's discretion to continue the mission.

A score of 3-5: If unable to lower the score to 0-3, it is the Principal Investigator's discretion to continue the mission.

A score of 6 or higher: If unable to lower the score, it is the AFIT FTSO's discretion as to whether or not to continue the mission.

IF YOU ARE NOT READY TO FLY... DON'T!

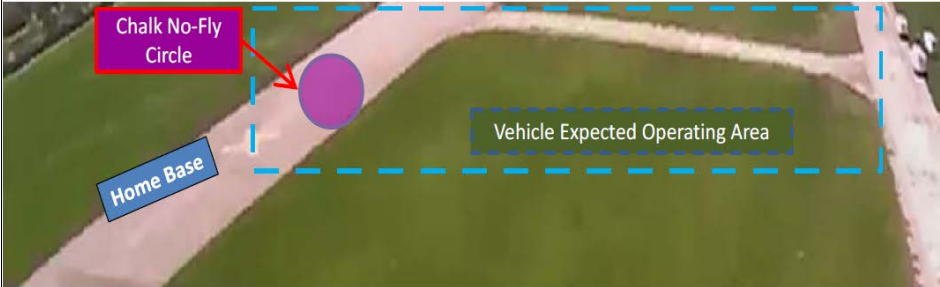
TEST DESCRIPTION

Objective 1 – Verify Vehicles’ Manual and Guided Mode Response to Gain Settings

TEST SCENARIO 1														
Description	The objective of this test is to verify that the UGVs and UAS respond appropriately to commands. The UGVs will be tested in manual mode, and the UAS will be tested in manual and guided modes. Gain setting tweaks will be applied as necessary until working gain settings are achieved.													
Stakeholders	Laura Lucas													
Success Criteria	<p>Successful if:</p> <p>The following modes are tested with the specified parameters.</p> <table><tr><th>Mode</th><th>Alt</th><th>Path Size</th></tr><tr><td>Radial Manual</td><td>7-10 m</td><td>Pilot Determined</td></tr><tr><td>Auto-Waypoints</td><td>7-10 m</td><td>10 m Box Path</td></tr><tr><td>Truck Manual</td><td>NA</td><td>Pilot Determined</td></tr></table>		Mode	Alt	Path Size	Radial Manual	7-10 m	Pilot Determined	Auto-Waypoints	7-10 m	10 m Box Path	Truck Manual	NA	Pilot Determined
Mode	Alt	Path Size												
Radial Manual	7-10 m	Pilot Determined												
Auto-Waypoints	7-10 m	10 m Box Path												
Truck Manual	NA	Pilot Determined												
Evaluation Criteria	<p><u>Satisfactory if:</u></p> <ol style="list-style-type: none">1. The safety pilot understands how the radial manual mode will respond and can use manual mode successfully.2. The safety pilot and team understand how the UAS will fly to the specified waypoints. <p>The safety pilot (Rick Patton) and the advisor (Dr. David Jacques) have authority over whether or not to proceed. If either individual does not give their consent to proceed, no more flight objectives will be accomplished.</p>													
Data Requirements	none													
Algorithms	none													
Expected Results	<ol style="list-style-type: none">1. The vehicles will move in manual mode2. The UAS will execute the waypoint and all vehicles will be recovered													
Assets	<ol style="list-style-type: none">1. AFIT X8 multi-rotor with Pixhawk autopilot and mission planner GCS2. AFIT Wave Relay MANET nodes													

Test Methodology	Test Procedures <ol style="list-style-type: none"> 1. BEFORE TAKEOFF: <ol style="list-style-type: none"> a. Setup GCS and operating area IAW AFIT Document 5028. b. Plan desired flight path of UAS to ensure entire test is conducted in front of test team with no direct overhead flights. c. Complete all required preflight checklists for UAS. d. Check that weather is within limits and determine launch/recovery locations and headings. e. Open airspace and obtain launch approval. 2. LAUNCH: <ol style="list-style-type: none"> a. Ensure that all present personnel are aware of launch. b. Ensure, at a minimum, one assigned observer will maintain visual contact with the UAS and can assist safety pilot. c. Position multi-rotor for ground launch at desired rally position. d. Arm multi-rotor. e. Safety pilot performs manual takeoff of multi-rotor. f. Safety pilot announces that aircraft is airborne. g. Climb to pre-briefed transition altitude. h. Transition to pre-briefed test-point entry position. 3. EXECUTE TEST POINTS: <ol style="list-style-type: none"> a. Safety pilot flies in radial manual mode until he gives go-ahead. b. Set waypoints one at a time on vehicle autopilot. c. Safety pilot switches into guided mode. d. Allow vehicle to perform flight plan and observe flight characteristics. e. Safety pilot switches into manual mode. 4. RECOVERY: <ol style="list-style-type: none"> a. Navigate aircraft to pre-briefed recovery transition location. b. Transition aircraft to safety pilot control or observation. c. Ensure landing area is clear of personnel and equipment! d. Begin descent and entry into landing pattern. e. Safety pilot announces landing to all present personnel. f. Execute recovery. 5. AFTER RECOVERY: <ol style="list-style-type: none"> a. Close airspace with range control. b. Remain clear of propeller. c. Disarm multi-rotor. d. Disconnect battery prior to moving aircraft by hand. e. Power off RC transmitter (as required).
-------------------------	---

Objective 2 – Demonstrate Multi-Rotor UAS Automatic Positioning

TEST SCENARIO 2	
Description	<p>The objective of this test is to determine the algorithm's capability to autonomously position the relay vehicle relative to the rover vehicles and a virtual obstacle. This will be accomplished through the collection of GPS position and attitude measures for each vehicle in the vehicles' telemetry logs on the GCS. The purpose of collecting this data is to determine the relative duration of uninterrupted C2 time for the UGVs during the communication relay mission. In other words, this data is collected to determine the algorithm's effects on teams of heterogeneous vehicles consisting of two UGVs and a multi-rotor UAS when an obstacle is present. The factors tested include the path taken by the rover vehicles around a chalk circle, which represents the surface of a simulated obstacle. The test will be accomplished as though there were a physical obstacle obstructing communication and transit through the area marked out with chalk.</p> <p>During the test, the rover vehicles will be controlled in manual mode by one operator, allowing the safety pilot to stay focused on the UAS. The rover vehicles will be moved away from the GCS with the transmitter power set low, until the GCS loses the ability to communicate with them, as indicated by the percent of telemetry packets received in the GCS software. The relay vehicle will then be moved to the centroid or average position of the GCS and rover vehicles, and communication will be reestablished. The relay vehicle will autonomously navigate to guided waypoints sent from a command algorithm run on the GCS. This will be completed for a multi-rotor UAS at 4-6 m altitude following UGVs. The vehicles will operate at 2-5 m/s. The region of operation is displayed below.</p>  <p>The image is an aerial photograph of a grassy field with a paved path. A purple circle is drawn on the grass, labeled 'Chalk No-Fly Circle' with a red arrow. A blue rectangle is labeled 'Home Base'. A dashed blue line outlines a larger area labeled 'Vehicle Expected Operating Area'.</p>
Stakeholders	Laura Lucas
Success Criteria	<p>Successful if:</p> <p>Required data was collected in accordance with the communication relay mission description.</p> <p>Note: Since the UAS is not required to land, Objective 2 flight test may be accomplished multiple times within the maximum duration of flight.</p>

Evaluation Criteria	<p><u>Satisfactory if:</u></p> <ol style="list-style-type: none"> 1. The relay vehicle maintains altitude outside the circle, with minimal deviation, and without demonstrating aggressive or dangerous maneuvering to accomplish the mission. 2. The relay vehicle demonstrates a relationship with the rovers in which it tends to move into a position above the UGVs' average position (middle of the team), unless it is prevented by the circle. 3. All safety features of the system perform adequately to retrieve control of each vehicle at any time. <p>The safety pilot (Rick Patton) and the advisor (Dr. David Jacques) has authority over whether or not to proceed until all data have been collected.</p>
Data Requirements	<p>Required</p> <ol style="list-style-type: none"> 1. Telemetry from UGVs. 2. Telemetry from multi-rotor UAS.
Algorithms	<ol style="list-style-type: none"> 1. Python code for positioning
Expected Results	<ol style="list-style-type: none"> 1. Telemetry data collected
Assets	<ol style="list-style-type: none"> 1. AFIT X8 multi-rotor 2. Two (2) AFIT Traxxas RC Trucks 3. AFIT Wave Relay MANET nodes
Test Methodology	<p>Test Procedures</p> <ol style="list-style-type: none"> 1. BEFORE TAKEOFF: <ol style="list-style-type: none"> a. Setup GCS and operating area IAW AFIT Document 5028. b. Preprogram the first test point for the relay vehicle. c. Complete all required preflight checklists for UAS. d. Check that weather is within limits and determine launch/recovery locations and headings. e. Open airspace and obtain launch approval. 2. LAUNCH: <ol style="list-style-type: none"> a. Ensure that all present personnel are aware of launch. b. Move UGVs to operating area and initialize. c. Start positioning algorithm on GCS. d. Position multi-rotor for ground launch at desired rally position. e. Arm multi-rotor. f. Safety pilot performs manual takeoff of multi-rotor. g. Safety pilot announces that aircraft is airborne. h. Climb to pre-briefed transition altitude. i. Transition to pre-briefed test-point operating area.

	<p>3. EXECUTE TEST POINTS:</p> <ul style="list-style-type: none"> a. Set parameters for test point. b. Manually move UGVs. c. Allow UGV positions to update on map. d. Switch UAS over to guided mode to start mission. e. Document start time. f. Allow UAS to perform maneuvers for at least 10 minutes. g. Document stop time. h. Switch UAS to manual mode. <p>4. RECOVERY:</p> <ul style="list-style-type: none"> a. Navigate aircraft to pre-briefed recovery transition location. b. Transition aircraft to safety pilot control or observation. c. Ensure landing area is clear of personnel and equipment. d. Begin descent and entry into landing pattern. e. Safety pilot announces landing to all present personnel. f. Execute recovery. g. Stop algorithm. <p>5. AFTER RECOVERY:</p> <ul style="list-style-type: none"> a. Ensure telemetry on GCS is saved. b. Close airspace with range control. c. Remain clear of propeller. d. Disarm multi-rotor and UGVs. e. Disconnect battery prior to moving vehicle by hand. f. Power off RC transmitters (as required).
--	--

SAFETY PLAN

1. QUALIFICATION AND TRAINING

- a. Dr. David Jacques – Lead Faculty member of the AFIT UAS program. Experienced with UAS simulation and real world testing. Successfully completed the Camp Atterbury Range Safety Course.
- b. Dr. John Colombi – SENG-651 UAS Course instructor. Several years' experience with AFIT UAS simulations and testing. Successfully completed the Camp Atterbury Range Safety Course.
- c. Mr. Rick Patton – CESI employee and safety pilot with many years of experience flying RC aircraft in congested air space. Owns and operates hobby RC aircraft. Successfully completed the Camp Atterbury Range Safety Course.
- d. Mr. Jeremy Gray – ANT center contract employee and Wave Relay operations instructor. Successfully completed this test for his (predecessor) thesis. Experience with operating MAVProxy and Mission Planner GCS software. Flight simulator training with small UAS (Sig Rascal). Experienced with maintaining UAS hardware. Successfully completed the Camp Atterbury Range Safety course.
- e. Ms. Laura Lucas– AFIT student performing thesis research. SENG-651 class project experience with AFIT UAS architecting, integration and testing. Successfully completed the Camp Atterbury Range Safety Course.

2. GENERAL MINIMIZING CONDITIONS

The following general minimizing procedures and considerations will be followed for the duration of this flight test program:

1. All test flights will be conducted in day Visual Meteorological Conditions (VMC) conditions.
2. Communications will be maintained between the ground operator, safety observers, safety pilot and test crews at all times.
3. If flight operations occur at the alternate location, the safety pilots will maintain positive radio communications with Himsel AAF Unicom at all times.
4. Flying over non-participating personnel and facilities will be avoided.
5. Hardware fail-safes will be utilized to minimize impact of lost communications between the aircraft and RC transmitter.
6. To minimize probability of in-flight low battery power, all flight durations will be timed and remain below 20 minutes. Thereafter, the flown battery will be replaced by a fully charged battery before the next test flight can be continued. All batteries will be charged prior to flight testing and marked charged.
7. Personnel without assigned roles for test will be observers of flight operations while outside flight test trailer. Minimize all unnecessary conversations and distractions during flight.
8. A multi-purpose fire extinguisher is located in the rear of the trailer in the event of a fire.
9. Utilize “Knock-It-Off” and “Terminate” procedures IAW AFI 11-214 paragraph 3.4.
10. Minimum altitude for quadrotor flight test is 3 meters AGL unless a lower altitude is approved for test requirements.
11. To minimize exposure of UAS flying overhead, test crew will only enter the UAS landing strip to change the beacon setting upon instruction by project team lead.
12. Maintain visual contact at all times.

13. If propulsion battery is connected, the propeller will be considered powered at all times. As such, avoid the propeller area of the aircraft.
14. Flight patterns performed by multi-rotor aircraft will be performed in front of and never overhead of the test team.

3. TEST HAZARD ANALYSES (THA's)

- A. Battery Fire
- B. Collision with Object
- C. Collision with Personnel
- D. Loss of Communication between GS laptop and UAS
- E. Loss of Communication between Safety Pilot Controller and UAS
- F. Partial loss of Flight Control (Failure of 1 control servo)
- G. Total loss of Flight Control (Failure of Pixhawk)
- H. Loss of GPS signal

		Mishap Severity Category			
		Catastrophic – I Death, System/Facility Loss, Severe Environmental Damage (e.g. Class A Mishap)	Critical – II Severe Injury, Occupational Illness, or Major System/Facility/Environmental	Marginal – III Minor Injury, Occupational Illness, or Minor System/Facility/Environmental	Negligible – IV Less than Minor Injury, Occupational Illness, or System/Facility/Environmental Damage
Probability of Mishap Occurring During the Test	Very Likely (A) Highly expected to occur – Many significant concerns even after mitigation applied.	1	3	7	13
	Likely (B) Expected to occur – Significant concerns remain after mitigation applied.	2	5	9	16
	Less Likely (C) Not expected but possible – Some concern exists even with mitigation applied.	4	6	11	18
	Unlikely (D) Unexpected – Minor concerns after mitigation applied.	8	10	B, C 14	19 D, E, H
	Very Unlikely (E) Highly unexpected – Little or no concern after mitigation applied.	12	15	A, F, G 17	20

[The appropriate letter of each THA is in the appropriate test hazard box.]

TEST HAZARD ANALYSIS (THA)	Page 1/9
TEST SERIES Laura Lucas Thesis Testing	MISHAP CAT/PROBABILITY III/Very Unlikely
PREPARED BY Ms. Laura Lucas	SIGNATURE
AFIT FLIGHT TEST SAFETY OFFICER Chad S. Hale, Lt Col	SIGNATURE
<p>HAZARD: Battery Fire</p> <p>CAUSE:</p> <ol style="list-style-type: none"> 1. Uncontrolled discharge of power from the battery leading to overheating and fire (thermal runaway) 2. Overcharging of battery leading to thermal runaway due to charger malfunction or human input error 3. Battery circuitry or subsystem component failure or wiring malfunction 4. Battery puncture <p>EFFECT:</p> <ol style="list-style-type: none"> 1. Loss of UAS or UGV 2. Injury to personnel 3. High temperature, toxic fire <p>MINIMIZING PROCEDURES:</p> <ol style="list-style-type: none"> 1. (1, 2,3) All batteries will be placed in fireproof metal containers to prevent damage during transportation. 2. (1, 2,3) All batteries will be charged using authorized battery chargers and by personnel trained in the proper recharging techniques. Battery will be placed in fireproof pouch during charging. 3. (2) All batteries will be charged in approved locations while monitored and placed in fire proof pouches. 4. (1,2,3) Only the proper battery types for the specified aircraft will be used 5. (1, 2,3) Only authorized Electronic Speed Controllers (ESCs) for the specified battery size will be utilized. 6. (1, 2,3) Load balancer will be used when charging flight batteries. 7. (2) Downed aircraft will be approached with caution due to the increased possibility of a battery fire. 8. (1, 2,3) Damaged batteries will be safely stored away from other flammable items and within a fireproof metal container. <p>CORRECTIVE ACTIONS:</p> <p>If the battery begins to smoke while charging:</p> <p>Move battery in fireproof pouch outdoors Keep battery in fireproof pouch and place it on a hardened surface away from flammable objects. If the battery catches fire during ground operations:</p> <ol style="list-style-type: none"> 1. Announce battery fire and avoid toxic fumes created by the battery fire. 2. The person nearest to the fire extinguisher will use the fire extinguisher to put out the fire. 3. The person in communication with the field controller will notify the field controller of the emergency via the radio. <p>If the battery catches fire while in flight:</p> <ol style="list-style-type: none"> 1. Announce battery fire. 2. The pilot in command will immediately land the aircraft (make attempt to land on hard surface). 3. All personnel will remain away from the aircraft until the safety pilot deems it safe to approach and put out the fire with the fire extinguisher. 4. The person in communication with the field controller will notify the field controller of the emergency via the radio. <p>REMARKS: None</p>	

TEST HAZARD ANALYSIS (THA)	Page 2/9
TEST SERIES Laura Lucas Thesis Testing	MISHAP CAT/PROBABILITY III/ Unlikely
PREPARED BY Ms. Laura Lucas	SIGNATURE
AFIT FLIGHT TEST SAFETY OFFICER Chad S. Hale, Lt Col	SIGNATURE
<p>HAZARD: Collision with Object</p> <p>CAUSE:</p> <ol style="list-style-type: none"> 1. Bird strike 2. Collision with real-world obstructions <p>EFFECT:</p> <ol style="list-style-type: none"> 1. Loss of UAS 2. Property damage <p>MINIMIZING PROCEDURES:</p> <ol style="list-style-type: none"> 1. (1, 2,3) Safety observers will be used to augment safety pilot. 2. (2) Communicate with the tower before testing to verify clear airspace. 3. (3) Identification of ground based obstructions (hazard) in area of operation before testing. 4. (3) Flight path will be adjusted in order to avoid ground based obstructions. <p>CORRECTIVE ACTIONS:</p> <ol style="list-style-type: none"> 1. Announce collision with object. 2. Discontinue testing and verify there are no injuries. 3. Assess extent of damage. 4. Notify tower if hit or near miss with non-AFIT aircraft occurs. 5. Document exact damage with photos/video. 6. Follow mishap reporting procedures per section 2 of Project Description (page 2). 7. Examine and, if possible, repair the UAS. 8. If operational, perform a trim flight to verify functionality. <p>REMARKS: None</p>	

TEST HAZARD ANALYSIS (THA)	Page 3/9
TEST SERIES Laura Lucas Thesis Testing	MISHAP CAT/PROBABILITY III/ Unlikely
PREPARED BY Ms. Laura Lucas	SIGNATURE
AFIT FLIGHT TEST SAFETY OFFICER Chad S. Hale, Lt Col	SIGNATURE
<p>HAZARD: Collision with Personnel</p> <p>CAUSE:</p> <ol style="list-style-type: none"> 1. Personnel interference during takeoff/landing 2. Loss of control of vehicle <p>EFFECT:</p> <ol style="list-style-type: none"> 1. Personnel injury 2. Loss of UAS <p>MINIMIZING PROCEDURES:</p> <ol style="list-style-type: none"> 1. (1) Launch/landing area will be cleared of all nonessential personnel during these phases of flight and launch and recovery of the aircraft will be announced loudly to all personnel. 2. (1, 2) All personnel will maintain situational awareness of vehicle/flight status and personnel in and around the test area. 3. (2) Test crew will only enter the UAS landing strip to change the beacon setting upon instruction by project team lead. <p>CORRECTIVE ACTIONS:</p> <ol style="list-style-type: none"> 1. Discontinue testing and assess extent of injuries. 2. Coordinate through range control (812-526-1351) if injury at alternate location is severe and requires emergency services 3. Perform any necessary first aid until help arrives. 4. Follow mishap reporting procedures per section 2 of Project Description (page 2). 5. Verify suitability of crew composition to carry on. 6. If suitable, examine and, if possible, repair the UAS. 7. If operational, perform a trim flight to ensure functionality. <p>REMARKS: None</p>	

TEST HAZARD ANALYSIS (THA)	Page 4/9
TEST SERIES Laura Lucas Thesis Testing	MISHAP CAT/PROBABILITY IV/ Unlikely
PREPARED BY Ms. Laura Lucas	SIGNATURE
AFIT FLIGHT TEST SAFETY OFFICER Chad S. Hale, Lt Col	SIGNATURE
<p>HAZARD: Loss of Communication between GCS laptop and UAS</p> <p>CAUSE:</p> <ol style="list-style-type: none"> 1. Signal interference 2. Onboard APM transmitter /receiver failure 3. GCS transmitter /receiver failure 4. UAS flying out of range <p>EFFECT:</p> <ol style="list-style-type: none"> 1. Vehicle spirals to ground 2. Unplanned off-field landing 3. Loss of control of aircraft <p>MINIMIZING PROCEDURES:</p> <ol style="list-style-type: none"> 1. (1, 2,3,5) Verify serviceability of communication equipment prior to test. Verify integrity of the antennae. Verify communication equipment batteries are adequately charged. 2. (4) Limit operation within maximum range of previously conducted test with same autopilot configuration. 3. (1) Coordinate flight operations and frequencies with Atterbury authorities. 4. (1, 2,3,4) Lost link fail-safes (return to launch and loiter) will be pre-programmed. 5. (1, 2,3,4) Separate communication system for safety pilot. 6. (2, 3) Pre-flight checklist will be conducted. <p>CORRECTIVE ACTIONS:</p> <ol style="list-style-type: none"> 1. Ground operator will immediately announce lost communications so the test team can help visually track the UAS. 2. Attempt to re-establish communications with the UAS. 3. If link cannot be re-established, switch to manual mode. 4. Safety pilot will land the UAS manually. 5. Examine and repair communication system. 6. Disable all scripts running on GCS when manual mode is selected by safety pilot <p>REMARKS: None</p>	

TEST HAZARD ANALYSIS (THA)	Page 5/9
TEST SERIES Laura Lucas Thesis Testing	MISHAP CAT/PROBABILITY IV/ Unlikely
PREPARED BY Ms. Laura Lucas	SIGNATURE
AFIT FLIGHT TEST SAFETY OFFICER Chad S. Hale, Lt Col	SIGNATURE
<p>HAZARD: Loss of Communication between Safety Pilot Controller and UAS</p> <p>CAUSE:</p> <ol style="list-style-type: none"> 1. Signal interference 2. Onboard RC transmitter /receiver failure 3. Safety Pilot controller transmitter /receiver failure 4. UAS flying out of range 5. Automatic waypoint algorithm overrides safety pilot inputs <p>EFFECT:</p> <ol style="list-style-type: none"> 1. Vehicle spirals to ground 2. Unplanned off-field landing 3. Loss of control of aircraft <p>MINIMIZING PROCEDURES:</p> <ol style="list-style-type: none"> 1. (1, 2,3,5) Verify serviceability of communication equipment prior to test. Verify integrity of the antennae. Verify communication equipment batteries are adequately charged. 2. (4) Limit operation within maximum range of previously conducted test using same RC configuration. 3. (1) If at alternate location, coordinate flight operations and frequencies with Atterbury authorities. 4. (1, 2,3,4) Lost link fail-safes (return to launch and loiter) will be pre-programmed. 5. (1, 2,3) Separate communication system for auto pilot. 6. (2, 3) Pre-flight checklist will be conducted. <p>CORRECTIVE ACTIONS:</p> <ol style="list-style-type: none"> 1. Safety pilot will immediately announce lost communications so the test team can help visually track the UAS. 2. Attempt to re-establish communications with the UAS. 3. If link cannot be re-established, ground operator will set way points to return the UAS back to the launch area. 4. Ground operator will initiate automatic landing from the GCS. 5. Examine and repair communication system. 6. Disable all scripts running on GCS when manual mode is selected by safety pilot <p>REMARKS: None</p>	

TEST HAZARD ANALYSIS (THA)	Page 6/9
TEST SERIES Laura Lucas Thesis Testing	MISHAP CAT/PROBABILITY III/Very Unlikely
PREPARED BY Ms. Laura Lucas, Ctr	SIGNATURE
AFIT FLIGHT TEST SAFETY OFFICER Chad S. Hale, Lt Col	SIGNATURE
<p>HAZARD: Partial Loss of Flight Control</p> <p>CAUSE:</p> <ol style="list-style-type: none"> 1. Single servo failure 2. Connector to servo failure <p>EFFECT:</p> <ol style="list-style-type: none"> 1. Vehicle spirals to ground 2. Unplanned off-field landing 3. Loss of control of aircraft <p>MINIMIZING PROCEDURES:</p> <ol style="list-style-type: none"> 1. (1, 2,3) Visual inspection of the aircraft will be accomplished prior to flight. 2. (1, 2,3) Perform preflight control check. <p>CORRECTIVE ACTIONS:</p> <ol style="list-style-type: none"> 1. Announce control malfunction. 2. If at alternate location, notify Himsel AAF UNICOM of UAS status. 3. Attempt immediate landing away from personnel. 4. Verify there are no injuries. 5. Follow mishap reporting procedures per section 2 of Project Description (page 2). 6. Document exact damage with photos/video. 7. Examine and, if possible, repair the UAS. 8. If operational, perform a trim flight to ensure functionality. <p>REMARKS: None</p>	

TEST HAZARD ANALYSIS (THA)	Page 7/9
TEST SERIES Laura Lucas Thesis Testing	MISHAP CAT/PROBABILITY III/Very Unlikely
PREPARED BY Ms. Laura Lucas	SIGNATURE
AFIT FLIGHT TEST SAFETY OFFICER Chad S. Hale, Lt Col	SIGNATURE
<p>HAZARD: Total loss of Flight Control (Failure of APM)</p> <p>CAUSE:</p> <ol style="list-style-type: none"> 1. APM failure 2. Connector (power supply to APM) failure <p>EFFECT:</p> <ol style="list-style-type: none"> 1. Damage to UAS 2. Damage to property 3. Injury to personnel <p>MINIMIZING PROCEDURES:</p> <ol style="list-style-type: none"> 1. (1, 2,3) Visual inspection of the aircraft will be accomplished prior to flight. 2. (1, 2,3) Perform preflight control check. <p>CORRECTIVE ACTIONS:</p> <ol style="list-style-type: none"> 1. Announce loss of control. 2. If at alternate location, notify Himsel AAF UNICOM of UAS status. 3. Attempt immediate landing away from personnel. 4. Keep personnel away from landing path. 5. Verify there are no injuries. 6. Follow mishap reporting procedures per section 2 of Project Description (page 2). 7. Document exact damage with photos/video. 8. Examine and, if possible, repair the UAS. 9. If operational, perform a trim flight to verify functionality. <p>REMARKS: None</p>	

TEST HAZARD ANALYSIS (THA)	Page 8/9
TEST SERIES Laura Lucas Thesis Testing	MISHAP CAT/PROBABILITY IV/ Unlikely
PREPARED BY Ms. Laura Lucas	SIGNATURE
AFIT FLIGHT TEST SAFETY OFFICER Chad S. Hale, Lt Col	SIGNATURE
<p>HAZARD: GPS Signal Loss</p> <p>CAUSE:</p> <ol style="list-style-type: none"> 1. Signal interference 2. GPS receiver failure 3. Poor receiver/satellite geometry 4. Connector failure <p>EFFECT:</p> <ol style="list-style-type: none"> 1. Loss of navigation (autopilot will not fly waypoints) 2. Unplanned off-field landing <p>MINIMIZING PROCEDURES:</p> <ol style="list-style-type: none"> 1. (1, 2,3,4) Follow approved preflight procedures for ensuring GPS signal. <p>CORRECTIVE ACTIONS:</p> <ol style="list-style-type: none"> 1. Announce GPS loss. 2. Switch to manual control 3. Safety pilot maintains controlled flight. 4. If GPS is not re-acquired as determined by test team, recover the UAV using manual mode. <p>REMARKS: None</p>	

AFTER ACTION REPORT

Per ENOI 91-6, the After Action Report should be submitted to the FTSO no later than 7 calendar days from the completion of the test.

1. Use this section to briefly describe how the test was carried out. Were there any unusual events?

The test went as planned. The wind picked up unexpectedly, to just within operating range (about 15 kts). However, the flight test was successful, and the aircraft was recovered.

2. What test execution/safety lessons were learned during the test event?

The existing multirotor program information worked well for this operation.

ACRONYMS

AFIT	Air Force Institute of Technology
AFLCMC	Air Force Life Cycle Management Center
AFRL	Air Force Research Laboratories
AGL	Above Ground Level
ANT	Autonomy & Navigation Technology
C2	Command and Control
CESI	Cooperative Engineering Services, Inc.
FOV	Field of View
FTSO	Flight Test Safety Officer
GCS	Ground Control Station
GPS	Global Positioning System
IAW	In Accordance With
LED	Light Emitting Device
LIPO	Lithium POLymer
LOS	Line of Sight
MANET	Mobile Ad-hoc NETwork
MFR	Military Flight Release
NIMH	NIckel-Metal Hydride
RAMS	Radio Aircraft Modelers Society
RC	Radio Control
SENG	Systems ENGineering
UAS	Unmanned Aerial System
UGV	Unmanned Ground Vehicle
VMC	Visual Meteorological Conditions
WPAFB	Wright-Patterson Air Force Base

REPORT DOCUMENTATION PAGE				Form Approved OMB No. 0704-0188	
Public reporting burden for this collection of information is estimated to average 1 hour per response, including the time for reviewing instructions, searching existing data sources, gathering and maintaining the data needed, and completing and reviewing this collection of information. Send comments regarding this burden estimate or any other aspect of this collection of information, including suggestions for reducing this burden to Department of Defense, Washington Headquarters Services, Directorate for Information Operations and Reports (0704-0188), 1215 Jefferson Davis Highway, Suite 1204, Arlington, VA 22202-4302. Respondents should be aware that notwithstanding any other provision of law, no person shall be subject to any penalty for failing to comply with a collection of information if it does not display a currently valid OMB control number. PLEASE DO NOT RETURN YOUR FORM TO THE ABOVE ADDRESS.					
1. REPORT DATE (DD-MM-YYYY) 23-03-2017		2. REPORT TYPE Master's Thesis		3. DATES COVERED (From - To) Sept 2015 - Mar 2017	
4. TITLE AND SUBTITLE Enhanced Cost Minimization Algorithm for Control Architectures				5a. CONTRACT NUMBER	
				5b. GRANT NUMBER	
				5c. PROGRAM ELEMENT NUMBER	
6. AUTHOR(S) Lucas, Laura, L., MS				5d. PROJECT NUMBER	
				5e. TASK NUMBER	
				5f. WORK UNIT NUMBER	
7. PERFORMING ORGANIZATION NAME(S) AND ADDRESS(ES) Air Force Institute of Technology Graduate School of Engineering and Management (AFIT/EN) 2950 Hobson Way Wright-Patterson AFB OH 45433-7765				8. PERFORMING ORGANIZATION REPORT NUMBER AFIT-ENV-MS-17-M-200	
9. SPONSORING / MONITORING AGENCY NAME(S) AND ADDRESS(ES) Air Force Research Lab, Aerospace Systems Directorate Wright-Patterson AFB OH 45433-7765 Mr. Paul Fleitz COMM 312-798-4628 Email: paul.fleitz.us.af.mil				10. SPONSOR/MONITOR'S ACRONYM(S) AFRL/RQQC	
				11. SPONSOR/MONITOR'S REPORT NUMBER(S)	
12. DISTRIBUTION / AVAILABILITY STATEMENT DISTRIBUTION STATEMENT A. APPROVED FOR PUBLIC RELEASE; DISTRIBUTION UNLIMITED.					
13. SUPPLEMENTARY NOTES This work is declared as a work of the U.S. Government and is not subject to copyright protection in the United States					
14. ABSTRACT This research emphasized control for missions with multiple unmanned vehicles (UVs). Extensions to an existing unified control architecture were developed. Line-of-sight (LOS) obstructions and total communication power limitations, such as battery capacity for communicating in multiple rover scenarios, were combined into one problem. The operational mission is summarized as follows: The operator initiates control transmissions between base and the UVs, while a small aerial vehicle provides a relay supporting flexible communications. During this mission, the system strives to maintain LOS communication with as many friendly UVs as possible. Automated enhanced placement software was designed to keep UVs visible to the relay. Manually determined relay placement might reduce performance and threaten safety; therefore, autonomous placement is under development. While there was documentation regarding midpoint placement...					
15. SUBJECT TERMS Optimization, Numerical Geometry, Visibility, BLOS, Communication, Telemetry, UAS, UGS					
16. SECURITY CLASSIFICATION OF:			17. LIMITATION OF ABSTRACT UU	18. NUMBER OF PAGES 129	19a. NAME OF RESPONSIBLE PERSON Dr. David Jacques (ENV)
a. REPORT U	b. ABSTRACT U	c. THIS PAGE U			19b. TELEPHONE NUMBER (include area code) david.jacques@afit.edu (937) 255-3636 x3329